Graduate School in Biochemical, Nutritional and Metabolic Sciences

UNIVERSITÀ DEGLI STUDI DI MILANO
FACOLTÀ DI AGRARIA

Assessment of potential biological activities of caseinophosphopeptides from a commercial purified mixture and from Grana Padano and Trentin Grana, after *in vitro* digestion.

PhD Course in Clinical and Experimental Nutrition

PAOLA DE LUCA

2014/2015

Tutor: Dr. Anita Ferraretto

INDEX

ABBREVIATIONS

$[Ca^{2+}]_i$ = Intracellular calcium concentration

$[Ca^{2+}]_o$ = Extracellular calcium concentration

$1,25(OH)_2D3$ = 1,25-Dihydroxycholecalciferol

Ca^{2+} = Free calcium ions

CPPs = Casein phosphopeptides

dekCPP = Decalcified Casein phosphopeptides

DMEM = Dulbecco's modified Eagle's medium

DMSO = Dimethyl sulphoxide

EMEM = Eagle's Minimum Essential Medium

FBS = Foetal Bovine Serum

Fura-2/AM = Fura-2 acetoxymethyl ester

GP = Grana Padano

KRH SD = Krebs Ringer Hepes buffer

LAB =Thermophylic lactic acid bacteria

RPMI 1640 =Roswell Park Memorial Institute Medium

TJ = Tight Junction

TN =Trentin Grana

TRPV6 =Transient receptor potential cation channel subfamily V member 6

ABSTRACT

Latte e prodotti caseari rappresentano una preziosa fonte di calcio, grazie alla presenza di peptidi derivati dalla caseina che prendo il nome di caseinofosfopeptidi (CPP). Essi sono caratterizzati dalla presenza di innumerevoli serine fosforilate, capaci di legare gli ioni calcio e renderli maggiormente solubili e biodisponibili per l'assorbimento da parte delle cellule intestinali.

E' noto che il processo digestivo e quello di assorbimento rappresentano una fase limite per i peptidi di origine alimentare. Di conseguenza i peptidi con attività bioattiva nei confronti della salute umana devono poter mantenere il loro potenziale anche dopo le suddette fasi. Questa è una prerogativa fondamentale per definire un nutriente come nutraceutico o un cibo come functional food.

Lo scopo della presente tesi è stato quello di valutare in seguito a digestione *in vitro* il potenziale biologico di CPP sia come miscela purificata da latte bovino, sia come componente di prodotti caseari, nello specifico formaggio.

CPP purificati da latte bovino e presenti sotto forma di aggregati con il calcio, forma riconosciuta esplicare funzionalità bioattive, sono stati somministrati a cellule Caco2 e HT-29 che derivano dall'adenocarcinoma del colon, ma che in seguito a differenziamento *in vitro* sono in grado acquisire caratteristiche morfo-funzionali tipiche delle cellule dell'epitelio intestinale deputato all'assorbimento dei nutrienti. Pur comportandosi in maniera differente a causa del diverso meccanismo che governa l'ingresso di calcio nelle cellule Caco2 (canale TRVP6) e HT-29 (canali depolarizzabili di tipo L-Type), dopo il processo digestivo, in entrambe le cellule si è verificato un aumento dell'ingresso del quantitativo di calcio e del numero delle cellule in cui tale ingresso avviene. In seguito a questi risultati, cibi completi e contenenti CPP, rappresentati da Grana Padano (GP) e Trentin Grana (TN) a tre diversi gradi di maturazione corrispondenta a bassa stagionatura (13 mesi), media stagionatura (13 mesi) e lunga stagionatura (26 mesi) sono stati a loro volta sottoposti a digestione *in vitro*. Grana Padano (GP) e Trentin Grana (TN) sono formaggi italiani a pasta dura, caratterizzati da un'elevata digeribilità ed elevato contenuto di calcio. La principale differenza tra i due è data dall'impiego del Lisozima durante il processo produttivo del GP. Per la produzione di quest' ultimo infatti, è concesso l'utilizzo di insilati che consentono la proliferazione di batteri quali il Clostridium butyricum ed il Clostridium Tyrobutyricum e le cui spore permangono a livello delle forme. Con l'avanzare del periodo di stagionatura queste germinano procurando l'esplosione delle forme. L'azione antibatterica del lisozima previene questo fenomeno. Allo stesso tempo accelera il processo proteolitico del formaggio in cui è contenuto. La digestione *in vitro* dei due campioni di formaggi alle diverse stagionature produce peptidi molto simili, ricchi in serine fosforilate e derivanti da α_{S1}, α_{S2} e β-caseina, di lunghezza variabile da 6 a 24 aminoacidi. La capacità di indurre l'uptake di calcio da parte dei digeriti di GP e TN diversamente da quanto riportato per i CPP purificati è stata valutata in un un modello *in vitro* di epitelio intestinale più completo rispetto al precedente, costituito dalla co-coltura delle linee cellulari già utilizzate (Caco2 ed HT-29). I risultati hanno evidenziato che i digeriti dei campioni di formaggio alle diverse stagionature hanno indotto l'ingresso di calcio nelle cellule intestinali senza differenze significative tra i diversi campioni di formaggio digerito utilizzati.

Successivamente è stata valutata la capacità di aumentare l'apposizione di matrice ossea in cellule Saos-2 in coltura, simili agli osteoblasti umani.

Tutti i digeriti sono stati in grado di aumentare notevolmente la mineralizzazione nelle cellule Saos-2, in maniera statisticamente significativa rispetto ai controlli e del tutto in linea con i risultati ottenuti in seguito alla somministrazione di noti induttori della mineralizzazione della matrice ossea, quali la vitamina D nella sua forma attiva ed il Desametasone.

Questi risultati hanno posto importanti presupposti affinchè i CPP, sia come tali, potenzialmente impiegabili come integratori o aggiunti a preparazioni alimentari, sia di fisiologica derivazione dalla digestine di latticini, possano essere definiti nutraceutici e /o functional foods. Il loro ruolo potrebbe essere giustificato nell'ottica del miglioramento della salute umana soprattutto in quei casi in cui il fabbisogno di calcio aumenta (crescita, gravidanza, osteoporosi, ecc).

Introduction

CALCIUM HOMEOSTASIS IN THE INTESTINAL CELLS

Calcium is an essential micronutrient for human metabolism and health. The main dietary sources are milk and dairy products (78%), while a minor contribution is given by fruits and vegetables (20%), and even by meat and fish (5%). The dietary calcium absorption is related to the chemical nature of the food source and to the individual nutritional, metabolic and physiological status. Compounds such as phytate, phenolic compounds, oxalate, lactose, phosphorus, and vitamin D, introduced with calcium may affect its absorption. For example, cereals and legumes contain phytates that are able to bind calcium creating an insoluble form or poorly soluble complexes in alkaline pH, making calcium ions unavailable for absorption (Kitts & Yuan, 1992). Moreover, the intestinal absorption of calcium and other minerals is drastically inhibit by some pectins (Gueguen L & Pointillart A 2000). The bacterial fermentation of different non-digestible oligosaccharides and carbohydrates, lowering the pH of intestinal environment, is able to increase the calcium absorption from the intestine distal part. However, several species of fibers (cellulose, hemicellulose, lignin and non-cellulosic polysaccharides) do not seem to directly influence the absorption of this ion. (Gueguen L & Pointillart A 2000). Calcium phosphate is the predominant form of calcium in the body (99%) and the main constituent of bone mineral (Bronner, 1988). The skeletal tissue retains and accumulates the main part of the ingested calcium. The calcium deposition rate in bones is higher in the newborn and decreases until the end of the individual development. During the life, the removed calcium rate from the bones tends to equalize the deposition rate (Bronner & Pansu, 1999). The bone deposition and removal, and the body homeostasis of calcium ions are regulated by hormones such as calcitonin, parathyroid hormone and vitamin D.

There are two known calcium absorption pathways: transcellular and paracellular. Transcellular pathway is secondary active transport, situated in the basolateral membrane, and it requires ATP hydrolysis by the Ca^{2+} dependent ATPase; it can occur when the Ca^{2+} concentrations in the intestinal lumen is lower than those in plasma, and it is also stimulated by $1,25(OH)_2D_3$. This pathway is a saturation process that happens when the luminal concentrations is up to 5 mM. In contrast, the paracellular pathway is a passive transport through the tight junctions (often described as vitamin D independent) and occurs if the Ca^{2+} concentration increases causing the formation of a transepithelial electrochemical gradients. In this case, the absorption pathway displays linear or diffusive kinetics between 5 and 200 mM Ca^{2+}.

Actually, the intestinal calcium internalization pathway (transcellular or paracellular pathway) depends on the amount and concentration of ionized Ca^{2+} in the intestinal lumen. The transcellular transport occurs for 50% in duodenum, decreasing to 20% in jejunum and 0% in ileum but on the evidence that the transcellular component depends on the Ca^{2+} content of the diet, this values are merely guidelines. Thus, when the transcellular $1,25(OH)_2D_3$ dependent transport is upregulated by low Ca^{2+} intakes, the paracellular flow contributes for perhaps <10% of duodenal absorption. In contrast, a high intake down-regulates transcellular absorption, so the paracellular flow increases up to > 90% of duodenal absorption. At high Ca^{2+} concentrations, the jejunum and ileum paracellular flow is the predominant way of absorption, because the absorptive capacity of the duodenum is diminished (Kellett, 2011).

The transcellular intestinal Ca^{2+} absorption, can be regulated by genomic or non-genomic pathways (Figure 1). The first is a facilitated diffusion pathway and represents the most widely accepted model; it involves three elements: TRPV6 (CaT1), a member of the transient receptor potential vanilloid subfamily, calbindin-D_{9K} and PMCA1b (the predominant form in intestine) (Choi & Jeung 2008; Hoenderop et. al, 2005; Peng et al., 2003). At duodenum level, apical Ca^{2+} enters into the enterocytes through TRPV6, which is activated by hyperpolarization and is relatively unresponsive to L-type channel inhibitors (Peng et al., 1999; Suzuki et al., 2008). Transport across the apical membrane is strongly promoted by an electrochemical gradient. The cytosolic calcium diffusion is 70-fold facilitated by binding to calbindin-D_{9K}, which acts as a Ca^{2+} carrier. Finally, Ca^{2+} is transported across the basolateral membrane against the electrochemical gradient through PMCA1b. About 80% of Ca^{2+} follows this route, the remaining 20% uses the Na^{+}/ Ca^{2+} exchanger.

The facilitated diffusion model is strongly up-regulated by $1,25(OH)_2D_3$ that binds the vitamin D receptor (VDR) or a low- Ca^{2+} intake and downregulated by high dietary Ca^{2+} intake or low $1,25(OH)_2D_3$. $1,25(OH)_2D_3$ (Johnson & Kumar, 1994). In fact, according to the immunocytochemistry and quantitative polymerase chain reaction, the protein and mRNA expression levels of TRPV6, calbindin-D_{9K}, and PMCA1b, are highest in duodenum and decrease distally; they are also present in cecum and colon (Armbrecht et al., 2003; Hoenderop et al., 2000; Zhuang et al., 2002). The rapid non-genomic vesicular transport pathway is based on chick duodenum model, which expresses calbindin-D_{28K} (Khanal & Nemere 2008b; Larsson et al., 1998). Vitamin D, by the $1,25(OH)_2D_3$-MARRS (membrane-associated, rapid

response steroid-binding) receptor, stimulates the entry of Ca^{2+} increasing Ca^{2+} concentration in the subapical region in few minutes, disrupting actin filaments (Nemere, 2005).

The resulting endocytosis vesicles are transported by microtubules in order to fuse with lysosomes and, finally, with the basolateral membrane to secrete Ca^{2+} and calbindin-D_{28K} into the bloodstream (Figure 1).

Lysosomal/basolateral fusion may involve the control of the local Ca^{2+} concentration by the entry through basolateral L-type channels together with the efflux through PMCA1b, according to the observation of a rapid Ca^{2+} recycling across the basolateral membrane (Khanal & Nemere 2008a).

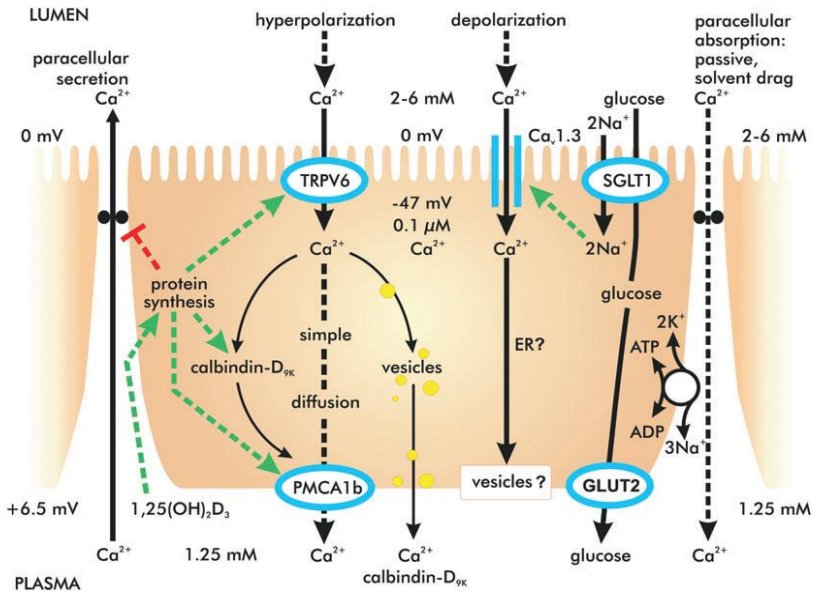

Figure 1. Calcium transport in rat jejunum. The pathway represented in the middle of the picture describe the transcellular absorption regulated by alternative depolarization and repolarization of the apical membrane, respectively, during and between digestive periods. The two transcellular active pathways for Ca^{2+} absorption show complementary roles: one way is mediated by TRPV6, which is activated by hyperpolarization of the apical membrane, and the other is mediated by Cav1.3, which is activated by depolarization. Three potential routes are controlled by TRPV6 related mechanism: a) the facilitated diffusion pathway by calbindin-D_{9K}; b) simple diffusion of free Ca^{2+}; c) the vesicular transport pathway, in which Ca^{2+} and calbindin-D_{9K} are simultaneously released into the plasma by vesicle fusion with the basolateral membrane. TRPV6, calbindin-D_{9K} and PMCA1b are also genomically upregulated by vitamin D. Cav1.3 is activated by Na^+/glucose co-transport (SGLT1) and by other depolarizing nutrients, including amino acids and oligopeptides. The transcellular pathway is not established yet, but it is independent of calbindin-D_{9K} and, probably, vitamin D. Absorption through Cav1.3 also regulates apical GLUT2 insertion. Paracellular absorption is shown as a minor component, on the base that Cav1.3, alone or in conjunction with TRPV6, offers alternative explanations for some phenomena currently attributed to paracellular flow. Dashed lines: with arrowhead, activation; with bar, inhibition (Kellett, 2011).

The way in which the intestinal Ca^{2+} absorption occurs under the depolarizing conditions of digestion is a fundamental issue. The digestion products of peptides, amino acids and disaccharides are strong depolarizing agents and they are generated throughout jejunum and ileum, which are the absorptive regions with the longest transit time for food. Nutrient-induced paracellular flow and/or activation of L-type channels represent the two possible mechanisms that might operate under depolarizing conditions. As a consequence, jejunum and ileum offer the major parcellular pathway of Ca^{2+} absorption because, exhibiting the longest transit time for food, have a much more depolarizing environment than duodenum after a meal.

It was established that intestinal epithelial cells do not express L-type channels, since enterocytes are activated by hyperpolarization (Petersen & Fedirko, 2001). This theory is supported by the discovery of ECaCs: they do not contain the S4 voltage sensor, normally located in L-type channels, and are activated by hyperpolarization in the range of -60 to -150 mV (Figure 2). Hence, TRPV6 was found in the duodenum, which is characterized by a polarizing environment due to a very short chime transit time. The most widely accepted mechanism of transcellular Ca^{2+} absorption, therefore, does not explain the fundamental issue of absorption during digestion.

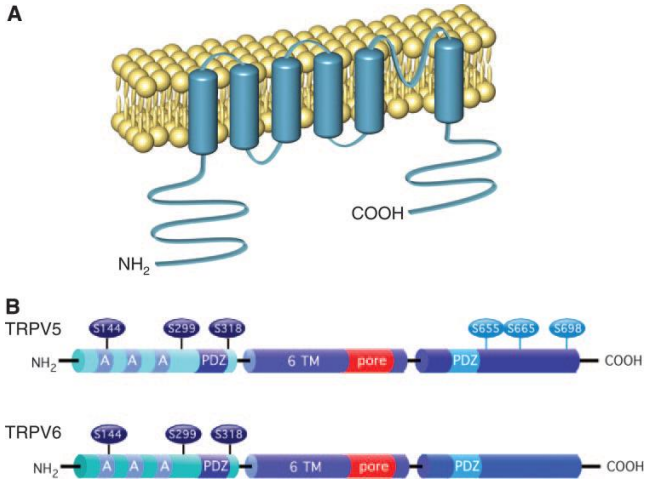

Figure 2. Structural organization of TRPV6. **A)** The epithelial Ca^{2+} channels is a 83 kDa protein composed by 730 amino acids. TRPV6 contains a core domain consisting of 6 transmembrane (TM) segments. In addition, a large cytosolic amino and carboxy terminus contains ankyrin repeats. Between TM5 and TM6 there is a short hydrophobic stretch considered the pore-forming region of these channels. Inner and outer side of the membrane are specified. **B)** potential regulatory sites in the amino and carboxy tail of TRPV6 including ankyrin repeats, PDZ motifs and conserved PKC phosphorylation sites (Hoenderop er al., 2005).

There is clear evidence that L-type channels are expressed in the apical membrane of Atlantic cod enterocytes (Larsson et al., 1998). Imaging experiments performed on isolated cells, loaded with Fura-2, revealed that K^+-induced depolarization, at 10 mM Ca^{2+}, caused a wave of Ca^{2+} entering across the apical membrane and exiting through the basolateral membrane in about 1 minute (Larsson et al., 1998). The resulted increase in intracellular Ca^{2+} levels was mimicked by Bay K 8644 and blocked by nifedipine (5 mM).
A role for apical Ca^{2+} entry was confirmed by single-pass perfusion of rat jejunum in vivo; entry could not involve TRPV6, which lacks the S4 voltage sensor and is opened by hyperpolarization, i.e., between -60 and -150 mV (Hoenderop et al., 1999; Peng et al., 1999). Furthermore, TRPV6 is located predominantly in duodenum, (Hoenderop et al., 2000; Zhuang et al., 2002) which has a relatively polarizing environment, modest glucose absorption, and negligible apical GLUT2 insertion.

In jejunum, the depolarizing conditions pointed to an apical L-type channel. A homology-based polymerase chain reaction approach was used in order to amplify transcripts of the non-classical neuroendocrine Cav1.3 α1 pore-forming subunit and an associated β3 subunit from jejunal mucosal cDNA (Morgan, et al. 2007); other L-type channel was not detected. Western blotting and immunocytochemistry were performed to localize protein expression of both subunits in the apical membrane. L-type characteristics were displayed by Ca^{2+} absorption (Morgan, et al. 2007; Morgan, et al. 2003).
Cav1.3 is a second channel capable of active transcellular Ca^{2+} absorption in intestine. It is activated by membrane depolarization and can operate under conditions of weak membrane depolarization at low-voltage thresholds, such as those generated around -47 mV by nutrient absorption. Cav1.3 and TRPV6 are respectively strongly activated at V_m values from +10 mV to -20 mV and from -60 mV to -150 mV.This suggests that the two transports have complementary roles in Ca^{2+} entry. The above mentioned characteristics show that TRPV6 and Cav1.3 contribute independently to absorption (Nakkrasae et al., 2010).
On the bases of this hypothesis, rapid changes in Ca^{2+} absorption during digestion occur as a consequence of alternate depolarization and repolarization, during and between digestive periods; the changes are achieved by alteration in the contribute of Cav1.3 and TRPV6 in response to changes in V_m. In this view, Cav1.3 plays the dominant role during digestion, especially when Ca^{2+} diet is plentiful, so TRPV6 activity is genomically downregulated and inhibited by changes in V_m if glucose concentration reach 30–100 mM at the apical membrane (Mace et al., 2007).
Amino acids, peptides and other depolarizing digestion products may activate Cav1.3 and inhibit TRPV6.
Moreover, depolarization is enhanced by an increased synthesis of disaccharidases and nutrient transporters. On the other hand, TRPV6, under the polarizing conditions between meals, plays a dominant role as a powerful scavenger.

When Ca^{2+} concentration in the lumen is lower than in plasma, TRPV6 can be activated by apical membrane repolarization and up-regulated by vitamin D in order to prevent massive loss of body Ca^{2+}. This mechanism explains the fundamental role of the vitamin D and TRPV6 in Ca^{2+} homeostasis. The interplay between TRPV6 and Cav1.3 is essential to maintain a strict control of free Ca^{2+} concentration in the extracellular space over the entire range of dietary intake.
Cav1.3 mediates the entry of Ca^{2+} by a second active transcellular pathway and regulated by depolarizing nutrients and hormones. In particular, rapid glucose- and prolactin-induced Ca^{2+} absorption through Cav1.3 is independent of calbindin-D_{9K} and probably of vitamin D. TRPV6 is activated by hyperpolarization; hence, Cav1.3 is able to act in a way different from TRPV6 , for example it operates optimally during dietary Ca^{2+} intake and under the depolarizing conditions of digestion. (Kellett, 2011).

MECHANISMS OF CELL CALCIUM REGULATION

Calcium is an important second messenger and a regulator of cellular functions. It is involved in many cellular responses, such as muscle contraction, nerve transmission, secretion, and also plays an important role in regulating cell growth, differentiation and apoptosis.
The concentration of intracellular calcium, $[Ca^{2+}]_i$ (0.1-0.2 µM) is lower than extracellular calcium $[Ca^{2+}]_o$ (1-2 mM). The maintenance of this gradient and the rapid increase in $[Ca^{2+}]_i$ (10-20 times in a few milliseconds), observed after stimulation with an agonist, are the result of coordinated action of several mechanisms that include: influx and efflux of calcium through the cytoplasmic membrane, intracellular calcium stores and buffer systems (Figure 3).
The entry of calcium from the extracellular environment occurs through different type of channels located in the plasma membrane: (Kitts & Yuan, 1992; Nelson & MM, 2006).

- **ROCCs** (Receptor-Operated Ca^{2+} Channels): calcium channel regulated by a receptor formed by a ligand binding site and a channel included in the same protein or part of the same complex. These channels open as a consequence of competitive binding to the receptor without the involvement of diffusible second messengers.
- **GOCCs** (G protein-Operated Ca^{2+} Channels). channels directly coupled to receptors by means of G protein.
- **SOCCs** (Stores-Operated Ca^{2+} Channels). channels activated by depletion of intracellular stores. Mechanism of activation is still unclear.
- **SMOCCs** (Second Messenger-Operated Ca^{2+} Channels): channels activated by a second messenger. The opening of these channels is controlled by a diffusible cytosolic messenger whose production is due to ligand-receptor interaction.
- **VOCCs** (Voltage-activated channels): channels detected in excitable cells, such as nerve and muscle fibers, and in no-excitable cells, such as fibroblasts. The opening of these channels occurs after a depolarization of the plasma membrane. The VOCCs can be divided into different classes according to their electrophysiological characteristics and sensitivity to different inhibitors.

Cells shows different ways to buffer or sequester calcium in order to prevent a prolonged and uncontrolled increase in $[Ca^{2+}]_i$.
The transport processes located in the plasma membrane are able to guarantee the maintenance of an adequate level of cytosolic free calcium ions and consist of two main systems for extrusion ions, ensuring the maintenance of the concentration gradient: the Ca^{2+}-ATPase and Na^+/Ca^{2+} exchanger. The Ca^{2+}-ATPase is an ubiquitous eukaryotic cell active transport system which can bind intracellular calcium with high affinity and release it in the environment outside the plasma membrane by consuming ATP. The Na^+/Ca^{2+} exchanger is present only in a few cell types, especially in excitable cells, coupling the release of one calcium ion against gradient to the entry of three sodium ions into cells following the gradient (Putney et al., 1999) .
There are other key mechanisms involved in the maintenance of ion homeostasis, such as the binding to cytosolic proteins and the accumulation in intracellular compartments. In the cell, as well as in mitochondria and Golgi apparatus, where calcium concentrations are extremely high, the calciosome, a specialized endoplasmic reticulum sub-compartment, is the main organelle involved in storage and in the rapid exchange of calcium after cell stimulation. Studies about skeletal muscle (Lamb and Stephenson 1992) have shown that Ca^{2+}-ATPase, present in the membrane of

this organelle, allows the accumulation of calcium in the sarco/endoplasmic reticulum against the gradient trasporting two calcium ions into the lumen of the reticulum for each molecule of hydrolyzed ATP.
Most of the calcium in the intracellular stores is not in ionic form, but is bound to low affinity (Kd = 1-4 mmol/ L) and high binding capacity (25-50 calcium moles/mole of protein) proteins, which enhance the ability to storage of the endoplasmic reticulum (Wasserman & Fullmer, 1995). These proteins are: calsequestrin, present mainly in muscle cells, and calreticulin, common in a greater number of cell types. The release of calcium from intracellular stores is due to inositol 1,4,5 triphosphate (IP3): it derives from the cleavage of phosphatidyl-inositol-4 ,5-bisphosphat by the action of phospholipase C, coupled with a G protein. The IP3 acts as a second messenger by binding to its receptor, located in the membrane of the endoplasmic reticulum, and activates calcium channel in response to the ion release in the cytosol (Berman, 1999).
This process depends critically on $[Ca^{2+}]_i$: at low concentration (<0.3 mM) calcium acts as a co-agonist of IP3 (thus exerting a positive control on his release from the endoplasmic reticulum), whereas at higher concentration exerts a negative control on the release of Ca^{2+}-induced by IP3, inhibiting the receptor and thus preventing further release of Ca^{2+} (Orrenius et al, 2003). Inside the eukaryotic cells, there are also systems able to buffer large transient increases in $[Ca^{2+}]_i$ that could lead to the activation of enzymatic reactions harmful for the cell. This proteins show an heterogeneous affinity and ability to bind Ca^{2+}, which take place within a cell Ca^{2+}-dependent enzymatic action (for example, phosphorylase) or regulatory (eg calmodulin). This plays an important role in the modulation of a variety of physiological processes (such as Ca^{2+}-ATPase activity of the membrane), as well as representing the cytoplasmic protein important in binding Ca^{2+}, thanks to its high concentration (approximately 1% of total cellular proteins) and the presence of four binding sites for Ca^{2+}.

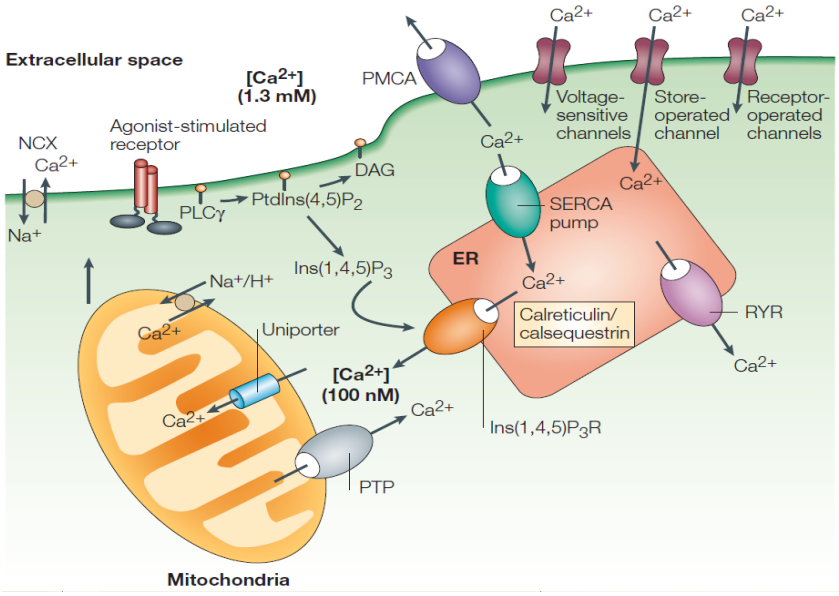

Figure 3. **Intracellular Ca^{2+} homeostasis.** The extracellular Ca^{2+} can enter into the cell through the voltage-gated channels permeable to Ca^{2+} (VOOCs), the channels sensitive to the concentration of intracellular Ca^{2+} (SOOCs), the channels G protein-coupled receptors (ROCCs). Ca^{2+} in the endoplasmic reticulum is released into the cytosol through channels opened by IP3. The PLC hydrolyzes PIP2, producing IP3 and DAG. The baseline intracellular concentration of calcium is recovered by the extrusion of the ion mediated by Ca^{2+}-ATPase present on the plasma membrane (PMCA) and on the membrane of the endoplasmic reticulum (SERCA), or by the antiport Na^+/ Ca^{2-} (Orrenius et al, 2003).

CASEIN PHOSPHOPEPTIDES (CPP_S)

A family of phosphoproteins (αs1-, αs2-, β- and κ-caseins), called caseins, constitutes about 80% of the bovine milk proteins. They constitute a good nutritional source of aminoacids even if in their native state they do not explicate any known biological activity (Schlimme & Meisel 1995).
Caseins contain a series of peptides, inactive in the precursor protein, but able to demonstrate a biological activity once released by the gastrointestinal digestion (Meisel & Frister 1988; Naito et al., 1972). These peptides are able to behave like opioid receptor agonist (casomorphines) and antagonist (cosoxines) peptides, anti-hypertensive (casochinines) and anti-thrombotic (casoplatelines) peptides and immunostimulating peptides (immunopeptides) (Meisel & Schlimme, 1990; Shah et al., 2000).
CPPs (αs1-, αs2-, β-caseins derived phosphorilated peptides) are a particular type of these biologically active peptides that are able to bound and solubilize minerals, such as calcium, involving its serine-associated phosphate groups, preventing their precipitation in the calcium-phosphate salt form. This action increases the bioavailability of calcium fraction in the small intestine, and particularly at the ileum level (Berrocal, et al. 1989; Erba, et al. 2002; Meisel and Olieman 1998). Indeed, the unphosphorilated peptides are not able to bind calcium, while the casein phosphorilation increases both the binding capacity and the resistance to proteolysis (FitzGerald 1998).
The high calcium bioavailability of milk and dairy products has been attributed to the CPPs formation, along the digestive tract; moreover the high number of phosphorilated serine residues, -Ser(P)-, and the consequent high negative charge density, are responsible for the resistance of CPPs to further proteolytic digestion and for their accumulation in the distal small intestine. (McDonagh and FitzGerald 1998).
All the CPPs share a highly polar "acidic domain" constituted by three serine phosphate cluster and glutamyl residues: -Ser(P)-Ser(P)-Ser(P)-Glu-Glu-. This sequence is highly conserved between the species and it is the characteristic Ca^{2+} binding motif that, due to the phosphorylated serines, it is relatively resistant to further hydrolysis. Moreover, they could prevent the metal ion precipitation at alkaline pH in the distal small intestine (Cruz-Huerta et al, 2015; Ferraretto et al., 2001 JNutr; Nongonierma & FitzGerald, 2015).

The extraction of CPPs can be performed *in vitro* starting from the bovine sodium caseinate, using a pancreatic enzymatic preparation presenting the tryptic as the main activity (Sato, et al. 1991).
Their binding ability varies from 0.4 to 0.6 mg of Ca^{2+} mg^{-1} of CPPs, whereas the ion solubilizing ability varies from 7.4 to 24 mg of Ca^{2+} mg^{-1} of CPPs. There is an evident distinction between the ability to bind and to solubilize calcium; moreover depending on the used enzymatic preparation, the ability to solubilize calcium changes, probably on the base of the aminoacidic sequence (McDonagh and FitzGerald, 1998).

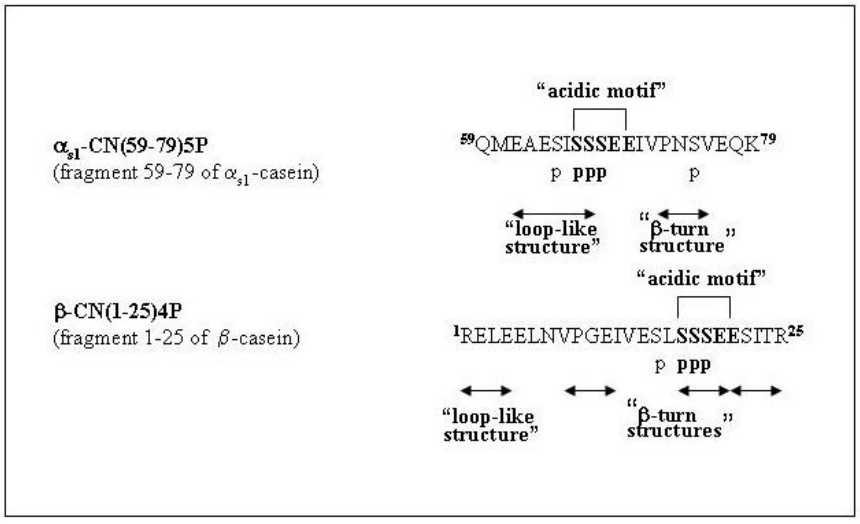

Figure 4. Primary structures of the αs1-CN (59-79)5P and βCN(1-25)4P CPPs purified from bovine caseins. The "acidic motif" characteristic of all CPPs is indicated in bold characters. S means the phosphorylated serine.

The calcium affinity constant, as determined by capillary electrophoresis, is comprised between 10^2 -10^3 M^{-1} (Meisel & Schlimme, 1990); this low affinity could facilitate the ion release during the intestinal absorption.
In the last few years, the studies about the physic-chemical CPPs property and the structure-calcium binding correlation have been focused on the two CPPs that form in highest amount during the intestinal enzymatic digestion: β-CN(1-25)4P and αs1-CN(59-75)5P. The primary sequences of these two peptides are reported in Figure 4.

Biological activity of CPPs

The first indications about a potential physiological role for CPPs came from the 1950, when Mellander demonstrated that the tryptic digestion-derived casein phosphopeptides were able to increase the bone calcification level in rachitic children without a contemporary vitamin D administration (Mellander & Olsson, 1956). Subsequently it was demonstrated that their administration induced an increased calcium absorption in rats (Patrick & Bacon, 1957) , and their presence in the diet of ovariectomized female rats was able to reduce the bone mineral density loss (Tsuchita et al., 1996).
The proved ability of CPPs to prevent the precipitation of calcium in the presence of phosphate has suggested the possibility that CPPs could enhance the amount of soluble calcium in the intestinal lumen, thereby increasing the mineral availability for absorption in the small intestine (Kitts & Yuan, 1992). Nevertheless, experiments *in vitro* with intestinal preparations and animals (pigs and rats) fed a soy protein rich diet implemented with CPPs, however, have provided conflicting results, and especially they do not have clarified in any way the molecular mechanism used by these peptides to increase absorption of calcium (Pointillart & Gueguen, 1989; Sato et al., 1986).
On the contrary, *in vitro* cell studies demonstrated with no doubts that CPPs can affect diverse biological function. The first direct evidence of an interaction between intestinal cells and CPPs came from the observation that in presence of CPPs and extracellular calcium, HT-29 and Caco2 cells, two known human intestinal in vitro cell models, are induced to uptake calcium ions from the extracellular milieu (Ferraretto et al., 2001). This activity was subsequently recognized to be due to the presence of a structural CPP conformation, conferred by both the phosphorylated 'acidic motif' and the preceding N-terminal portion, necessary for the interaction with the cell plasma membrane (Ferraretto et al., 2001). Instrumental to this CPP aptitude is the formation of stable aggregates with calcium ions, in fact the cellular response, i.e, the increased intracellular calcium concentration, follows a dose-response relationship similar to that reported for the formation of aggregates, with a maximum at 4 mM extracellular calcium concentration and a CPP dose of 1280 μM, if a purified commercial mixture, or 200 μM, if a single purified CPP (Gravaghi et al., 2007).
More recent studies have also provided results concerning differences between the intestinal cell lines used, HT-29 and Caco2, in their response to CPPs, evidencing that, regardless of the slight differences (mostly at the quantitative levels) between the two cell lines, the ability of these cells to take up extracellular calcium under CPP stimulation is a molecular attitude expressed upon differentiation (Cosentino et al., 2010). Another demonstration of the interaction between CPPs and intestinal cells can be derived by two works (Kawahara, et al. 2004; Kitts and Nakamura 2006) presenting experimental evidences that a particular CPP sequence, commercially available as CPP-III, (Meiji Seika, Tokyo, Japan), consisting of about 90% casein phosphopeptides such as bovine αs2-casein (1-32) and β-casein (1-28) and enriched in calcium, modulates the intestinal immune system by enhancing the mRNA expression of TNF-α as well as IL-6 (a cytokine with functions of modulator of cellular differentiation, proliferation and apoptosis) in a dose dependent manner.
The use of primary human osteoblast-like cells, established in culture from trabecular bone samples obtained from waste materials during orthopaedic surgery, has revealed interesting and new potentialities for CPPs when administered. Analogously to what monitored in intestinal in vitro cell lines, CPPs stimulate calcium uptake by primary human osteoblast-like cells and induce an increase in the expression and activity of alkaline phosphatase (ALP), a marker of human osteoblast differentiation. Moreover, the higher fraction of available calcium due to CPPs enhance calcification nodule formation by human SaOS-2 in vitro cell culture (Donida, et al., 2009).

GRANA PADANO AND TRENTIN GRANA CHARACTERISTICS

Grana Padano (GP) is one of the oldest cheeses in the dairy tradition of Northern Italy and its recognition as a PDO product dates back to October 30, 1955, when it was issued the Presidential Decree no. 1269 on the "Recognition of denominations about the processing methods, product characteristics and production area of the cheese." Since 1926 this product is supported by a similar cheese called Trentin Grana (TN), belonging to the same Consortium (Consortium for the Protection of Grana Padano), to bring together all the producers, ripeners and dealers of these cheeses. While the use of Lysozyme in the production of GP is permitted, in TN the use of this additive is not allowed, assimilating into this Parmigiano Reggiano other extra-hard cheese, whose production regulation does not cover the use of this additive. The following diagram shows the Grana Padano production process:

RAW MILK
A maximum of two milkings, generally a morning and an evening

SURFACING NATURAL CREAM

MILK P.S.
for separation from fat surfaced

MILK IN BOILER copper

ADDITION OF SERUM ENGAGEMENT
culture of lactic bacteria obtained from incubation of cheese whey from the previous day

ADDITION OF RENNET VEAL

Coagulation
by heating the milk to a temperature 31-33ºC

BREAKING CURD

COOKING
stirring, final temperature 53-56ºC

STOCK UNDER SERUM
for a time of 30-70 minutes at Temperature that does not exceed the end of cooking

It enables granules of curd resting on the bottom of the boiler and cluster

FORMING
2 days

SALTING
by immersion in natural brine
for a time comprised between 16-25 days
depending on the type of forms, the salt concentration, the level of salting required

STEWING
in order to dry the form

SEASONED
T ° 15-22ºC for at least 9 months
in ripening rooms where humidity, ventilation and temperature are controlled
Pile driving of the forms in the fixed time periods

MARKING
after appropriate control CSQA

As the main component of milk is water, the cheese will have very low humidity, resulting in concentration of all nutrients. Despite the composition variability due to not-standardized products, Grana Padano and Trentin Grana are characterized by a high protein content, while the use of low-fat milk causes a reduction in lipids compared to proteins. In contrast, in the starting raw material a protein predominance is observed.

The tables below show the analytical characterizations of the two cheeses.

	TN: Consortium Source up to 100	**GP: Consortium Source**	**GP: IEO Source**
Energy value (Kjoule-Kcal)	1565KJ-376Kcal	1597KJ-384Kcal	1690Kj-409Kcal
Proteins	32.18 g	33 gr	33.9 gr
Lipids	27.52 g	28 gr	28.5 gr
Carbohydrates		Absent	3.7 gr
Soluble phosphopeptides		1.5 gr	3.7 gr
Free Aminoacids		6 gr	-
Conjugated linoleic acids (CLA)		170 mg	-
Calcium	986 mg	1165 mg	1169 mg
Potassium		120 mg	120 mg
Phosphorus	640 mg	692 mg	692 mg
Selenium		12 µg	12 µg
Iron		140 µg	200 µg
Magnesium		63 mg	63 mg
Sodium chloride		1.6 gr	1.6 gr
Zinc		11 mg	4 mg
Copper		500 µg	490 µg
Iodine		35.5 µg	36 µg

Table 1. Comparison of the average nutritional content (g or mg per 100 g of product such as) of TN and GP provided by the consortium and by IEO (European Institute of Oncology).

As can be observed, the analytical compositions are substantially overlapping, both cheeses are characterized by high protein titles, greater than 30% and by high lipid levels. The calcium concentration is relevant in both cases.

Grana cheese consumption and nutritional implications

The cheeses can be defined as highly nutritious elements because they are characterized by a concentration of proteins, fats, minerals and vitamins that is 4-10 times higher then the starting raw materials. This is carried out following the removal of the water in serum form and after the curing period. Among the food principles involved in this concentration, the proteins are the main role because they increase about 10-fold compared to the initial content, while fats increase 8 times. The lactose is not affected by this concentration, because the majority remains in the serum or in any case is used by the dairy microflora that is established during curing. For this reason, in the medium-long ripening cheeses as GP and TN they can become part of the diet of people who are lactose intolerant.

Proteins

The grana cheeses are characterized by a high protein quantity (greater than 30%) with a high content of lysine and other essential amino acids such as valine, leucine ect. The only tryptophan amino acid is highly deficient together with cysteine. Nonetheless a portion of 50 g of GPs or TN is able to cover a large proportion of the essential amino acid requirements of the adult (body weight 70 kg) as viewable in Table 2.

Amino acids	**mg/g food protein[1]**	**Requirement [2] (mg/die)**	**Amino acids GP (mg/100g of food)[3]**	**Provision (mg)**	**% coverage requirements**
Ile	18	1134	1390	695	73.5
Leu	25	1575	2820	1410	107.4
Lys	22	1386	2470	1235	106.9
Met+Cys	24	1512	1160	580	46
Tyr+Phe	13	819	3740	1870	274
Thr	13	819	1100	550	80.6
Trp	6.5	409.5	310	155	45.4
Val	18	1134	1910	955	101.1

[1] FAO-WHO

[2] Assuming a body weight (bw) of 70 kg and ingestion of protein 0.90 g/kg of p.c.

[3] Table of food

Table 2. Recommended Contribution of essential amino acids in adults and percentage of their fulfillment through the ingestion of 50 g of GP.

Following proteolysis, the grain cheese digestibility increases because it is delivered to digestive enzymes a substrate already partially hydrolyzed. Furthermore the presence of free amino acids (FAA) and short chain peptides stimulate the secretion of gastric pepsin and HCl. Among the products of casein degradation, the major proteins present in the curd, there are also several bioactive peptides such as caseinophosphopeptides (CCP), molecules resistant to intestinal digestion that can form highly soluble stable complexes with the Ca^{2+} which facilitate the absorption intestinal. Other interesting peptides are casomorphins or opioid peptides that act in the intestine stimulates the absorption of amino acids, intestinal transit and water balance (Matar et al., 1996). ACE inhibitors or hypotensive peptides are additional milk bioactive peptides with reducing blood pressure capacity. A recent study (Crippa et al., 2011) and numerous literature data showed that these peptides may have a complementary role to drug treatment for individuals who are required to reduced pressure level of 10mmHg. In particular, the study above mentioned shown that taking ACE-inhibitory peptides following consumption of 30 g of GP cheese, a decline in both systolic and diastolic blood pressure is shown.
The action mechanism of these peptides involves the inhibition of the ACE that is known to catalyze the conversion reaction Angiotensin I to Angiotensin II, potent vasoconstrictor associated to what is the Renin-Angiotensin system that regulates blood pressure; the consequences of this action are the Angiotensin II reduction, the inhibition of bradykinin breakdown and hypotension. In order to perform the action of these peptides, they must be absorbed still intact by the intestine, they must resist to the plasma peptidase attack of finally, they must reach the target sites (Cerutti, Tecniche Nuove, Parma, 63). In addition to the peptide VPP (Val-Pro-Pro) and IPP (Ile-Pro-Pro), other peptides were recently discovered and, after artificial synthesis, they are *in vitro* tested, highlighting the same ACE-inhibitory effect (Mullally, et al., 1996). The concentration of ACE inhibiting peptides IPP and VPP in cheese is influenced by various factors such as the dairy microflora present and the possible use of starter cultures, the pre-treatment of milk (microfiltration, pasteurisation) and ripening conditions; in relation to the latter factor it must be said that the ACE-inhibitory activity, obtained following the proteolysis, increases to a certain point. Later, the activity decreases with increasing curing time (Sforza et al, 2011). The concentration of such peptides in cheese as the GP and the TN varies from 5% to 15% (Bachmann, et al., 1997).
GP and TN are excellent sources of branched amino acids, in fact the value of the Valine, Isoleucine and Leucine

summation is 6.12 mg/100 g of edible part, and it is higher than other animal and plant foods; this information is notable in the case of physical activity because these amino acids are an important energy source in muscles, promoting protein synthesis and preserving the muscle protein mobilization. The branched amino acids are then responsible for the brain serotonin synthesis inhibition, responsible for the precocious fatigue sense onset (Arsenio et al., 1996).

Lipids

The GP and TN are cheese with an average lipid content of 28.92% and 41.28% on the edible part of the dry matter content that is mostly represented by triacylglycerols; the free fraction of these (3.5% of total lipids after 10 months) is an excellent source of readily available energy. From the fatty acid profile point of view, the unsaturated fatty acid that is most represented is the oleic acid followed by palmitic acid even if prevails the saturated fraction. However, in this latter fraction, there is a good presence of stearic acid which, being easily unsaturable to oleic acid, can be considered as nutritionally unsaturated, but the corresponding desaturase decreases its activity after the 35th year of life. In addition, the saturated fatty acids up to 10 carbon atoms are used for energy purposes, therefore they does not necessarily have negative connotations. Saturated fatty acids having a recognized role of increase the cholesterol level are lauric acid (C12:0), palmitic (C16:0), but above the myristic (C14:0) (Kris-Etherton & Yu, 1997). According to the INRAN database, myristic acid represents only 2.7% of the cheese such as, while there is a higher presence of palmitic (7.3%) and negligible is instead the lauric acid (0.8%). From this point of view GP cheese has a beneficial fatty acid nutritional profile. As for the cholesterol content, it is equal to 150 mg / 100 g of product. Assuming an ingestion of 50 g of cheese, this quantity represents about 40% of the daily permitted for that molecule (300 mg/day). Important is the conjugated linoleic acid (CLA) content, a family of molecules which both *in vitro* (Parodi, 1999) and on animal models (Ha et al., 1987; Ip et al., 1994) showed anti-tumor properties, directed towards the breast cancer and the colon cancer. Among the epidemiological studies, the Scandinavian study, showed that a consume of two dairy product servings with high fat content causes a reduction of 13%in tumor incidence, in the district colorectal (Larsson et al., 2005). On animal models, a small concentration of 0.5 g kg^{-1} is already widely effective in reducing cell proliferation, differentiation and/or apoptosis of breast cancer cells, as evidenced figure 5. The reduction in fat mass and the increase in lean body mass, the protection from atherosclerosis, the angiogenesis control and the insulin resistance prevention, were other beneficial actions.

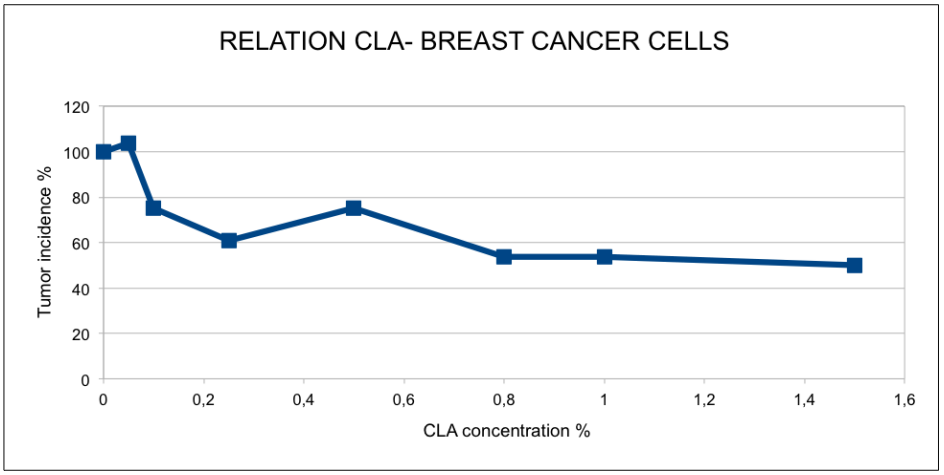

Figure 5. Relation between CLA and breast cancer in rats.

Calcium and vitamins

GP and TN are characterized by high calcium bioavailability (see table 3) (Magnano et al., 2011); assuming an intake of 50 grams of cheese/day, the intake of this mineral is around the middle of the daily requirements for a adult healthy. A survey from the INN (INN. Tabelle di composizione degli alimenti, (1994) Roma) the contribution of dairy products to the total intake of calcium is approssimately of 70%, of this 28.3% is provided by cheeses such as TN or GP, with lipid title of 20-30% on a wet basis.

Recent study show that the segment population from 18 to 29 years is characterized by a diet rich in lipids, also favored by a high intake of dairy products. In this situation, the consumption of foods with high ratio Ca^{+2}/lipids as Grana cheese, is favorable to achieve an equilibrium between a fat and calcium content. The GP and TN are cheeses with higher content of calcium per gram of fatty substance and are also foods with higher value ratio Ca^{2+}/energy.

Food	Ca^{2+} (mg)/energy (kcal)	Ca^{2+} (mg)/lipids (g)
Grana cheese	3.07	40.95
Nuts	0.28	2.92
Beans	0.44	54.80

Table 3. Ratio between Ca^{2+}/lipids and Ca^{2+}/ Energy in some foods with abundant calcium content (effetti benefici del formaggio GP D.O.P. nella dieta dello sportivo, adapted).

The high calcium availability in GP can increase the mobilization rate of adipose tissue (Zemel et al., 2004). This is important to reduce the chronic inflammation, that is induced by the accumulation of adipose tissue in the abdomen, and that is one of the main causes that contribute to the metabolic syndrome onset. This abdominal adiposity is often associated to the insulin-resistance, and it is caused by a greater synthesis of JNK-1. This latter, in an abnormal way, induces the Insulin Receptor Substrate (IRS) phosphorylation, reducing the affinity for the insulin.
The integrity maintenance of the skeletal system is important in order to prevent injuries of varying nature and the diet, by providing minerals and vitamins, strongly influences the bone tissue health. Particularly critical is the formation of a high and early peak bone mass (maximum density and maximum hardness) that normally occurs in the second decade of life; After this age, the bone resorption prevails on bone mineral matrix apposition (Matkovic et al., 1990). Osteoporosis is characterized by low bone mass and by deterioration of bone microarchitecture. The factors that increase the bone mass are different and they are associated in various ways in the individual subject:

• genetic factors and family history, hormonal factors (estrogen and androgens, growth hormone);

• nutrition (Ca^{2+} intake, vitamin D and probably vitamin C and K);

• lifestyle (physical activity, exposure to UV rays, smoking, excessive consumption of coffee);

• congenital diseases, chronic and prolonged pharmacological treatments (corticosteroids).

There is a bone density level above which no fractures occur and below which instead the incidence increases progressively; this value is called "fracture threshold". Although, a diet with an adequate amounts of Ca^{2+} is fundamental, but there are many disagreements about the real amount to be introduced; according to the new RDAs both sexes in adulthood should take 1000 mg/day of calcium, which would increase to 1200 mg/day after 60 years of age, with no further increases for women in menopause. There are several studies that have shown that a pediatric calcium increase allows to reach a bone mass higher peak in young age (Riggs et al., 1987; Matkovic et al., 1990). Calcium supplementation with high bioavailability as that contained in the GP and in TN, play a primary role in achieving that peak (Matkovic et al., 1979), even taking Grana Padano prepubescent would have a greater effect on bone density than the single calcium supplementation (Chan, et al., 1995; Creff & Bernard 1984). This result was attributed to the fact that the grain cheeses have in addition to high content of calcium also other elements (magnesium, sodium, vitamin D, etc).
The calcium is closely related to vitamin D. In fact, this latter influences the calcium absorption and its metabolism. It is shown that the active form of this vitamin also acts on cell growth. It induces cell apoptosis and cell involution with chromatin condensation and DNA fragmentation; also it has a specific role in the mammary gland differentiation (Moorman et al., 2004). There are several studies that show a significant inverse relationship between calcium intake and cancer only at high level of vitamin D (Cho, 2004). Regarding the need for vitamin D, set to be around 10-15 mg/day, an intake of 50 g of cheese can satisfy 1.8-2.7% of the daily requirement. However, there is a correlation between

vitamin content of the starting raw material and that into the finished product, and this especially for fat-soluble vitamins that remain bound to the lipid fraction.
The GP and TN cheeses are also an excellent source of vitamin B12. In fact, a portion of 50 g is able to coat 75% of the daily requirement of an adolescent or an elderly person; this figure is also particularly interesting for those people who follow a vegetarian diet for which the intake of this vitamin is difficult. Regarding other vitamins, the contributions do not appear to be particularly high.
In view of all these benefits, there are also some potential negative effects.
It is known for some time that, the high salt (NaCl) consumption, is considered one of the main risk factors associated with the hypertension development, typical disease of industrialized countries reaching values up to 20% in the adult population. The damage that can achieve a high blood pressure consist of vascular disease, damage to the heart (heart failure, heart attack), kidney (renal failure), brain (stroke) and eyes (hemorrhages, retinitis etc.). Damage can occur after several years into the disease and it is favored by other risk factors such as diabetes, smoking, obesity and excessive cholesterol in the blood.
The Grana Padano consortium has been active on this front with a Na content reduction, from the original 2 g/100 g to 1.6/100 g. Table 4 shows the Na content of the main cheese consumed in our country.

Cheeses	Sodium content (mg) of 100 gr of edible product Source: IEO	Content compared with Grana Padano
Pecorino Romano	1890	+290 mg
Asiago	760	-840 mg
Montasio	757	-843 mg
Fontina	686	-914 mg
Fiordilatte	200	-1400 mg
Crescenza	350	-1250 mg
Gorgonzola	600	-1000 mg

Table 4. Salt (NaCl) content in the main Italian table cheeses and respect to the GP.

Cholesterol and fatty acids

There are various dietary guidelines that emphasize the reduction of cholesterol and trans fatty acids. This is important in order to reduce the occurrence of cardiovascular disease (CVD) in humans; on the basis of these assumptions the food industry created a range of foods low in fat content among which different types of dairy products. Dairy products are an important quantitative and qualitative source of lipids and this characteristic is the reason why, to date, a definite correlation between dairy consumption and effects on cardio-vascular health has yet not found. In addition to genetic factors, it is important to consider when assess the effects of the consumption of milk and dairy products, food style and the level of disaggregation of dairy products which can be considered as a group indistinct or split in function of the product type or the fat content.
The consumption of dairy products (and therefore, of cheeses) highlights two contrasting aspects: intake of cholesterol and saturated fatty acids (SFA) vs. content of conjugated linoleic acid (CLA) and peptides ACE inhibitors. If the first is surely associated with negative events charged to the district cardio-vascular system, for the second several studies show, in direct and indirect way, a protective action in load of the circulatory system. The inverse relationship between consumption of cheeses (without distinction of fat content) and CVD has been highlighted only for the female sex, probably because women consume a lower quantity of these products. Literature has evidenced that the rapport between consumption of dairy products and effects on cardiovascular health is influenced by the provision in saturated fatty acids (Hu et al., 1999) and by the diet in which the dairy are inserted . A study clearly show that fats derived from milk increase LDL large and sparse, with low potential atherosclerosis (Sjogren et al., 2004).
If we consider the role of saturated fatty acids, it can be noted that a decline in the recruitment of these components implies a decrease in the incidence of CVD, but only when the SFA are "replaced" by polyunsaturated fatty acids (PUFAs). While the integration with carbohydrates causes no positive effect and also, increasing the share of triglycerides and the small and dense LDL fraction (predictive of CVD risk), increments the risk because it implies a reduction of the HDL cholesterol. Actually, it's important to say that different saturated fatty acids have several feeback on cholesterol levels: stearic acid (18:0) has no effect on cholesterol when compared with the monounsaturated oleic acid (18:1), while the fatty acids with small dimensions like myristic acid (C14) or palmitic acid (C16) tend to increment the plasma level of cholesterol and LDL.
This explains the reason why the consumption of dairy products is not clearly related to deleterious actions on the cardiovascular system, even if cheeses are important sources of SFA and cholesterol.

Allergy Lysozyme: Lysozyme is a protein of 14.3 kDa formed by a single chain of 129 amino acids that can be found in egg white and in human saliva. Thanks to his proven antibiotic action it's used in the processing of the GP, because this enzyme is able to hydrolyzing the link β (1-4), glycosidic that connects the N-acetylmuramic acid residues of the polysaccharides constituting the wall of Gram positive, (Proctor et al., 1988) and consequently to prevent the late swelling of cheeses, caused by the spore germination of Clostridium and Clostridium tyrobutyricum butiricum during the maturing [F. Wasserfall, M. Teuber. Action of egg white lysozyme on Clostridium tyrobutyricum; Appl. Environ. Microbiol. (1979) 38: 197]. The Lysozyme is legally permitted as an additive in the production of cheese (European Parliament and Council Directive No.95/2 /EC) with doses of 25-30 mg/l of milk, corresponding to about 300-350 mg/kg of finished product (Bottazzi et al., 1999; Bärtschi et al., 2006); in the GP this concentration is reduced, because it is present in a quantity of about 155 mg / Kg. Even if it derives from egg, food able to produce allergic reactions especially for children in pediatric age (8-58% of individuals sensitive to egg are sensitive also to the lysozyme) (Bishop et al., 1990) to date there are few and controversial evidence about the allergenic role of this substance, as a result of consumption of GP (Iaconelli et al., 2008). It seems that the attack by proteolytic enzymes active during the maturing of cheese could lead to a reduction in the presence of active lysozyme (or better, to a reduction of its epitopes) in the finished product (Rossi et al., 2011; Polverino de Laureto et al., 2002) or else the same Lysozyme is able to give life to conformational isomers during the maturing (Schneider et al., 2011). About this, we report some results of several studies effectuated on children in the pediatric age (Marseglia et al., 2012) and adults (Rossi et al., 2011).

In the first study, 21 children have subjected to a test of oral stimulation with increasing amounts of GP and TN matured at 12 and 24 months in order to assess if individuals allergic to egg protein could also be allergic to lysozyme in GP. The results proved that when individuals sensitive to egg white assumed the GP of 12 months, in a small number of them occurred both immediate and long-term allergic reaction; in particular itching, nausea, abdominal pain, vomiting, dermatitis, rhinitis, bronchial asthma, urticaria and angioedema. These events decreased with the assumption of GP with 24 months and when the children considered where not sensitive to lysozyme. The authors of this study have concluded that a possible relationship between the severity of the allergic reactions and the amount of IgE-specific lysozyme is possible only when this level is greater than 7 kU/l in accordance with the data of H.A. Sampson, D.G.Ho. [H.A. et al., 1997; Celik-Bilgili et al., 2005) and that the seasoning of the product can act positively against this problem, because it's probable that lysozyme itself is affected by a sort of hydrolysis of its epitopes. In the study of 25 adults sensitive to egg protein were analyzed in order to assess the response, both in terms of clinical and immunological, to the somministration of 30 g of GPs and TN of 16 and 24 months of age (Rossi et al., 2011). The results reported by the authors have shown no allergic reaction and variation in the level of IgE "lysozyme-specific" when equivalent to basal level, equal to100. The assumption of the GP with 16 months did not cause changes in levels of IgE and IgA when compared with the levels found for the TN 16 months. A significant relationship between IgA and IgE has also been observed when the GP was provided to patients sensitive to lysozyme, confirming that this molecule is able to cross the blood barrier. In the complex, therefore, no adverse reaction was recorded after ingestion of the GP compared to TN. By the metabolic point of view, ingestion is followed by a rapid absorption (peak plasma within 1 h) and rapid decrease with reset of the dose within 48 h after (Hashida et al., 2002).
Lysozyme in GP does not seem to constitute a danger for adults and for children while there is a risk, even if it is limited, in the children sensitive to albumen but we must not forget that, however, in pediatric age allergenicity due to the protein in cow's milk and, in particular β-lactoglobulin (60-80% of cases), casein, α-lactalbumin and serum albumin is the most common.
Both works underlined also a consistent presence of biogenic amines, with prevalence of histamine; it is known that the possible adverse effect of these substances on the organism (dermatitis, urticaria) and that the concentration tends to increase with the increase of the months of ripening, it is possible that their presence is correlated to the activity of lysozyme that, modifying the proteolytic microflora, could determine a variation in the levels of biogenic amines (Neviani, 1994).

Ripening and lysozyme effects on main food components of grana cheeses

The Grana cheese is a product which is characterized, from the biochemical point of view, for the succession of complex hydrolytic events which manifest themselves both in load of its components and of their derivatives. The analysis performed on multiple samples of GPs and TN to different months of ripening (10-25 months) has revealed that the Ca content does not drop too much, indeed tends to remain constant over time, at values of around 0.85-0.9%, as it can be seen in the chart below.

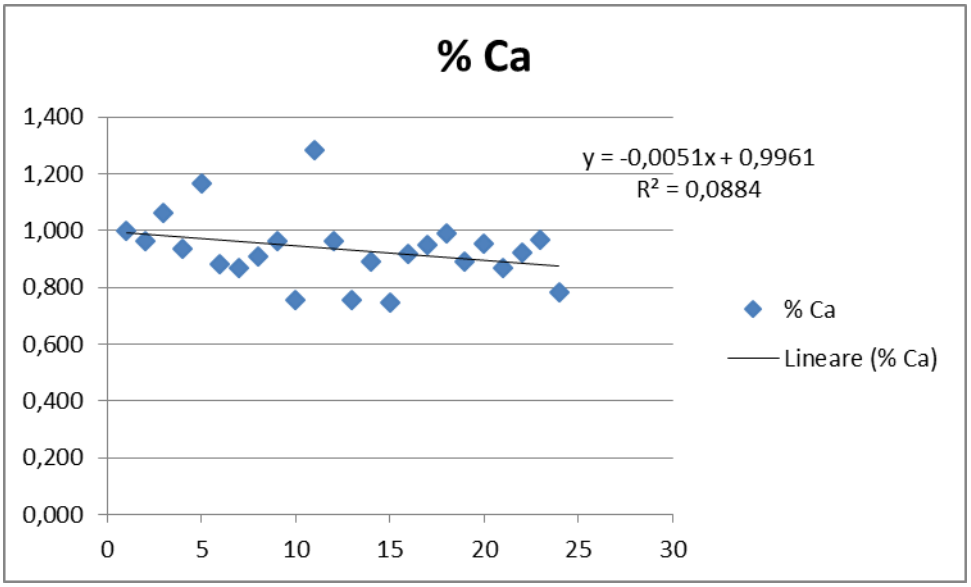

Figure 6. Calcium content variation in GP and TN at different months of aging (data provided by the Institute of Nutrition- facoltà di Agraria, UCSC Piacenza).

Regarding the sodium, it is known that during the ripening occurs the formation of crystals, the individual rather than in the form of aggregates, based on calcium phosphate, calcium lactate, sodium chloride and tyrosine that differ in their dimensions, structure and moment of formation (Bianchi et al., 1993; Bottazzi et al., 1993). The first crystals, calcium phosphate, has been identified at the end of the fermentation process that is performed by the thermophilic lactic microflora (Streptococcus thermophilus, Lactobacillus delbrueckii subsp. Delbrueckii, Lactobacillus delbrueckii subsp. Lactis, Lactobacillus helveticus) and consist in globular masses, with a porous external appearance, irregular surface and a diameter of between 8-10 µm and µm up 15-20. These crystals are limited to the first 48 hours of making cheese; in fact, during the progress of the ripening period and seasoning, it was observed any significant increase in the volume and number of crystals. Other types of needle-like crystals of the property have been highlighted; these clusters become visible to the naked eye at the end of seasoning when, reached the size of 100-150 pm, they form white granules, friable, sandy. Formations of this type, based on calcium lactate, representing a typical character of the cheeses grained, only if they do not present themselves in a number too high. At the maturation end, appears another crystalline formation of 0.3-0.5 cm in size, the color is gray with a slightly greenish, consistency and lack of bitter taste on the palate. Such structures are granules of Tyrosine, easily removable from the paste and which sometimes is accompanied by the presence of aggregates of NaCl visible to the SEM (scanning electron microscope) (Bottazzi et al., 1994). The sodium chloride content of cheese is expressed both on a wet basis (in relation to 100 g of cheese) that in relation to the cheese moisture content; this last value is representative of the salinity of the aqueous phase in which are enzymes involved in chemical and biochemical processes responsible for the cheese ripening. The NaCl content in the aqueous part increases in sudden manner in the step of "extraction of the cheese mass" from the boiler (0.10 g/100g) to the first month of age (2.64 g /100g), that is shortly after the exit from the brine. With increasing age of the cheese can be observed a salt concentration increase in the aqueous phase, up to reach values of 4.11- 7.84 g/100g of cheese at 12-96 months of ripening respectively. The trend observed is related to the lost of moisture that the cheese undergoes during ripening (Malacarne et al., 2006).

The proteolysis of casein is considered to be one of the main events that determine the typical sensory characteristics and the quality of aged cheeses GP and TN. Excluding the k-casein that participating in the process of cheese making is not present, during the curing process the residual milk proteins (β caseins, αs_1, αs_2) are subjected to degradation by proteases typical of the milk (plasmin), the rennet (chymosin and pepsin) and the proteolytic enzymes (carboxypeptidase and aminopeptidase) released from lysed cells of LAB (lactic acid bacteria) (Fox et al., 1996; Gatti et

al., 1999). After their action occurs a decrease in the protein content which in the marketed product reaches the 10-15% of the departure content (Addeo et al., 1992; Ferranti et al., 1997). In fact is known that in the GP aged for 12 months the average content of free amino acids (FAA) increases up to values of 18.28 to 22.16 %. In the following months, probably for the prevalence of the degradation process, these values remain similar. Thus ASN (asparagine) and GLN (Glutamine) declined by deamination ASP (aspartic acid) and GLU (glutamic acid), while the serine content steadily increases (Resmini et al., 1993). This behavior is not standardized, because it has been seen that cheeses with different ages may contain similar quantities of amino acid, while beetwen samples with the same age amino acid content may undergo variations; for all these reasons, the content of FAA is not a valid index to determine the age of the product (Resmini et al., 1993; Masotti et al., 2010). The variability appear to be due to the microbial composition of the whey used in the various dairies (Rossetti et al., 2008) as well as to slight differences in the characteristics of the milk, in the processing technology and in the ripening conditions that occur throughout the year (Choisy et al.,1997). The peptide fraction contained in Grana cheese can be divided into three different categories: oligopeptides, phosphopeptides and large nonpolar peptides. As for the main oligopeptides it is interesting to note that Grana Padano, Parmigiano Reggiano and Grana Trentin have a very similar composition, probably because they have the same enzymes. However, the evolution of the peptidic fractions during ripening is typically distinguished between the three cheeses: the oligopeptide content of Grana Padano derived from αs and β casein is relatively low in the first month of ripening, after it increases (from 10 to 16-19 g/kg cheese) between the 4-8 and 14-38 months of maturation to settle back down or even slightly decrease (Resmini et al., 1996; Ferranti et al., 1997). In the Parmigiano Reggiano and Trentin Grana the amount of oligopeptides is lower and has a less regular pattern. The reason for this different behavior can be attributed to the different techniques of production but also to the different proteolytic activity; GP seems to be faster because of lysozyme that, anticipating the lysis of LAB promotes the release of cytoplasmic enzymes for degrading activity. The rapid identification of oligo peptidic pattern is now possible by several chromatographic techniques, as reported by several authors (Ferranti et al., 1997; Sforza et al., 2003); Table 5 is displayed a typical pattern composition; this allows to advance considerations on the curing time of the product even though then the actual amount of peptides differs when samples of the same age originate from different dairies. It can be assumed that small differences in making cheese technique induce strong variability of fat percentage, thermal parameters, etc. leading to changes in proteolytic events and lipolysis occurring during cheese ripening.

Peptide molecular weight (Dalton)	Identification
260	Glu-Leu (o Ile)
294	Glu-Phe
1348	βCN (16-25)3P[c]
1703	βCN (16-28)3P[c]
1870	βCN (15-28)4P[c]
2764	α_{s1}CN(1-23)
1707	α_{s1}CN(24-38)
1237	α_{s1}CN(24-34)
4238	α_{s1}CN(80-114)
3860	α_{s1}CN(83-114)
3602	α_{s1}CN(85-114)
1881	βCN(193-209)

Table 5. GP peptidic composition, identified by chromatography column ESI-MS (Sforza et al., modified).

Another consideration is the oligopeptides produced by the plasmin action: these peptides are found in both types of cheese and their presence is permitted also by thermal inactivation of Chymosin (Sforza et al., 2004). The plasmin, the main among proteases present in milk, has an important role as it acts on the distribution of β-casein and αs2 (Grufferty et al., 1988); this activity seems to be at least up to 16^{th}-24^{th} month of ripening (Sforza et al., 2003). The plasmin hydrolysis of the β-casein (composed of 209 amino acids) leads to the formation, at pH values of 4.6, Y of caseins (Y1-

Y2-Y3) corresponding respectively to the polypeptide fragments 29-209, 106-209, and 108 -209 containing the portion COOH of β-casein (Eigel et al., 1979; Gaiaschi et al., 2001). The peptides complementary to Y caseins contribute to forming the so-called "proteose-peptone fraction" of the milk (Andrews et al., 1983), responsible for the majority of the peptides of low molecular weight resulting from β-casein, which are found in seasoned cheese for long period (Addeo et al., 1992; Addeo et al., 1994).
In a GP seasoned 14 months, there is a series of phosphopeptides which derived from the peptide "β-CN f7-28 4P" (deriving from the hydrolysis of the β native casein, containing four residues phosphorylated serine) (Ferranti et al., 1997). Mainly, there are two conditions that, acting in opposite directions, can influence the amount of such phosphopeptides in the GP: the action of plasmin and its enzymatic degradation by microbial protease. The effects of the proteolytic activity of microbial origin become relevant in an advanced stage of cheese ripening (16^{th}-18^{th} month of seasoning) balancing the formation of the peptide due to hydrolysis of the bond Lys28 Lys29 of β-casein by plasmin. At the decrease of β-casein content is associated the increase of its peptidic fractions that become evident, respectively, at 15^{th} (Y1) and 22^{th} (Y2 -Y3) months of ripening (Addeo et al., 1995; Gaiaschi et al., 2001) in particular, if casein Y1 increases at the beginning of ripening and then decreased with the progress of proteolysis, Y2 Y3 remain constant over time (Masotti et al., 2010). Since the hydrolysis of β-casein by plasmin is a significant event, the Y casein may be considered as one of the main parameters useful to assess the cheese age and then, its quality (Addeo et al., 1995; Restani et al., 1996).
As regards the caseins αs1 (199 AA) and αs2 (207 AA), are three polypeptides which are derived from degradation by the chymosin and plasmin:
α_a fragment corresponding to amino acid 24-199 of casein αs1;

• α_b represent the fragments 35-199 of αs1 casein and the amino acid 25-188 of casein and casein αs2;

• α_c detectable with the 80 to 199 amino acid fragment derived from casein α_s.

Their formation takes place early and then it take different performance from the 4^{th} month of seasoning. It been shown that if the fragment αa decreases (from 3:38 ± 0:54 g/100g of cheese on the 4^{th} month to 1.23 ± 0.37gr/100 grams of cheese at 22^{th} month) due to early thermal inactivation of chymosin (active mainly on location 23-24 dell'αs1-CN) (X) (xxx), the fragment αb remains constant (2:47 g/100 g of cheese) because there is a constant balance between formation by hydrolysis of αs1casein and cleavage to shorter peptides; the fragment αc increases during aging because of the action of plasmin (1.95 ± 0.75gr / 100g of cheese on the 4^{th} month in 3.28 ± 0.19gr / 100g at 22^{th} month.

Compositional differences are also observed when comparing the crust and the dough of grana cheese: the total content of free amino acids present in the crust is 5-10% lower when compared to the average content of amino acids of the dough. This is due to a slowing down of the proteolytic processes in the most superficial part of the shape due to the reduced moisture content. The slowdown of the proteolytic activity is manifested by the accumulation of high molecular weight peptides and the presence of still intact casein fractions (fraction αs2) that, by contrast, they are rapidly degraded in the remainder of the form (Pellegrino et al., 2003). This confirms that the ripening o cheese a long period of maturing takes place in centripetal direction and leads to the appearance of a typical peptide pattern, useful to advance any considerations about the content of the crust in the grated parmesan cheese where the same can be present in precise amounts (maximum 18% of the total- DPCM 1991).

Decarboxylation of amino acids and biogenic amines

Biogenic amines are nitrogen compounds that are formed as a result to the decarboxylation of amino acids or to amination and transamination of aldehydes and ketones. The chemical structure of biogenic amines can be aliphatic (Putrescine, Cadaverina, spermine, Spermidine), aromatic (tyramine and phenylethylamine) or heterocyclic (Histamine and Tryptamine). Among these compounds, some have a key role in cell life, other (Histamine, Putrescine and Tyramine) at high concentrations can be toxic to humans; in addition, by reaction with nitrites, histamine can form nitrosamines that have carcinogenic properties.

In the cheeses, the amine formation occurs as a result of enzymatic decarboxylation by lactic acid bacteria (Santon, 1996); even the level of such compounds can reach, in cheeses ripened for a long period or products in not optimal hygienic conditions, extremely high values in the order of 1000 ppm (Fernandez-Garcia et al., 2000; Cerutti, Tecniche Nuove, Parma, 63). The quantity and quality of amine present are also conditioned by:

- availability of free amino acids,
- the presence of microorganisms capable of synthesizing decarboxylated enzymes: it is essential the microflora selection in order to better govern the process
- conditions of temperature and pH suitable to their development,
- from the salt content of the cheese as well as by specific essential cofactors to the enzymatic activity (Middlebrooks et al., 1998).

In addition, the hygienic quality of the starting milk is fundamental, because with a high lactobacilli, streptococci and Enterobacteria content, is possible to obtain a cheese with a high amine level (Edwards & Sandine, 1981).

Influence of Lysozyme

Lysozyme and aging period, can influence the cheese oligopeptidic pattern. For this reason, calcium milk product digestibility is greater than that of the plants. In a recent study (Rossi et al., 2011) it showed that there is a positive correlation between the presence of lysozyme, peptide content and calcium digestibility. In fact, TN cheese samples showed values of digestibility lower than GP samples at the same maturation degree. This observation was also justified recalling the proteolytic action of lysozyme against cheese casein (the main protein calcium associated). The Lysozyme activity is responsible of the presence of a larger number of peptide residues calcium associated with a molecular weight of 1000-2500Da in GP respect to TN.

Fat

The fat component of cheeses at medium and long aging period, such as GP and TN, determine the structural and rheological properties of the dough; the fat lipolysis of GP and TN cheese is due to the combined action of lipolytic enzymes of different origin, but in particular by the lipase of lactic acid bacteria. These microorganisms release different amount of fatty acid from which, through mechanisms of degradation derive low molecular weight compounds that contribute to the flavor. The free fatty acids content (FFA) increases gradually and regularly throughout the curing cycle. The lipolysis index (FFA mg/100 mg of total fat) is positively correlated with the age of the cheese but negatively with the moisture content and pH. The breakdown for the individual FFA on the total content does not show significant variations even if palmitic acid, which at the beginning of seasoning makes up about 30% of the FFA, tends to decline in parallel with the increase of oleic acid (22%); also butyric acid, relatively low at the beginning, tends to increase during aging (Sandri et al., 1997). A greater degree of lipolysis of the fatty acids with a short chain (C4-C8) compared to long chain (C16-C18) was also recorded (Sandri et al., 1997; Malacarne et al., 2006). The lipolytic activity intensity can vary in relation to different factors such as enzyme concentration, pH, temperature, water activity, salt content, etc. However, at beginning the salt should not inhibit the lipolysis significantly, on the contrary to what occurs for the proteolysis. Lipolysis is also influenced by the cheese ripening time, by storage and all procedures that interfere with the maturation processes (Collins et al., 2003).

SMALL INTESTINE

STRUCTURE OF THE SMALL INTESTINE

The small intestine originates from the pyloric valve that separates the stomach and ending with the ileocecal valve that connects to the large intestine; it are compose by two portions: the duodenum with a horseshoe shape, where open into the ducts from the liver and pancreas and jejunum-ileum (also called portion mesenteric) fully covered by the peritoneum. The small intestinal mucosa is characterized by folds, villi and microvilli that increase the absorbing surface (Arienti, 2010). It is bounded to the intestinal lumen by a continuous monolayer of epithelial cells coupled together by specialized protein structures called tight junctions (TJ); the latter are involved in the paracellular transport, as they form small pores which permit the passage, from the intestinal lumen into the interstitial space, of small hydrophilic molecules such as minerals including calcium, amino acids and polypeptides (Mariani et al., 2006). All along the gastrointestinal tract epithelium, which is the interface between the inner and outer cellular environment, rests on a basement membrane and is supported by a complex of well-organized connective tissue (lamina propria) consisting of fibroblasts, blood vessels, lymphatic vessels, nerves and smooth muscle cells. The epithelium of the intestinal villi (finger-like protrusions of the mucosa) is composed mainly of enterocytes, highly specialized cells that allow the transport functions of nutrients released during digestion, from the intestinal lumen into the bloodstream. The enterocytes present, from the histological point of view, a luminal membrane raised in lowercase and digits called microvilli which together confer to the mucosa the appearance of a brush; for this reason, it is alluded to such a structure with the name of brush-border (brush border) (Arienti, 2010). The small intestine is therefore the main site in which thanks to the microvilli, occurs the mixing of the intestinal contents, secretion exo / endocrine, metabolic transformation and absorption of nutrients. Other epithelial cell types present, in addition to the absorbing enterocytes are the stem cells of the crypts, mucus goblet cells, enteroendocrine cells and the cells that produce antimicrobial proteins (Paneth cells). In Figure 7 it is shown the morphological organization of the small intestine.

Absorptive Enterocytes

Absorptive enterocytes are polarized epithelial cells that have, on the apical surface of the plasma membrane, a specialty called brush border (or brush border). The brush border is a structure consisting of microvilli, fingerlike protrusions of the cytoplasm, coated from the plasma membrane and closely adjacent between them. Each human enterocytes of the small intestine has about a thousand-three thousand microvilli and their presence increases the absorbing surface. The collection of microvilli, villi and circular folds are estimated to increase the inner surface of the small intestine up to 200 m^2. On the surface of microvilli it is present the glycocalyx, a dense network of long polysaccharide chains which, besides performing a protective function of the cell membrane, possesses enzymes able to influence digestive processes. The main functions performed by these highly specialized cells are the digestion of nutrients in the intestinal lumen, thanks to the presence, at the level of the microvilli membrane, of various hydrolytic enzymes, and the absorption of nutrients, thanks to the presence of several proteins channel and carriers used for their absorption. (Castano et al., 2008; Colombo.& Olmo 2007; Shimizu, 2010).

Mucus Goblet cells (or Goblet Cells)

These cells are capable of producing the mucin, a dense substance formed by glycosaminoglycans, proteoglycans and glycoproteins that, once secreted, hydrates and becomes mucus, whose function is to lubricate and protect the intestinal epithelium trapping any pathogens. Goblet cells, together with the absorbing enterocytes, are the two main cell types present in the villi (Castano & Donato 2008; Colombo & E. Olmo 2007).

Paneth cells

These cells are found on the bottom of the crypts of Lieberkühn and produce glycoproteins, including lysozyme, which has an antibacterial effect (Castano & Donato 2008; Colombo & E. Olmo 2007).

Enteroendocrine cells

These cells are part of the endocrine system and the enteric secrete hormones such as gastrin, cholecystokinin, secretin and serotonin (Castano & Donato 2008; Colombo & E. Olmo 2007). These hormones are involved in the modulation of the digestive process.

M cells

The M cells have the ability to internalize antigens present in the lumen of the digestive system and to welcome in deep introflections on the opposite side of B and T lymphocytes, dendritic cells and macrophages. M cells are found in the gut epithelium at particular lymphoid aggregates called Peyer Plaques that are part of the MALT (mucosa-associated lymphoid tissue). The role of the MALT is to ensure the humoral immune response and cell stimulations resulting in local. (Castano & Donato 2008; Colombo & E. Olmo 2007).

Stem cells

They are pluripotent cells that are the source of all epithelial cells in the crypts and villi. These cells are found at the base of the crypts of Lieberkühn and divide continuously to cope with the rapid replacement of the intestinal epithelium that occurs approximately every 3-5 days (Castano & Donato 2008; Colombo & E. Olmo 2007).

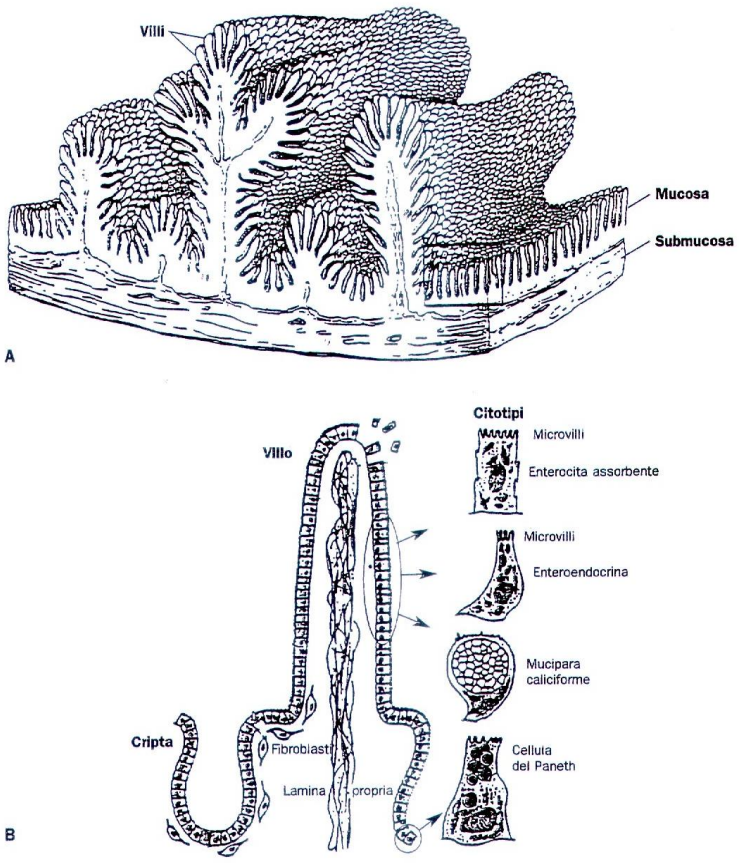

Figure 7. A) Three-dimensional structure of the small intestine; B) cell types present in the gut epithelium and their location (Figure taken from AM Costantini et al., 2006).

The transport of a substance from the lumen through the epithelium can occur by different routes:

- transcellular, by diffusion across the apical membrane, the cytoplasm, the basolateral membrane;
- paracellular pathway through the tight junctions;
- transcytotic mediated via interactions with specific receptors on the apical membrane, internalization into vesicles that migrate through the cytoplasm with release of the contents across the basolateral membrane, on the opposite side of the cell;
- via mediated by specific transporters that allow the internalisation across the apical membrane and / or the efflux across the basolateral membrane.

Functions of the intestinal epithelium and interaction with nutrients

Thanks to the presence of different cell types, the intestinal epithelium is able to perform four important functions: barrier, signal transduction, digestion and absorption of nutrients.

Barrier

The first function of the intestinal epithelium is to form a barrier between the intestinal lumen and our organism. This can be classified as physical barrier and biological barrier. The first includes the presence of a junctional complex between the different cell types of the intestinal epithelium, essential to the integrity of the epithelium. This physical barrier is formed by tight junctions, junctions anchors wing, desmosomes and gap junctions. In particular, the tight

junctions are the main responsible for the paracellular permeability and they promote the passage of ions and small hydrophilic molecules but, at the same time, they form a physical barrier to the passage of large molecules, bacteria and food antigens. On the contrary, the biological barrier is composed of a large detoxification system, by the ability to carry Immunoglobulin A (IgA) and to secrete antimicrobial peptides capable of inhibiting the invasion of the body by pathogens and toxic compounds (Shimizu, 2010).

Recognition and signal transduction

The enteroendocrine cells, localized in the intestinal epithelium, possess receptors capable of recognizing the presence of nutrients in the lumen. The recognition of these nutrients activates the production and secretion, on the basolateral side, of different types of hormones capable of modulating the digestive processes, as well as the onset of satiety. In addition, the enterocytes possess different Toll-like receptors able to recognize and bind bacterial components such as the lipolisaccaride (LPS), peptidoglycan and flagella. These bonds are able to trigger signaling cascades that lead to the production and secretion of multiple biological compounds including the inflammatory cytokines. Then the cells of the intestinal epithelium are able to transform the signals arising from the intestinal lumen into signals within the organism. (Shimizu, 2010).

Digestion

The main digestive function of the small intestine is carried out by the pancreatic enzymes and bile that are secreted in the duodenum. Enterocytes present, the level of the membrane of the microvilli, various hydrolytic enzymes are deputies mainly to the terminal digestion of macronutrients in the diet. This digestion permits the release of nutrients into a suitable form for absorption.
The various hydrolytic enzymes and the functions they carry out are summarized in Table 6.

BRUSH BORDER ENZYMES	MAIN SUBSTRATES AND THEIR ACTION	PRODUCTS
Maltase-Glucoamylase	Oligosaccharides up to 9 residues; cleaves α-1,4 glycosidic bond	Glucose
Sucrase-isomaltase	Sucrose and branched oligosaccharides; cleaves α-1,4 bonds and α-1,6 non-reducing end	Glucose and fructose Glucose
Lactase-Phlorizin hydrolase	Lactose hydrolyzation	Glucose and galactose
Trehalase	Trehalase hydrolyzation	Glucose
Enteropeptidase	Trypsinogen activation by proteolytic cleavage	Trypsin
Aminopeptidase	Peptides; cleaves the N-terminal aminoacid bond	Amino acids, peptides
Carboxypeptidase P	Peptides; cleaves the C-terminal proline	Amino acids, peptides
Endopeptidase	Peptides	Peptides
Dipeptidases I and II	Cleavage of peptides containing methionine, and glycine	Amino acids
Alkaline phosphatase	Dephosphorylation of different phosphorylated substrates	Dephosphorylated molecules

Table 6. Description of key hydrolytic enzymes present in the enterocytes brush border (Table is modified by Salvatore F. (Salvatore, 2013), Ganong WF et al. (Ganong & Barrett, 2005) and by R. Holmes et al. (Holmes & Lobley, 1989).

Digestive enzymes

The enzymes involved in the digestive process are the endopeptidases and the exopeptidases that cleave polypeptide chains into fragments, attaching them respectively in correspondence of some specific amino acid residues (gastric pepsin) rather than starting from the amino or carboxyl end. They are different peptidase at level of the enterocytes brush border (peptidase Microvillous), besides the hydrochloric acid (which mainly function denaturant), pepsin (in the stomach) and pancreatic enzymes (pancreatic carboxypeptidase and endopeptidase) and they cut the longer peptides. These enzymes present specific function for the substrate on which they operate (table 6). The peptidases show a cytoplasmic and external distribution indicating that the larger oligopeptides are hydrolyzed on the microvillar membrane, while and tri-peptides are partially hydrolyzed on the membrane and in part absorbed as such. Of this latter, the majority is hydrolyzed in the cytoplasm, and it passes to the bloodstream as amino acids, with a few peptides not cleaved (Mariani et al., 2006; Rinni et al., 2006).

Amino acids detachment of 3-8 aminoacids from the C-terminal peptide end

Brush border peptidases	Action	Products
Oligopeptidase (different types)	Amino acids detachment of 3-8 aminoacids from the C-terminal peptide end	Amino acids, dipeptidases
Aminopeptidase A	Dipeptide splitting with acid amino in amino terminal end	Amino acids
Aminopeptidase I	Cut dipeptides containing methionine	Amino acids
Aminopeptidase III	Cut dipeptides containing Glicine	Amino acids
Dipeptidil aminopeptidase IV	Cut dipeptides containing Proline with free C-terminal end	Peptides and amino acids
Carbossipeptidase P	Cut dipeptides containing Proline with free C-terminal end	Peptides and amino acids
ϒ-glutamin transpeptidase	Cut ϒ-glutamine bonds	ϒ glutamine and/or peptides
Folate conjugase	Cut pteroil glutamate	Monoglutamate
Cytosolic Peptidase		
Endopeptidase (different)	Cut the majority of the peptides	Amino acids
Aminotripeptidase	Cut tripeptides	Amino acids
Proline dipeptidase	Cut the X-pro bonds in dipeptides containing Proline	Proline, Amino acids

Table 7. Brush border and cytoplasm peptidase of epithelial cells lining the intestinal villi. From "The molecular basis of nutrition"; G. Arienti.

Calcium absorption at physiological levels

Calcium is the mineral most represented in the skeleton of vertebrates, and it has a central role in the regulation of many physiological processes and it requires particularly complex homeostasis maintained by the action bowel, kidney and skeletal hormones. The net absorption of calcium in the diet is the sum of transcellular active processes, vitamin D-dependent and paracellular. The passage through the paracellular tight junctions is not influenced by nutritional or physiological state of the individual and it is prevalent in normal or high recruitment. The ileum is the site with a greater absorption, under high calcium intake conditions. In this case dominates the paracellular pathway and the "vitamin D-dependent" route is inhibited. This latter is the result of three different processes, all strongly induced by the active metabolite of vitamin D (1.25 dihydroxy-vitamin D3). The calcium ion can cross the apical enterocyte membrane by the transporter CAT1, operating at low concentrations of calcium or by epithelial calcium channels that instead prevail at elevated intracellular calcium concentrations, in the order of 10 mM. The output by the cell is made by an active mechanism of extrusion due to the Ca^{+}-ATPase pump whose activity is stimulated by 1.25 Vitamin-D. In the absence of vitamin-D, the calcium uptake is reduced by 90%. Among the factors that affect the availability of calcium distinguish those endogenous (age, sex, pregnancy etc ...) and exogenous ones, such as changes in diet or the presence of substances that alter the solubility of the ion as phytates, oxalates, fiber ect. The intestinal absorption of calcium, in general, represents 30% of the daily calcium ingested (Mariani et al., 2006; Rinni, et al., 2006).

IN VITRO MODEL OF HUMAN INTESTINE

Since that has not yet been possible to stabilize the *in vitro* culture cells from human intestine biopsies, fetal or adult who present the structural and functional properties of the physiological intestine, there are a commercially available cancer cell lines as hypothetical model of intestinal epithelium. Among these, the cell lines that are derived from human colon adenocarcinoma represent a considerable advantage, not only for experimental cancer research but also in basic biological processes study of the mucosa and for the screening and characterization of agents capable to induce benign phenotype differentiation in tumor cells. This cells, from one stage of totally undifferentiation, are able to achieve complete differentiation, acquiring the typical phenotype of mature enterocytes (Ferraretto et al., 2007). In this regard, the Caco-2 cell line from human colon adenocarcinoma has provided a lot of information. These cells are stabilized in order to study cancer and related therapies for their ability to induce tumors in mice; they have been identified as the population able to undergo "spontaneously" to a differentiation process, aquising the intestinal absorbent phenotype, when cultured in the post-confluence conditions (Pinto et al., 1983), following the use of special culture media (Jumarie et al., 1991; Lentz et al., 2000; Li et al 2004), or with successive sub-cultivations without reaching the post-confluent stage (Ferraretto et al., 2010). In the HT-29 cell line, however, the enterocytic differentiation requires the various inducers, such as the use of a culture medium with low glucose content (RPMI containing 2 g l^{-1} of glucose), the addition of 5 mM Sodium Butyrate to the RPMI medium, the replacement of glucose with galactose as the main source of sugar in DMEM medium, the treatment with drugs such as Foscolina (activator of adenylate cyclase), colchicine, the Nocodazolo or Taxol (inhibitors of the cytoskeleton) (Zweinbaum et al., 1985; Ferraretto, 2006; Ophir 1995). With Caco-2 or HT-29 cells *in vitro* differentiated it is possible to perform studies of absorption and transport of various molecules. In fact they represent the main cell models employed as enterocytic epithelial barrier.

Caco2 cell line

Isolated for the first time by J.Fogh in 1977, the Caco-2 tumor cells, localized at the level of the crypt of intestinal villi, useful for the study of the enterocyte absorbent. In a particular experimental condition, characterized by cells in post-confluence or in the presence of differentiating agents such as fetal bovine serum (FBS) and a specific content into glucose in the culture medium (Ferruzza et al., 2012) the Caco2 cells formed a monolayer polarized characterized by the presence of tight junctions, microvilli well organized and "domes" (domes), because of the 'existence of a one-way flow of ions and water and the expression of specific enzymatic markers, such as enzymes of the brush-border sucrase-isomaltase (YES) and alkaline phosphatase (ALP) (Pignata et al., 1994). In addition, the recognized value of these cells which model of intestinal epithelium, has been strengthened by the identification of some barrier properties. The cell line Caco-2, differentiated post-confluence, showed a monolayer of cells in phenotype mainly absorbent expressed intestinal transporters specific for sugars, amino acids, oligopeptides, bile acids, vitamins and micronutrients. A limiting factor of these studies has been shown, however, by coexistence of cells of the colon and enterocytes in a specific population of Caco-2; to this it is added the fact that most of the culture conditions, implemented to differentiate the cells into postconfluenza, are not sufficiently representative of physiological conditions in the intestines (Ferraretto et al., 2007). In this regard it was developed a new technique capable of generating a cell line Caco-2 at different stages of differentiation without changing the culture conditions and without having to reach the stage of postconfluenza (Ferraretto et al., 2007) thus permitting how to choose, within the same cell population, the cell stage most appropriate, in terms of morphological and physiological, the performance of precise analysis.

HT-29 cell line

The cells HT-29 cells are considered to mucus-secreting phenotype, similar to the mucus goblet cells, which suitably differentiated, constitute an excellent model of polarized intestinal epithelium, having the ability to generate gradients of nutrients and electrolytes between the inside and the outside of the cell. The apical portion of HT-29 cell is characterized by a brush border with the microvilli. The microvilli membrane, presents the secretory function responsible for the secretion of numerous hydrolytic enzymes such as ALP, peptidases, saccarases involved in carbohydrate digestion. The basolateral portion is instead characterized by protein complexes (pump Na^+-K^+/ATPase) adapted to the transport of substances and by cells that express the major histocompatibility complex (MHC class I and II), that synthesize receptors for IgA , that perform the transport function for the same through the cytosol, that express receptors for hormones and peptides (Pinto et al., 1982; Zweibaum et al., 1985). The morphology of the HT-29 cells depends by the type of medium and by the content of glucose present therein; it is known that, if the culture medium used is DMEM (Dulbecco's modified Eagle's medium) with high glucose content (4.5 g /l) the HT-29 cells show an undifferentiated phenotype that, morphologically, is represented by a not polarized multilayered epithelial cells, with sporadic apical microvilli and without junctional apparatus (Gravaghi, et al., 2007). HT-29 cells instead show a differentiated fenotype when they grow in RPMI medium (Roswell Park Memorial Institute medium) or at a low concentration of glucose (13.9 mmol/l) or in modified DMEM (Dulbecco's Modified Eagle medium) or when the

Glucose is gradually replace by Galactose. Morphological analysis has been shown in fact that the cells grown in RPMI form a polarized monolayer with well-developed brush border on the apical surface, constituted by elongated and abundant microvilli. At the level of the contact points between cells becomes evident the complete junctional apparatus, comprising occluding junctions, adherens junctions and desmosomes. The cells adapted to grow in medium containing galactose show the presence of a monolayer with a lower number of apical microvilli and follicular structures, in addition to the presence of transport vesicles on the apical side (Gravaghi, et al., 2007).

EFFECT ON THE ENTEROCYTE ENZYME FUNCTIONALITY

Alkaline Phosphatase (ALP)

The intestinal alkaline phosphatase belongs to a superfamily of enzymes capable of performing a wide range of activities, including those of hydrolases and transferases isomerases (Lallès, 2010). As a general rule, the alkaline phosphatase enzymes are homodimeric and each of the monomers contains five cysteine residues and three metal ions, two atoms of Zn^{2+} and one of Mg^{2+} essential for enzyme activity. These enzymes catalyze the hydrolysis of monoesters of phosphoric acid and transphosphorylation reactions (Lallès, 2010; Millán 2006). In particular, the intestinal alkaline phosphatase is a glycoprotein, anchored to the apical membrane of the enterocytes, which has a high activity in the duodenum which is followed by a progressive decrease along the jejunum and the ileum. Furthermore, the activity level of this enzyme shows a gradient increasing from crypts to villi related to the differentiation degree of intestinal epithelial cells. For this reason, the alkaline phosphatase is used as enzyme for a long time index of the differentiation in the enterocitic sense (Lallès, 2010). Several diet components, including protein, fat and carbohydrates, are known to modulate the intestinal alkaline phosphatase expression or activity (Lallès, 2010; Sefcíková et al., 2008). A fat rich diet, particularly triglycerides containing saturated fatty acids and medium-long chain, cause the specific activity increase of the ALP before to induce weight gain (Lallès, 2010; Sefcíková et al., 2008; Mozes et al., 2004). It appears that the increase in the activity of this enzyme is strongly correlated with a greater absorption of fat in the intestine (Lallès, 2010; Lallès 2014). Contrary unsaturated fatty acids or polyunsaturated, cause a decrease in the activity of this enzyme. Even a diet rich in proteins and amino acids, with the exception of L-cysteine and L-tryptophan that are potent inhibitors of the ALP, or rich in carbohydrates and simple sugars, such as lactose, starch, cereals and cellulose, it is able to stimulate the functioning of the enzyme. In addition to macronutrients, other dietary components, including minerals and vitamins, may affect the activity of this enzyme. The free phosphorus coming from the diet has an inhibiting effect while the phosphate bonds, the Ca^{2+} and vitamin K are able to enhance the activity of the ALP (Lallès, 2010; Lallès, 2014).

Dipeptidyl peptidase IV (DPP IV)

The DPP IV is a serine protease expressed in soluble form at the level of the membrane of different epithelial tissues, including the intestine. It belongs to the family of prolil oligopeptidase and it conducts its hydrolytic activity of different types of peptides, selectively removing dipeptides which have in second place a proline or an alanine. This enzyme plays an important role in several biological processes, in fact by means of its proteolytic activity is able to activate or inactivate the peptides, growth factors and cytokines. For example, it plays an important role in the homeostasis of glucose because it is able to inactivate, by proteolytic cleavage, incretins. Some studies have shown that the use of inhibitors of DPP IV could promote a better glycemic control in subjects with diabetes mellitus type II. The DPP IV is also able to inactivate, by proteolytic cleavage, different peptides of significant medical importance. At the level of the intestinal epithelium it is involved, together with the other peptidases of the membrane, in the terminal digestion of the peptides present in the intestinal lumen arising from the degradation of proteins introduced with the diet (Lambeir et al., 2003). The DPP IV bowel appears to be inhibited by three amino acids (Met, Leu and Trp) and eight dipeptide (Phe-Leu, Trp-Val, His-Leu, Glu-Lys, Ala-Leu, Val-Ala, Leu and Ser-Gly -Leu) resulting from the digestion of proteins introduced with the diet (Nongonierma et al., 2013). Furthermore it is also inhibited by peptides derived from the digestion of milk proteins (Lacroix et al., 2013).

Amino Peptidase N (APN)

Aminopeptidase N belongs to the family of aminopeptidase, enzymes that catalyze the hydrolysis and release of amino acids from the amino terminal portion of proteins and peptides. In particular, the APN is an enzyme capable of releasing, in a preferential, neutral amino acids. The APN is a membrane glycoprotein with zinc dependent catalytic activity, expressed in different tissues including enterocytes of the intestinal epithelium and the epithelium of the proximal tubule of the kidney. In the epithelium of the small intestine performs the task of hydrolyzing small oligopeptides present in the intestinal lumen, the amino acids released are transferred directly to specific membrane transporters (Taylor A. 1993).

Aim of the study

Milk and dairy products are an excellent source of bioavailable calcium thanks to the presence of casein protein derived, named "casein phosphopeptides" (CPPs). These latter are characterized by a high content of phosporilated serines, responsible for binding with calcium ions. When the calcium-CPPs aggregates are formed, the calcium ions become more soluble and bio-absorbable for intestinal epithelium.
In order to improve the calcium fraction absorbed by ileum, that represent the intestinal tract in which this ion is concentrated and where absorption takes place after a calcium load meal, CPPs were studied in both human and animal (FitzGerald, 1998) but the difficulties of studies have provided conflicting results (Ferraretto A & Fiorilli A 2010). In the past, studies using *in vitro* cell cultures have revealed different roles of CPPs, such as the anti-proliferative effects on cultured mammalian intestinal cells (Ganjam et al., 1997), the modulation of cell viability in human cells cultures (Hartmann et al., 2000) and the modulation of the intestinal immune system (Otani et al., 2001). In the last five years, CPPs have been recognized to increase the intracellular calcium in differentiated human intestinal cancer cell lines Caco2 and HT-29 (Cosentino et al, 2010b). Together with the importance of the increase in the calcium fraction it is worth to remember that calcium ion influx may play a role as messenger of cellular events related to the control of proliferation, as well cell viability (Munaron et al., 2004). In fact the abnormal cell proliferation is related to pathological conditions such as inflammation and cancer (Brown et al., 2005; Wright et al., 1994).
Anyway, digestion and absorption are limiting steps for the peptide bioavailability (Bruno et al., 2013).
The initial goal of this thesis was to evaluate the biological potential of a commercial mixture of CPP after *in vitro* digestion. In fact, the peculiar characteristic to define a nutrient as "nutraceutical", or a whole-food as "functional food", is the ability to retain or increase the bioactive potential even after digestion and absorption phases.
In particular, a commercial mixture of CPP was subject to an *in vitro* digestion, then it was administered to Caco2 and HT-29 cells, two different cell lines from human colon adenocarcinoma. These cells are able to acquire morpho-functional characteristics typical of the intestinal absorptive and mucus secretory cells of human intestine, after appropriate *in vitro* differentiation.
In this context, the main difference between this two cell types is the different mechanism of calcium absorption. Caco2 cells present the TRVP6 channels, that are activated when the extracellular calcium concentration is low, according to the saturable kinetics that takes place in duodenum. HT-29 cells, instead, present depolarizing L-type calcium channels, characteristic of the jejenum and ileum tract in wich calcium is absorbed through paracellular way, for example after a meal.

The biological potential retain of CPPs after *invitro* digestion was evaluated essentially by:

- Study of the supramolecular structure evolution of the Ca–CPP complexes
- Analysis of CPP-induced calcium uptake in intestinal like cells.

The capacity of milk protein–derived peptides to increase the calcium fraction that can be absorbed by our intestinal cells, have been a subject of growing commercial interest in the context of health-promoting functional foods. Since CPP are from casein, the second aim of this thesis was to evaluate, after *in vitro* digestion, the biological potential of two whole foods containing CPPs, consisting by Grana Padano (GP) and Trentin Grana (TN) at three different periods of ripening: low (13 months), medium (19 months) and long aging (26 months). They are two hard Italian cheeses, characterized by a high digestibility and high calcium content. The main difference is given by the use of lysozyme during the GP production process. It is known that this additive accelerates the proteolytic processing of GP cheese (Sforza et al., 2003).

For this experimental step, a new model of the *in vitro* human intestinal epithelium has developed for the first time in our laboratory. This is a co-culture between Caco2 and HT-29 cells, that together are able to mimic a better model of human intestinal epithelium in which multiple cell types physiologically coexist.

In order to evaluate the biological potential of GP and TN, at beginning they are subject to an *in vitro* digestion process. Subsequently, after digestates administration was evaluated:

- calcium uptake in an *in vitro* model of human intestinal epithelium represented by a co-culture of Caco2 and HT-26 cells;
- bone mineral matrix formation in human osteoblast-like cells represented by Saos-2 cells.

Materials and methods

CPPs DIGESTION AND THEIR ADMINISTRATION IN INTESTINAL-LIKE CELLS

Materials and reagents

Cell culture media, L-glutamine, antibiotic–antimycotic solution, sodium pyruvate, trypsin-EDTA solution, EGTA and all other reagents, unless otherwise specified, were purchased from Sigma-Aldrich (St. Louis, MO, USA). Foetal bovine serum (FBS) was provided by EuroClone Ltd (West Yorkshire, UK). Fura-2 acetoxymethyl ester (Fura-2/AM) was provided by Calbiochem (La Jolla, CA, USA).

Casein phosphopeptides (CPPs)

The CPP preparation (Peptigen®110) represents a purified tryptic casein hydrolysate containing a very high level of CPPs and it was kindly provided by MD Foods Ingredients Amba (Videbaek, Denmark). Quality parameters of the preparation such as calcium content, CPP and protein content, Ser/P ratio26 and their ability to induce calcium uptake in intestinal cells were previously studied (Cosentino et al., 2010a). Two main components, an N-terminal tryptic peptide 1–25, obtained from beta casein, bearing four phosphate groups, and a 62–79 peptide obtained from alpha s1 casein, with three phosphate groups, were identified by The MALDI-TOF/MS analysis (Cosentino et al., 2010a).
The MS spectra showed that the average molecular weight was 2500 (Cosentino et al., 2010a). The composition of CPP preparation is the following: 95% CPP content; 6.6% calcium content; 3.2% phosphorus content; N/P ratio: 7.8 mol mol−1; Ser/P ratio: 0.97 mol mol−1, which is in accordance with data published (Ellegard et al., 1999). For all experiments CPP solutions were prepared at 1280 μM peptide concentration, corresponding to the maximum activity able to induce the intracellular calcium rise (Gravaghi et al., 2007; Cosentino et al., 2010b) (Cosentino et al., 2010a).
The main feature of these CPPs, hereafter Ca–CPPs, is the presence of calcium in the stock powder preparation. As determined previously (Cosentino et al, 2010a), a fraction of the pre-loaded calcium is stably associated with Ca– CPP complexes, an amount independent from the extra calcium present in the solution.
According to the procedure already described (Cosentino et al., 2010a) an aliquot of Ca–CPPs was decalcified, by the chelating ion exchange resin Chelex100 (Bio-Rad Laboratories, Hercules, CA, USA) and this second CPP preparation was named dekCPP. Furthermore, after dissolution in a calcium-containing solvent, dekCPP becomes Ca–dekCPP. In order to prepare the Ca–dekCPP complexes, the solvent used to solubilize the dekCPP powder, was added with calcium.

In vitro digestion of Ca–CPPs and Ca–dekCPP

Enzymes and bile salts were purchased from Sigma-Aldrich (St. Louis, MO, USA).

40 mg of porcine pepsin (EC 3.4.23.1, catalog no. P-7000) was suspended in 1 ml of 0.1 M HCl; 20 mg of pancreatin (catalog no. P-1750) and 120 mg of bile extract (catalog no. B-8631) were solubilized in 10 ml of 0.1 M $NaHCO_3$. 500 mg of Ca–CPPs (50× concentrated, with respect to the final concentration) were dissolved in 3 ml of double distilled water adjusting the pH to 2 using 5 M HCl. The same protocol was used for dekCPPs, but $CaCl_2$ (two calcium ions per peptide chain) was added in order to reproduce the calcium amount embedded in Ca–CPP complexes. After, the two samples were simultaneously subjected to simulated digestion, as follows: adding 5 mg of freshly prepared pepsin solution and incubating the samples in a shaking water bath at 37 °C for 90 min. The gastric digests were kept in ice for 10 minutes in order to stop the pepsin digestion. The gastric digest pH was raised to 6 using 1 M $NaHCO_3$ before intestinal digestion. Subsequently, 8.75 mg of the pancreatin–bile extract mixture were added and was incubated for another 2 h.
After incubation, the intestinal digestion step was stopped using an ice bath for 10 min. The pH was adjusted to 7.2 by 0.5 M NaOH. The intestinal digestates were heated for 4 min at 100 °C to inhibit proteases and then they were immersed in an ice bath to decrease the temperature. Afterwards, 1 ml of each samples were centrifuged at 12 000 g, for 30 min at 4 °C (TL-100 Ultracentrifuge, Beckman Coulter), in centrifuge tubes polyallomer® (Beckman Coulter, Brea, CA, USA).
The supernatants were transferred and stored at −20 °C. Finally, double distilled water was added to correct the osmolarity to 300 ± 20 mOsm kg^{-1} (cryoscopic osmometer Osmomat 030, Gonotec GmbH, Berlin, Germany) (Jovaní et al.,; 2001 Ortega et al., 2009).
Before and after digestion Ca–CPPs and Ca–dekCPPs were subjected to the Lowry protein assay (Lowry et al., 1951), showing a protein recovery of 82%.

LC/MS/MS analysis

Thanks to LC/MS/MS, peptides were analyzed by means of an Orbitrap XL instrument (Thermo Fisher, Waltham, MA, USA) equipped with a nano-ESI source coupled with a nano-ACQUITY capillary UPLC (Waters, Milano, Italy). Peptides were separated by the support of a capillary BEH C18 column (0.075 mm × 100 mm, 1.7 μm, Waters) using aqueous 0.1% formic acid (A) and CH_3CN containing the mobile phases represented by 0.1% formic acid (B). Peptides

were eluted by means of a linear gradient from 5% to 50% of B a 300 nl min^{-1} flow rate in 45 minutes. Mass spectra were acquired over an m/z range of 400–1800; the ten most intense doubly-, triply- or quadruply-charged ions detected in each spectrum underwent to CID fragmentation (dependent scan acquisition mode) and MS/MS spectra were acquired over an m/z range of 50–2000. In order to interrogate the Swiss-Prot protein database, MS and MS/MS data were used by Mascot (Matrix Science, London, UK). Settings were as follows: taxonomy, other mammalia; enzyme, no cleave; mass accuracy window for parent ions, 10 ppm; mass accuracy window for fragment ions, 50 millimass units; no fixed modification; variable modifications, phosphorylation of serine, threonine and tyrosine, oxidation of methionine.

Laser light scattering

Aliquots of CPP concentrated stocks, dissolved in double distilled water, were diluted in phosphate-free KRH with the same calcium concentration employed to monitor the CPP biological effect. The laser light scattering apparatus has been designed in the laboratories of *Department of Medical Biotechnology and Translational Medicine, University of Milan* to be quite sensitive, thanks to four optical channels. It includes a diode laser (λ = 532 nm) and a temperature controlled cell. Both independent static (SLS) and dynamic (QELS) laser light scattering measurements at room temperature were performed on each sample. Through the correlation function of the scattered intensity, dynamic measurements yield the translational diffusion coefficients of particles in solution and then, via the Stokes–Einstein relation, their average hydrodynamic diameter. Information on the mass of particles in solution were obtained by parallel static measurements of the average scattered intensity.

Small angle X-ray scattering (SAXS)

SAXS measurements were performed at the ID02 high-brilliance beamline at the ESRF (Grenoble, France); room temperature, with a very short exposure time (0.1 s), was maintained in order to avoid any radiation damage. The parameters used were the following: a beam cross section of 0.3 mm × 0.8 mm and a wavelength of 0.1 nm, in the region of momentum transfer, $q = (\pi/\lambda)\sin(\theta/2)$, 0.017 $nm^{-1} \leq q \leq 4.65$ nm^{-1}, where θ is the scattering angle. Samples were placed in plastic capillaries (KI-beam, ENKI, Concesio, Italy) disposed horizontally onto a six-places sample holder, allowing for nearly contemporary measurements on sample and reference cells. The measured SAXS profiles showed the scattered radiation intensity I(q) as a function of the momentum transfer (q). Several spectra were taken in relation to the empty cells and to the solvent. They were carefully compared and subtracted to each sample spectrum. With respect to laser light scattering analysis, a SAXS analysis was carried out to assess the structure of the particles in solution on a more local, internal, scale. The experimental I(q) profile was then fitted with the internal form factor (PInt) characteristic of structures obtained by random condensation of functional monomers, in which the resulting statistic of the subchains is Gaussian. For equal reaction probability of the functional groups:

$$PInt = 1/(1 + \langle Rg\ 2\rangle\ q2/3)$$

Where ⟨Rg 2⟩ is the average radius of gyration squared of the subchain, proportional to the correlation length within the entanglement network (Pedersen et al., 2002). We also tested the model developed for the casein micelles internal structure, which consists of calcium phosphate nanoparticles reticulated in the peptide matrix (Bouchoux et a., 2010), This model is not suitable for the internal structure of CPP aggregates and has been rejected.

Cell culture

The human colon adenocarcinoma cell lines Caco2 (BS TCL 87) and HT-29 (BS TCL 132) were purchased by Istituto Zooprofilattico Sperimentale di Brescia (Brescia, Italy). Caco2 cells were cultured in 75 cm^2 plastic flasks (VWR International PBI, Milan, Italy) in EMEM (Minimum Essential Medium Eagle's) growth medium supplemented with 15% heat-inactivated foetal bovine serum (FBS), 2 mM L-glutamine, 1 mM sodium pyruvate, 0.1 mg l^{-1} streptomycin, 1 × 105 U l^{-1} penicillin, and 0.25 mg l^{-1} amphotericin-B. The differentiation of Caco2 cells was achieved according to the well-established procedure (Ferraretto et al., 2007). Briefly, it consists of successive sub-cultivations without reaching the post-confluent stage. HT-29 cells were grown in 75 cm^2 plastic flasks (VWR International PBI) in RPMI 1640 medium (Roswell Park Memorial Institute), supplemented with 10% heat-inactivated foetal bovine serum, 2 mM L-glutamine, 0.1 mg l^{-1} streptomycin, 1 × 105 U l^{-1} penicillin, and 0.25 mg l^{-1} amphotericin-B, obtaining a population of differentiated and polarized cells, although with a high degree of heterogeneity (Hekmati et al., 1990).

All cell cultures, kept at 37 °C under a 5% CO_2–95% air atmosphere, were periodically checked for the presence of mycoplasma and were found to be free of contamination.

Measurement of cytoplasmic calcium content, $[Ca^{2+}]i$, at the single-cell level

Caco2 and HT-29 cells were seeded separately on glass coverslips (Ø = 24 mm) to determine cytoplasmic calcium $[Ca^{2+}]i$. Around to 50% of confluence, they are loaded with 2.5 μM Fura-2/ AM and 2.5 μM Pluronic F-127, in phosphate-free Krebs Ringer HEPES solution (KRH, 140.0 mM NaCl, 5.0 mM KCl, 2 mM $CaCl_2$, 0.55 mM $MgCl_2$, 6.0 mM glucose and 10.0 mM HEPES, pH 7.4) as previously described (Gravaghi et al. 2007). Fluorescence determination was performed with a microscope (TE 200, Nikon, Tokyo, Japan) connected to a CCD intensified camera (Extended Isis, Photonic Science, Millham, UK) and to a thermostated (TC-202 A, Medical System Corporation, Harvard Apparatus, Holliston, MA, USA) perfusion chamber (PDMI-2, the same commercial source). The intracellular free calcium $[Ca^{2+}]_i$ amount was calculated, within every single cell, using a fluorescence image acquisition and data analysis system (Applied Imaging, High Speed Dynamic Video Imaging Systems, Quanticell 700, Sunderland, UK), from the 340/380 nm images, using a calibration performed with external standards of calcium and Fura-2, according to the equation reported in ref. (Grynkiewicz et a., 1985).

Statistical analysis of cell population

Statistically significant differences ($p < 0.005$ or $p < 0.01$) were obtained using Student's t-test, two way ANOVA (IBM SPSS Statistics 22) and χ^2 test.

GRANA PADANO AND TRENTIN GRANA CHEESES CHARACTERIZATION

Grana Padano and Trentin Grana cheeses, at three maturation degree, corresponding to 13, 19 and 26 months of ripening, were kindly provided by the Grana Padano Production Consortium on behalf of Latteria Soresina (Soresina, Italy).
The samples at 13, 19 and 26 months of ripening, represent the short, medium and long maturation period, respectively.
Grana Padano and Trentin Grana, are very similar Italian hard cheeses produced in the northern part of Italy. They are cooked cheeses made from raw, partly-skimmed cow's milk supplemented with a natural whey starter and ripened for at least 9 months. The dominant microflora of the natural whey starter is represented by Thermophylic lactic acid bacteria (LAB) selected by the process of curd cooking. Lysis of LAB and the release of intracellular enzymes are the determining factors in the Grana Padano and Trentin Grana ripening (Sforza et al., 2004).
The important difference is the presence, in Grana Padano of the antibacterial molecule lysozyme. This latter is added during the production process of GP, in order to avoid the swelling of cheese forms due to the presence of *Clostridium butyricum* and *Clostridium tyroburyricum*.
These bacteria come from forage use for feed cows that provide the milk used for Grana Padano production.
In fact, it is permitted to silage use for Grana Padano. Silage are obtained from the grain whole plant that is chopped and stored in silos favoring the microorganism growth.
In detail, the Lysozyme is able to hydrolyze the β (1-4) glycosidic bond that binds the N-acetylmuramic acid residues of polysaccharides constituting the Gram positive wall thus preventing the bacteria spore germination during ripening.
The Trentin Grana cheese production does not require the lysozyme use and in this sense it is similar to the Parmigiano-Reggiano cheese.
During the ripening process, milk curd proteins (namely α_{s1}, α_{s2}, β and κ caseins) undergo an extensive degradation because of the endoproteases and exoproteases present in raw milk, in the rennet and released by the lactic bacteria present in the natural whey starter (Sforza et al., 2003).

Calcium content determination in GP and TN cheeses

In order to determine the calcium content in the GP and TN chesees, the procedure used was reported in table 8 (Method US-EPA n. 6010c (2000) - revision 3) and has planned to add, in a test tube, 0.3 g of grated cheese, 5 ml of nitric acid (HNO_3) and 1 to 65% ml of hydrogen peroxide (H_2O_2) 120/130 volumes. The obtained solution was placed into the microwave oven (Marsx Express) and subjected to mineralization by heating cycles variables in terms of both power and timing:

STEP	Watt	Power (%)	Time step	
1^{TH}	800	50	5 minutes	Reached 70°C in 10 minutes
2^{TH}	800	70	5 minutes	Reached 125°C in 10 minutes
3^{TH}	800	100	5 minutes	Reached 170°C in 10 minutes

Table 8. Step of calcium content determination. Method US-EPA n. 6010c (2000) – revision 3.

After cooling, filtration in 50 ml flask and some washings with Mill-Q or double distilled water was performed, in order to collect completely the sample that was then brought to volume. The reading was performed by ICP-OES (Inductively Coupled Plasma- Optical Emission Spectrometry) PERKIN ELMER mod. OPTIMA 2100 DV (Massachusetts, USA) at λ = 317-933 nm according to the method: US-EPA (Environmental Protection Agency USA) n. 3052 (1996) -revisione 0 "Microwave assisted acid digestion of siliceous and organically based matrices".

Determination of protein in GP and TN cheeses

The cheese protein content was determined by Kjeldahl method [ISO 8968-3:2004. Milk: Determination of nitrogen content; part 3: Block-digestion method (semi-micro rapid routine method)] consisting of an acid attack at high temperature to release the total nitrogen in the NH_4^+ form. The obtained solution was alkalinized with NaOH and distilled in a steam current, collecting the ammonia obtained in a solution of H_3BO_3 (Lewis acid) and titrating with 0.1 N H_2SO_4. The analysis was performed in duplicate and following *in vitro* digestion. In digestion tubes, the sample (0.3 g of grated cheese), 2 Kjeldahl catalyst tablets (1000 Kjeldahl cx, each containing 3.5 g of potassium sulfate K_2SO_4 and 0.105 g of copper sulphate) and 20 ml of sulfuric acid (H_2SO_4) at 98% were included. The catalysis was able to raise the acid boiling point then reduce the mineralization times. The mixture obtained was stirred slightly and the test tubes to be placed in the mineralizer for 90 minutes, after which they were cooled for approximately 15 minutes. The distillation was automatically performed using DISTILLATION UNIT BÜCHI 323 after sample basification by addition of 90 ml of 32% NaOH and 30 ml of H_2O. The distillate was collected as ammonia, in the collection solution consisting of 100 ml of Lewis acid and Methyl red and cresol Dibromo indicators. The titration was carried out using an automatic titrator (Crison Compact titrator) and H_2SO_4 to reach a final pH of 4.6 (which is expressed by the change in color from green to pale pink).
For the final calculation it was used the following formula:

PROTEIN % = (14 * ml drained H_2SO_4 * 0.1 * 6.38 * 100)/(sample grams * 1000)

where:
6.38 = multiplication factor that expresses the protein nitrogen content
0.1 = acid Normality
14 = nitrogen atomic weight

Dry content determination in GP and TN cheeses

The determination of GPs and TN samples moisture content was performed according to the method reported by ISO (100) expecting that known weight sample, covered by sand, was mixed with pre-dried and treated at 102 ° C for 3 hs. At the end of the treatment, the sample is weighed and, by setting a simple operation, it is determined the loss of mass (content of water evaporated). After weighing the capsules used to contain the sample and having noted the tare, the same were filled with a mixture consisting of 3 g of grated cheese and 20 g of sand; after they were transferred in dryer where they remained for the time necessary to eliminate the aqueous fraction of the sample. At the end of the drying process, the capsules were cooled and weighed again in order to obtain the values necessary to determine the moisture content. For the calculation, reference was made to the following formula:

MOISTURE% = ([(g initial tare +)-weight final] / g sample) * 100

Fat determination in the GP and TN cheeses

The GP and TN fat content was determined by Van Gulik method [ISO 3433:2008. Cheese: determination of fat content- Van Gulik method] by an appropriate Butyrometer whose characteristics are shown in [ISO 3432:2008. Cheese: determination of fat content; butyrometer for Van Gulik method]. The principle of the method involves the dissolution of the protein fraction with sulfuric acid; after the fat fraction is separated by means of repeated shakings and baths in hot water. Frequently amyl alcohol is added to the fat fraction in order to advance its separation. The amount of fat is directly shown by the Butyrometer scale. The cheeses were grated and inserted at the base of Butyrometer filled up to 2/3 with sulfuric acid. After this preliminary operation, the Butyrometer was closed and it was subjected to an alternation of operations. The total duration of the process was about 75 minutes, consisting in a 65 °C water bath and a manual agitation of the instrument. The aim was the quick dissolution of the protein fraction. Once the proteins were dissolved, 1 ml of amyl alcohol and sulfuric acid were added up to 35% of the graduated scale; this allowed the rise of the fat fraction from the body of Butyrometer. Before reading, a new sequence of baths and shaking were performed allowing the complete separation the fat fraction. The fat content was determined as follow:

B-A

where:
B = reading carried out at the base of the column of fat
A = reading from the height of the column of fat

Enzymatic digestion of GP and TN cheeses

The Perales method provided for a preliminary mechanical cheese grinding by a *miniTritatutto* (Girmi minitritatutto). 4.5 g of grinded product were subjected to enzymatic attack in order to extract the greatest amount of calcium.

The protocol required the preparation of 4 solutions:
1. Pepsin solution: 0.125 g of pepsin in 12 ml of 0.1 N HCl;
2. Pancreatin/ Bile solution: 0.05 g of pancreatin and 0.310 g of bile in 17.5 ml of 0.1 N Na_2CO_3;
3. 0.1 N HCl solution;
4. 0.1 M $NaHCO_3$ solution.

Each sample of 4.5 g was diluted in 25/30 ml of double distilled water, pH was adjusted using 6 N HCl, in order to get values close to 2, and the pepsin was added, in an amount equal to reach the final concentration of 0.02 g/g of sample. Purified water was added to the obtained solution, in order to reach the weight of 100 g, and it was incubated in water bath at 37°C for 2 h. This step was followed by cooling the solution in ice for 10 minutes. Two pH corrections were performed on these samples: the first by the addition of 0.1 N $NaHCO_3$, pancreatin (0.05 g/g of sample) and bile (0.03 g/g of sample) which raised the value to 5, the second with 0.5 M NaOH to a final value of 7.2. Within the two corrections, samples were incubated at 37°C for 2 h and cooled in ice. The volume and the final weight of each sample was determined before performing a centrifugation at 1300 × g (Sorvall Instruments RC5C). The supernatant obtained was separated and used for the determination of Calcium.
Simultaneously to the GPs and TN samples, a blank of digestion was create with the only difference in the absence of the cheeses.

Identification of casein phosphopeptides (CPPs) in cheese digesta UPLC-HR-MS/MS

CPPs from cheese digesta were isolated by selective precipitation with $CaCl_2$ according Cruz-Huerta et al. (2015). Extracts were separated by the Ultra-Performance Liquid Chromatography (UPLC) and the CPPs were identified by the High Resolution Tandem Mass Spectrometry (HR-MS/MS). The UPLC-HR-MS/MS analyses were carried out by coupling an Acquity UPLC separation module (Waters, Milford, MA, USA) to a Q Exactive hybrid quadrupole-Orbitrap mass spectrometer and an HESI-II probe for electrospray ionisation (Thermo Scientific, San Jose, CA, USA). The digested cheese extracts were separated using an Acquity UPLC BEH300 C18 column (150×2.1 mm, 1.7 μm) (Waters) kept at 40 °C, and using 0.1 ml 100 ml^{-1} formic acid (FA) in MilliQ-treated water (solvent A) and 0.1 ml 100 ml^{-1} FA in acetonitrile (solvent B). For the UPLC separation, a linear elution gradient was applied (6% to 60% of solvent B in 36 min) at a flow rate of 0.25 ml min^{-1}. The LC eluate was analysed by MS using Full MS and data dependent tandem MS analysis of five the most intense ions [$ddMS^2$(Top 5)]. The resolution was set at 70K and 17.5K, the AGC targets were 5×10^5 and 5×10^4, and maximum ion injection times were 50 ms and 100 ms for Full MS and $ddMS^2$ scan types, respectively. The MS data were processed and the CPPs were identified using the Proteome

Discoverer 1.4 software (Thermo Scientific) which was used to extract peaks from MS and MS/MS spectra and to match them against the database of *Bos taurus* (UniProt taxon ID 9913) caseins considering their genetic variants (Farrell et al., 2004). Phosphorylations of Ser and Thr were set as fixed modifications, while Asn deamidation and Met oxidation were set as variable modifications. The precursor mass tolerance was set to 5 ppm and fragment mass tolerance was 0.5 Da.

Osmolarity correction

After *in vitro* digestion, the osmolarity was corrected at the value of 308 ± 10 mOsm kg^{-1} (cryoscopic osmometer Osmomat 030, Gonotec GmbH, Berlin, Germany) adding double distilled water or D-Mannitol (Sigma M9546).

Protein assay of GP and TN digestates

Lowry method was performed in order to determinate protein content (Lowry ea al, 1951). The assay requires the use of Folin-Ciocalteu reagent, which consists in a solution of tungstic, molybdic and phosphoric acid sodium salts, able to react with tyrosine phenolic groups in the presence of cupric ions, a blue dye which shows a maximum of absorption around 750 nm.

Reagents:
- Albumin (BSA): 10 µg in 50 µl.
- Solution A: Sodium Carbonate (Na_2CO_3) 2% in 0.1 N Sodium Hydroxide (NaOH).
- Solution B: Copper sulfate ($CuSO_4$) 1%.
- Solution C: Sodium tartrate - potassium (Na/K tartrate) 2%.

First reagent: A + B + C in the ratio 100:1:1, blue color.
Second reagent: Folin-Ciocalteau diluted 1:1 in distilled water, yellow color.

According to the method a bovine serum albumin (BSA) standard solution, was prepared at a concentration of 10 mg in a final volume of 200 µl. The samples contained proteins were diluted in a final volume of 200 µl. The reaction blank was formed by 200 µl of double distilled water (the same volume of the samples). After, 1 mL of the following mixture: 2% Na_2CO_3 in 0.1 N NaOH, 1% $CuSO_4$, 2% Na^+/K^+ tartrate was added in all the samples, incubated then for 10 min at room temperature. Subsequently, 0.1 mL of Folin-Ciocalteu, diluted 1:1 with double distilled water, was added and samples were incubated 30 min at room temperature. The absorbance of the samples were red by the spectrophotometer at a wavelength (λ) of 750 nm. The samples protein concentration were calculated in relation to the standard absorbance.

CO-CULTURE CHARACTERIZATION

Cell culture media, L-Glutamine, antibiotic-antimycotic solution, trypsin-EDTA solution and all other reagents, unless otherwise specified, were purchased from Sigma (St. Louis, MO, USA). Foetal bovine serum (FBS) was from EuroClone Ltd (West Yorkshire, UK).

CELL CULTURE

HT-29 cell line

Maintenance in culture. The human colon derived adenocarcinoma cell line HT-29 (BS TCL 132) was provided by Istituto Zooprofilattico Sperimentale di Brescia (Brescia, Italy). These cells, after thawing, were routinely growth in DMEM (Dulbecco's Modified Eagle Medium) culture medium with high D-glucose content (4.5 g l^{-1}). The cells were cultured in 75 cm^2 plastic flasks (VWR International PBI, Milan, Italy) and kept at 37°C in a 5% CO_2-95% air atmosphere. The DMEM medium was supplemented with 10% heat-inactivated foetal bovine serum (FBS), 2 mM L-Glutamine, 0.1 mg l^{-1} streptomycin, $1 \cdot 10^5$ U l^{-1} penicillin, 0.25 mg l^{-1} amphotericin B. At confluence, the cells are detached from the growth substrate by enzymatic digestion (Trypsin-EDTA 0.05-0.02%) of the adhesion-mediating proteins and then sub-cultivated.

Differentiation in RPMI-1640. After detaching by trypsin-EDTA (0.05-0.02%) cells were resuspended in RPMI-1640 (Roswell Packard Memorial Institute) growth medium, seeded in a new 75 cm^2 flask and maintained till the following passage. The RPMI-1640 medium has a lower D-glucose content (2g/l) and it is supplemented with 10% heat-

inactivated foetal bovine serum (FBS), 2 mM L-Glutamine, 0.1 mg l^{-1} streptomycin, $1 \cdot 10^5$ U l^{-1} penicillin, 0.25 mg l^{-1} amphotericin B. When the confluence status was reached, the cells were detached from the substratum and sub-cultivated for about 20 passages.

Caco2 cell line

Maintenance in culture. The human colon derived adenocarcinoma cell line Caco2 (BS TCL 87) was provided by Istituto Zooprofilattico Sperimentale di Brescia (Brescia, Italy).

Cells were cultured in 75 cm^2 plastic flasks (VWR International PBI, Milan, Italy) in EMEM (Minimum Essential Medium Eagle's) growth medium supplemented with 15% heat-inactivated foetal bovine serum (FBS), 1 mM sodium-pyruvate, 2 mM L-Glutamine, 0.1 mg l^{-1} streptomycin, $1 \cdot 10^5$ U l^{-1} penicillin, 0.25 mg l^{-1} amphotericin B. After one day of post-confluence cells were trypsinized (Trypsin-EDTA 0.05%-0.02%), diluted (usually 1:3) and then seeded again in a new plastic flask. Each trypsinization and successive dilution in a new flask was considered as a cell passage. Cultures, kept at 37°C in a 5% CO_2-95% air atmosphere, were periodically checked for the presence of mycoplasma and were found to be free of contamination.

Differentiation by sub-cultivation

Caco2 differentiation consists of successive sub-cultivations in EMEM complete medium for at least 18 passages and without reaching the post-confluent stage, in according to the method previously mentioned (Ferraretto et al., 2007).

Co-cultures

HT-29 cells previously described were cultured in 75 cm^2 plastic flasks (VWR International PBI, Milan, Italy) in Roswell Park Memorial Institute medium 1640 (RPMI 1640) supplemented with 10% FBS, 2 mmol l^{-1} L-Glutamine, 0.1 mg l^{-1} streptomycin, 100.000 U l^{-1} penicillin, 0.25 mg l^{-1} amphotericin-B, containing 13.9 mmol l^{-1} of glucose for a minimum of 5-6 passages to obtain a population of differentiated and polarized HT-29 cells (Hekmati et al., 1990), with features of absorptive and mucus-like cells.

Caco2 cells were cultivated in EMEM complete medium as previously described (Ferraretto et al., 2007) for at least 18 passages to achieve a differentiated status. Later, Caco2 cells were plating with complete RPMI (Caco2 RPMI) and sub-cultivated for at least 2 passage.
Co-culture of Caco2 and HT-29 cells was assessed by plating a mixture (40000 cells cm^{-2}) of 70% Caco2 (28000 cells cm^{-2}), from 20^{th} to 40^{th} passage, and 30% HT-29 (12000 cells cm^{-2}), from 22^{th} to 40^{th} passage, in complete RPMI medium. Co-culture employed in experimental design were stopped at 5 different time points corresponding to 0, 3, 6, 10 and 14 days of post-confluence stage. Medium was changed every three days.
Cultures, kept at 37°C in a 5% CO_2-95% air atmosphere, were periodically checked for the presence of mycoplasma and were found to be free of contamination.

Saos-2 cells
Human Saos-2 cells (Saos-2 HTB-85, ATCC-LGC standards, Milan, Italy) were maintained in 75 cm^2 flasks containing Iscove's Modified Dulbecco's Medium (IMDM) supplemented with 10% FBS, 4 mM L-Glutammine, 0.1 mg l^{-1} streptomycin, 100,000 U l^{-1} penicillin, 0.25 mg l^{-1} amphotericin-B and maintained in a humidified atmosphere of 5% CO_2 at 37°C (Donida et al., 2009).

Transmission electron microscopy analysis (TEM)

Cells were fixed at room temperature (RT) for 60 min with 3% glutaraldehyde buffered in 0.1 M Sorensen phosphate buffer (pH 7.4), plenty rinsed with the same buffer and post-fixed in 1% osmium tetraoxide (OsO_4) in 0.1 M Sorensen phosphate buffer. Afterward, the staining with uranyl acetate 2% in H_2O, dehydration through an ascending series of ethanol and embedding araldite (Durcupan, Fluka, Milan, Italy), were performed as previously described (Ferraretto et al., 2007; Gravaghi et al., 2007). Ultrathin sections were obtained with an Ultracut ultramicrotome (Reichert Ultracut R-Ultramicrotome; Leika, Wien, Austria), stained with lead citrate before examination using a Jeol CX100 electron microscope (Jeol, Tokyo, Japan).

Immunofluorescence analysis of intercellular adhesion

Cells were seeded on glass coverslips, fixed at RT for 5 min with 4% paraformaldehyde in 0.1 mmol l^{-1} Phosphate-Buffered Saline (PBS) (pH 7.4), post-fixed in ethanol 70% at 4°C and stored at -20°C until use. Cells were washed with PBS (3 washes of 5 min each), permeabilized with 0.1% Triton X-100 in PBS for 15 min at RT and rinsed with PBS at RT. Cells were pre-incubated for 30 min with normal goat serum (1:10) diluted in PBS at RT to saturate the nospecific binding sites and incubated with primary and secondary antibodies in order to evaluate intercellular adhesion. Nuclei were highlighted with 4', 6-diamidino-2-phenylindole dihydrochloride (DAPI 1:50000 dilution in bi-distilled water; 5 min of incubation at RT) (Prignano et al., 2015). The technical negative control was represented by the secondary antibody with PBS and without the primary one.

Proliferation rate (MTT)

Cell proliferation was evaluated using a method that is based on the tetrazolium salt formation, displayed by the color development (MTT assay) (Mosmann, 1983). For this purpose, cells were seeded at the density of 40000 cm^{-2} in 1 ml of their medium into 24-well plates (Greiner bio-one CELLSTAR®, Milan, Italy) and grown until 50% of confluence. Then medium was replaced with the same containing 10 µl of MTT (5 mg ml^{-1} of Thiazolyl Blue Tetrazolium Bromide, Sigma, USA) added into each well and incubated for 4 h at 37°C. Subsequently, the medium was replaced with 500 µl of dimethyl sulfoxide, followed by resuspension in order to disrupt the crystals formed inside the cells. After, absorbance due to the formazan production was measured at 570 nm (Wallac Victor^2 1420 Multilabel Counter, Perkin Elmer, Beaconsfield, UK) in order to estimate cell proliferation.

Isolation of cell brush border containing fraction (P2)

Cells were seeded in 75 cm^2 flasks until full confluence, then they were harvested in ice-cold physiological saline solution, washed three times and pelleted. Cell extraction protocol was performed as described (Schmitz et al., 1973; Zweibaum et al., 1985) with minor modifications. Briefly, cell pellets (6-7 mg at T0 and 18-25 mg at T6 of proteins) were homogenized with 1 ml ice-cold Tris/Mannitol buffer (2 mmol l^{-1} Tris, Mannitol 50 mmol l^{-1}, pH 7.1) and disrupted by ultrasonication in ice bath, to avoid protein and enzyme denaturation given by heat. The homogenate was added with $CaCl_2$ to a final concentration of 20 mmol l^{-1} and it was placed at 4°C for 10 min with frequent mixing. After this incubation period, centrifugation (10 min, 950 × g, 4 °C) was performed and the obtained supernatant was subsequently centrifuged (30 min, 33500 × g, 4 °C) to yield a small pellet (fraction P2) containing the brush border membranes. This pellet was finally resuspended with a small aliquot of Tris/Mannitol buffer in order to determine the enzyme activity assays and the protein content.

Alkaline Phosphatase assay (ALP)

The principle of this method is based on the chromogenic yellow p-nitrophenol (PNP) production, that follows the dephosphorylation of p-nitrophenylphosphate substrate (PNPP) by ALP. The reaction takes place at alkaline pH and in the presence Mg^{2+} ion, to allow the correct enzyme function. The color intensity produced by the reaction is proportional to the enzyme activity (Buras et al., 1995). The protocol presumes that ALP activity is assayed in 20 µl of P2 fraction (2-12 µg) previously obtained for each sample. The 20 µl were resuspended with double-distilled water in a final volume of 50 µl. 0.5 ml of a reaction mixture composed by 200 mM PNPP, sodium bicarbonate ($NaHCO_3$) 0.3 M, magnesium chloride ($MgCl_2$) 15 mM and doubly distilled water, was added in all samples. At the same time, two blanks and two standard solutions were prepared. The two blanks contained 50 µl of double distilled water and 0.5 ml of the reaction mixture. The two standard solutions contained respectively 10 and 100 nmol PNP and 0,5 ml of the reaction mixture before described devoid of PNPP. All samples and standards were prepared in triplicate and incubated, together with the blanks, at 37 ° C for 25 min, away from light sources. After 25 min, the reaction was stopped by the addition of 1 ml of a 0.1 N NaOH solution in each sample, standard and blank. The absorbance was measured at λ = 410 nm, by using a spectrophotometer (Spectrophotometer uniSPEC2, LLG Labware).

All the standard and the sample absorbance values were subtracted with those of the blank, in order to obtain the value due to the product presence. The standard absorbance was used in order to create the standard curve necessary to quantify the amount of product in each sample. The specific activity was expressed as mU mg^{-1} protein (where mU = nmol product / min of incubation); 1 unit (U) is defined as the enzyme activity that hydrolyzes 1µmol of substrate in one minute (Ferraretto et al., 2007). This procedure was applied for each enzyme assay. The protein content was measured by means of the Lowry method (Lowry et al., 1951).

Dipeptydil peptidase-IV (DPP IV) assay

This method is based on the reaction between the β-naphthylamine, a colorless aromatic amine produced by the hydrolysis of Gly-Pro-4-methoxy-β-naphthylamide by the DPP IV, and the Bratton-Marshall reagent called N-(1-naphthyl)ethylenediamine. This reaction leads to the formation of blue *azo*-dye.

In general the reaction of Bratton-Marshall consists in a diazotization of the primary amine group of an aromatic amine following the addition, in solution, of sodium nitrite ($NaNO_2$) and hydrochloric acid (HCl). This leads to the formation of a diazotized amine salt and nitrous acid (HNO_2) the excess of which is neutralized by the addition of ammonium sulfamate ($H_2NSO_3NH_4$). Following the Bratton-Marshall reagent (N-(1-naphthyl)ethylenediamine) is added in order to form an aromatic azo dye by the binding to the amine (Review et al., 2013).
This paper protocol presumes the specific activity assay of DPP IV in 1 µl of P2 (0.7-4.0 µg), previously obtained for each sample (Morita et al., 1983). The P2 fraction was resuspended in 400 µl of the reaction buffer, formed by Tris-HCl (50 mM and pH 8.4), and DPP IV substrate (Gly-Pro-β-naphthylamide) at final concentration of 2 mM. In contemporary were prepared two blanks, each containing 400 µl of the reaction buffer, and two standard solutions containing 3 µM and 50 µM of the DPP IV hydrolysis reaction product called β-naphthylamine in a final volume of 400 µl. All samples and standards were prepared in triplicate and incubated, together with the two blanks, at 37 ° C for 30 min, away from light sources. After 30 min, the reaction was stopped by adding 300 µl of trichloroacetic acid (TCA to 32%), in each blank, sample and standard. Since the product obtained from the hydrolysis reaction catalyzed by DPP IV is colorless, it has been used the reagent of to obtain a colored compound. After, according to the Bratton-Marshall reaction 100 µl of sodium nitrite 0,3%, 100 µl of ammonium sulfamate 1.5% and finally, the reagent N-(1-naphthyl)ethylenediamine 0,1% (in Ethanol 95%), were added in sequence in each blank, standards and samples. The absorbance was measured at 560 nm (Spectrophotometer uniSPEC2, LLG Labware) and enzyme activity was calculated according to a standard curve and expressed as mU/mg protein (Lowry et al., 1951).

Aminopeptidase N (APN) assay

The assay principle is based on the substrate L-alanine-p-nitroanilide hydrolysis by APN that leads to the L-alanine and p-nitroaniline (compound of yellow color) formation. The intensity of the color produced is proportional to the enzyme activity (Ferruzza et al., 2012).

The protocol provides for the specific APN assay in 10 µl of P2 fraction (7-40 µg) previously obtained for each sample. The P2 and 1 mM L-alanine-p-nitroanilide substrate were resuspended with the reaction buffer, consisting of 30 parts of PBS + and one part of Tris (10 mM) - NaCl (150 mM), in a final volume of 1000 µl. Two blanks, each containing 1 ml of the reaction buffer, and two standard solutions containing, respectively in a final volume of 1 ml, 10 µM and 100 µM of p-nitroaniline (the APN hydrolysis reaction product) were prepared. All samples and standards were prepared in triplicate and incubated, together with the blanks, at 37 ° C for 30 min, away from light sources. After 30 min, the reaction was stopped in ice for 10 min. The absorbance was measured at 405 nm and enzyme activities were calculated according to a standard curve and expressed as mU/mg protein.

Transepithelial electrical resistance (TEER)

The tight junctions are responsible of the intestinal epithelium paracellular permeability and its regulation. Increase and decrease of intestinal permeability is associated respectively to decrease or increase of the transepithelial electrical resistance (TEER).

In order to monitor presence and development of tight junctions, among cells, the co-culture and parental cells trans-epithelial electrical resistance (TEER) was measured at confluence (T0) and after 3 (T3), 6 (T6), 10 (T10) and 14 (T14) days of post-confluence, with the instrument (Figure 8 panel A).

A

B

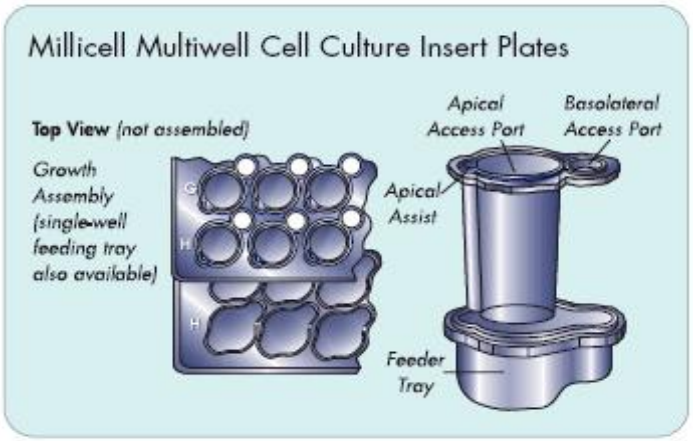

Figure 8. TEER instrument (panel A) and transwell (panel B).

For this purpose, 24-well plates (Figure 8 panel B) formed by an apical chamber, with a porous filter (0.7 cm^2), and a basolateral chamber were employed (transwell Millicell® Cell Culture Insert Plate PET 1 micron, 24 Millicell® Well Receiver Tray, Millipore Corporation, Billerica, MA 01821 USA).
Cells were seeded and maintained in their growth medium until the measure at all the time points above indicated. TEER values in the absence of cells were used as a blank and subtracted to the values correlated with the presence of the cells. Results were expressed in $\Omega \cdot cm^2$ and represented the main value from 3 to 6 chambers.

Statistical analysis

Statistically significant differences between two mean values were established by two-ways ANOVA followed by a Bonferroni post hoc t-test with the SPSS 20 statistical software (SPSS, Chicago, IL, USA). A p value <0.05 was considered significant and was represented by different letters for intra subject test, or symbols for inter subject test.

In detail, the Lysozyme is able to hydrolyze the β (1-4) glycosidic bond that binds the N-acetylmuramic acid residues of polysaccharides constituting the Gram positive wall thus preventing the bacteria spore germination during ripening.
The Trentin Grana cheese production does not require the lysozyme use and in this sense it is similar to the Parmigiano-Reggiano cheese.
During the ripening process, milk curd proteins (namely α_{s1}, α_{s2}, β and κ caseins) undergo an extensive degradation because of the endoproteases and exoproteases present in raw milk, in the rennet and released by the lactic bacteria present in the natural whey starter (Sforza et al., 2003).

Viability assay (MTT)

In order to assess the cell viability and the dose-tolerance threshold of the Caco2 and HT-29 cells in co-culture, following the administration of the Grana Padano and Trentin Grana digestates, the MTT viability assay (bromide 3-(4,5 -dimethylthiazol-2-yl) -2,5-diphenyltetrazolium) was used. The method is a colorimetric assay that assess the ability of mitochondrial dehydrogenases, in viable cells, to cut the MTT tetrazolium ring (yellow), with subsequent formation of formazan, visible through the formation of blue/purple crystals in cells. The amount of formazan produced was measured by a spectrophotometer and is directly proportional to the number of living cells (Twentyman et al., 1987).
Cells were plated at 40000 cells cm^{-2} in 24-well Multiwell and incubated overnight (37°C with 5% CO_2 in a humid environment). Subsequently, aliquots of 50-150-300 µl of the culture medium were replaced with the same amount of cheese digestates (for the samples) and fresh medium (for the controls). The treatment was performed after 2 and 24 hours, at 37°C and repeated in triplicate for each condition. At the end, the supernatant was removed from each well. 510 µl of MTT solution (10 µl of MTT and 500 µl of complete RPMI medium) was placed in all the wells, followed by an incubation for 3 h at 37°C. After that, the MTT solution was removed and replaced with 500 µl of dimethyl sulfoxide (DMSO), for 10 minutes at 37°C and under slow agitation, in order to solubilize the crystals inside the cells. After the incubation the absorbance of each well was red by a spectrophotometer (Wallac Victor2 1420 Multilabel Counter, Perkin Elmer) at 570 nm.

TEER measurement

TEER has also been used to evaluate various cell types as *in vitro* drug transport models (Artursson, 1990; Cho et al., 1989). Measurement of the transepithelial electrical resistance (TEER) in co-culture is used to monitor the integrity of the cell layer after direct contact with cheese digestates. Co-culture was seeded in complete RPMI-1640 medium in a 24 well plate (Transwell MillicellR Cell Culture Insert PET 1 mm, MillicellR 24 Well Receiver Tray, Millipore Corporation, Billeric, MA, USA) at 40000 cells cm^{-2} density and maintained until six days after the complete confluence. Then, 100 µl of growth medium was removed, the same volume of samples was added to the upper chamber and incubated for 2 and 24 hours. TEER was measured with a Millicell ERS system (Millipore Corporation). Blank was represented by TEER values in the absence of cells, while TEER values measured in cells not treated with cheese digestates were used as control.

Cytoplasmic calcium content misuration at single cell level

Cytoplasmic free calcium concentration $[Ca^{2+}]_i$, at a single-cell level was measured in co-culture cell model after treatment with two doses (100 µl and 200 µl) of GP or TN digestates. As a control blank of digestion was used at the same doses. Co-culture was seeded on a glass coverslips (24-mm diameter, thickness 0.13–0.17 mm) and loaded with 2.5 µM Fura-2 acetoxymethyl ester and 2.5 µM Pluronic F-127 in a Krebs-Ringer HEPES solution (KRH) containing: NaCl 125 mM, KCl 5 mM, KH_2PO_4 1.2 mM, $CaCl_2$ 2 mM, $MgSO_4$ 1.2 mM, glucose 6 mM and HEPES 25 mM, and were adjusted to pH 7.4 according to the procedure already described (Cosentino et al., 2010; Ferraretto et al., 2001) conventionally this buffer is namely KRH standard (KRH STD). As a further control, some experiments were carried out in nominally free calcium KRH buffer, in which the only difference respect to the KRH STD is the absence of $CaCl_2$.
The experiments were carried out by means of a thermostated (TC-202 A; Medical System Corporation, Harvard Apparatus, Holliston, MA, USA) perfusion chamber (PDMI-2, same commercial source) and a microscope (TE 200; Nikon, Tokyo, Japan) connected to a CCD intensified camera (Extended Isis; Photonic Science, Millham, UK). The fluorescence image acquisition and data analysis system (Applied Imaging; High Speed Dynamic Video Imaging Systems, Quanticell 700, Sunderland, UK) allowed to determine the $[Ca^{2+}]_i$ on single cells. The amount of intracellular free calcium, $[Ca^{2+}]i$, within the cells was calculated from the 340/380 nm images by means of a calibration performed with external standards of calcium and Fura-2, according to the equation of Grynkiewicz et al. (Grynkiewicz et al., 1985).

Induction of bone mineral matrix formation

Bone mineralization in human osteoblast-like cells was measured after cheese digestates administration.
In particular, Alizarin red stainings (ARS) (Jia-Li et al., 2014) was performed on Saos2 cells (human osteosarcoma cell line) at the end of 4 weeks of treatment with the basolateral compartment solution of transwells, colleted after the previously incubation of co-culture cells with digestates. This procedure simulate what happen after intestinal digestates absorption.
In detail, co-culture cells were plated on transwells (Transwell MillicellR Cell Culture Insert PET 1mm, MillicellR 24-Well Receiver Tray, Millipore Corporation, Billeric, MA, USA) and at six days of post-confluence were treated with 200 µl of digestates for 2 h. Later, the basolateral content mimicking the blood flow and representing the result of the intestinal absorption of digestates, was recovered and administered to Saos-2 cells in order to perform mineralization assay.
Saos-2 cells were plated in 12-well dishes at density of 50000 cells cm^{-2} in 4 ml of complete IMDM medium, until 70% of confluence. 800 µl of the basolateral compartment of transwells, above described, were added twice a week for 28 days. Further, in each wells 100 nM 1α, 25-Dihydroxy vitamin D3, (vit D) and 100 nM Dexamethasone (Dex) were added twice a week. At the same time, 50 µg ml^{-1} L-ascorbic acid and 10 mM β-glycerolphosphate, both acting as cell mineralization promoters, were added every day to all wells except the ones representing the negative control. Negative control samples were constituted by cells treated only with standard medium (CTR), while control was represented by cells treated with standard medium plus β-glycerophosphate and ascorbic acid (CTR plus). Blank was represented by wells with vehicles in absence of cells. After 4 weeks of treatments, cells were submitted to in vitro mineralization assay.

Evaluation of *in vitro* mineralization (Alizarin Red staining)

Saos-2 medium was removed and after, each well was washed with PBS, then 500 µl of 70% cold ethanol was added in for one hour at RT. Afterwards, wells were washed with deionized water and 500 µl of 40 mM Alizarin Red Solution were added at RT and all the samples were incubated and stirred in the dark for 20 min. The Alizarin Red staining solution was carefully aspirate and the cell monolayer was washed first with PBS and after with double distilled water. Extraction of calcium deposits was made with Cetylpyridinium chloride 10% (Sigma, C0732) for 30 minutes at RT to perform a quantitative mineralization analysis. Absorbance was measured at 550 nm (Kontron instruments Uvikon 922 spectrophotometer, Milan, Italy).

Results

CPPs DIGESTION AND THEIR ADMINISTRATION IN INTESTINAL-LIKE CELLS

LC-ESI-MS/MS.

After an analysis of the main molecular mass peptides derived from the *in vitro* digestion of CPPs, a number of short peptides from beta and alpha s1 casein were detected, most of which comprise one or more phosphorylated serines. In detail, peptides from beta casein mainly derive from the N-terminal portion as 1–25 or 33–55 polypeptide chain, while peptides from alpha casein come from the alpha s1 110–119 portion. Moreover, the peptides from beta casein are more abundant than those of alpha s1 casein and they are constituted by a smaller number of amino acids. In Table 9 these results are reported.

Parent protein	Position	Observed	M_r (expt)	M_r (calc.)	ppm	Peptide
Beta casein	1–6	394.7117	787.4078	787.4075	0.65	A.RELEEL.N
Beta casein	1–11	642.8264	1283.6362	1283.6357	0.98	A.RELEELNVPGE.I
Beta casein	1–16	953.4642	1904.9138	1904.9132	0.34	A.RELEELNVPGEIVESL.S + Phospho (S)
Beta casein	4–11	443.7116	885.4086	885.408	0.78	L.EELNVPGE.I
Beta casein	6–14	485.2662	968.5178	968.5179	−0.0052	E.LNVPGEIVE.S
Beta casein	6–16	625.3076	1248.6006	1248.6003	0.31	E.LNVPGEIVESL.S + Phospho (S)
Beta casein	7–16	568.7657	1135.5168	1135.5162	0.57	L.NVPGEIVESL.S + Phospho (S)
Beta casein	30–44	974.3999	1946.7792	1946.7782	1.61	K.IEKFQSEEQQQTEDE.L + Phospho (S)
Beta casein	33–45	845.8281	1689.6416	1689.6407	0.57	K.FQSEEQQQTEDEL.Q + Phospho (S)
Beta casein	33–48	1031.4194	2060.8242	2060.8212	1.5	K.FQSEEQQQTEDELQDK.I + Phospho (S)
Alpha s1 casein	41–70	971.2587	3881.0457	3881.0514	−0.5	L.SKDIGSESTEDQAMEDIKQMEAESISSSEE.I + 2 Oxidation (M); 7 Phospho (S)
Alpha s1 casein	43–58	972.3469	1942.6792	1942.6792	0.033	K.DIGSESTEDQAMEDIK.Q + oxidation (M); 2 Phospho (S)
Alpha s1 casein	109–118	590.7621	1179.5066	1179.506	1.08	Q.LEIVPNSAEE.R + Phospho (S)
Alpha s1 casein	110–118	534.2196	1066.4226	1066.422	0.53	L.EIVPNSAEE.R + Phospho (S)

TABLE 9. of the main molecular mass peptide identification from the enzymatically digested CPP sample by **L**C-ESI-MS/MS.

Laser light scattering

In order to characterize the Ca–CPP and Ca–dekCPP supramolecular complexes on the colloidal lengthscale and to follow their possible disaggregation upon digestion, the laser light scattering measurements were performed. Thanks to the interaction between negatively charged phosphorylated serines and positive divalent calcium ions, the aggregated structures are formed. In the present work, before digestion (pH 7.4), the fraction of calcium embedded within the aggregates is the same both for Ca–CPPs and Ca–dekCPPs, namely 2 Ca/CPPs mole/mole, as recalled before. For the CPPs bioactivity, the presence of aggregated structures is essential, as the fraction of calcium internalized by cells is actually the CPP-complexed calcium (Gravaghi et al., 2007; Cosentino et al., 2010a). Before digestion, both CPPs form aggregates with a similar average hydrodynamic radius and quite a high polydispersity (140 ± 25 nm).
Two experiments were designed to follow the evolution of the supramolecular complexes during the digestion process. In the first experiment, the solution pH was simply changed, from pH 7.4 down to pH 2 and back to neutral pH. The average overall size of the complexes was determined at the different stages of the experiment. These results may be fundamental to understand the behaviour of the supramolecular complexes, despite they obtained in the absence of digestive enzymes. In fact, the commercial CPPs here used, are produced by tryptic hydrolysis of sodium caseinate (Cosentino et al., 2010a) and they are similar to those produced by the enzymes operating along the physiological digestive process. In the second experiment, the *in vitro* digestion protocol, described in the Materials and methods section, is performed adding enzymes to the CPPs with the appropriate pH values. Laser light scattering experiments were performed on CPP solutions at the beginning, after acidification and/or pepsin addition, and at the end of the process. The measured size distribution of the CPP complexes at different pH values, characteristic of each digestion step, both for Ca–CPP (left side) and Ca–dekCPP (right side), is reported in Fig. 9. The complexes are classified into three size ranges (tens, hundreds and thousands of nm) and their relative importance is reported as relative scattered intensity. Results in Fig. 9 clearly show that, as compared to the initial stage (left bar in both groups), upon acidification the distribution shifts to smaller size (tens of nm) for both systems (central bar). As the pH is raised again, large aggregates quickly reform (right bar). This general behaviour is displayed by both systems.
The experiment performed on CPP solutions in the presence of different enzymes, pepsin and pancreatin at different pH, showed results in which the evolution of the overall size of the complexes is qualitatively similar. The interference of the scattered intensity coming from the enzyme preparations themselves, in this case, prevents a detailed assessment of the size distribution of the CPP complexes.

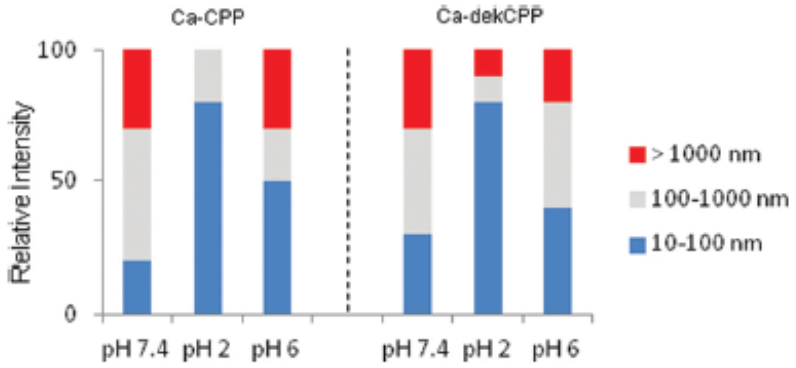

Figure 9 Size distribution of Ca–CPP (left side) and Ca–dekCPP (right side) complexes at different pH values, characteristic of each digestion step: initial, pH 2, pH 6. The complexes are classified as belonging to three size-ranges (tens, hundreds and thousands of nm) and their rela- tive importance is expressed as relative scattered intensity (%).

Small angle X-ray scattering (SAXS)

SAXS measurements assessed the internal structure of CPP complexes and its evolution during the digestion process. Spectra are reported in Fig. 10, both for Ca–CPPs and Ca–dekCPPs, at the three stages of simulated digestion, as before. The X-ray scattered-intensity profile, in the high-q region, corresponding to short distances within the aggregate (local structure), is similar for all spectra, showing a q−2 decay of I(q). This behaviour is characteristic of non-globular objects with fractal or entangled chain-like conformation. In the low-q region, corresponding to longer distances, the intensity profiles display a slight increase, relative to the overall structure of the aggregates, typically assessed by light scattering, as above. Although apparently not so far from the ones obtained on casein micelles, those results on the structure of CPP complexes (Bouchoux et al., 2010; De Kruif et al. 2012; Holt et al., 2003) nonetheless unravel interesting differences regarding the sites of calcium inclusion, connected to the absence, in Ca–CPPs, of excess phosphate.

Scattered intensity analysis has been performed following the model described in the Materials and methods section. We also tested and rejected the model developed for the internal structure of casein micelles, characterized by calcium phosphate nanoparticles reticulated in the peptide matrix (Bouchoux et al., 2010). The internal structure of the CPP + calcium complex was modelled as a collection of randomly condensing monomers. These monomers, the peptide chains, entangle thanks to the interaction of negatively-charged phosphorylated- serine residues and divalent positive calcium ions. On a local length scale, small compared to the mesh size of the entangled network, we could observe the structure of the individual flexible subchains. Results on the average radius of gyration of the subchains for the Ca–CPPs and Ca–dekCPPs are reported in Fig. 11 at different digestion steps: the initial condition (1), after acidification and pepsin action (2), and after pancreatin action. In addition, a shoulder is clearly visible in the SAXS intensity profile relative to the Ca–CPP sample in its initial state. The presence of inter-chain interactions between peptides that, in the entangled phase, assumes a preferential distance (d = 22 nm) confirm the experimental structure factor, reported in Fig. 10 and shows a peak (qpeak = 0.29 nm−1). Interestingly, after acidification and pepsin addition, this structure peak disappears, indicating that the internal structure of the Ca–CPP complexes becomes more flexible and irregular.

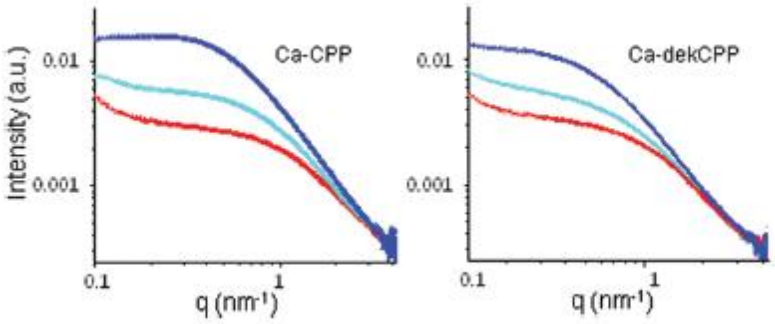

Figure 10. Ca–CPP (left) and Ca–dekCPP (right) SAXS spectra at different digestion steps: the initial state (blue), after gastric phase (cyan), and after intestinal phase (red). A shoulder is visible in the intensity profile corresponding to the initial state of Ca–CPPs. In the other spectra, the intensity profiles at low q display a slight increase, a sign of the aggre- gates' overall structure.

Effects of digested CPPs on intracellular calcium content

In differentiated Caco2 and HT-29 cells the changes in the intracellular calcium concentration, $[Ca^{2+}]_i$, induced by both Ca–CPPs and Ca–dekCPPs and their digested counterparts, all containing the same amount of calcium, were evaluated and analysed. In Fig.11 and 12, an example of the single cell responsiveness profiles to CPPs is reported. The percentage of the responsive cells, represent the effects of the different administrations, together with the increment in the cytoplasmic calcium concentration ($\Delta[Ca^{2+}]_i$), for any single cell and for the whole cell population (tot $[Ca^{2+}]_i$), and they are reported in Tables 9 and 10.

The administration of the Ca–CPP digested instead of its undigested counterpart produces calcium uptake in a higher fraction of Caco2 cells (70% vs. 15%), (Fig. 11 and Table 10) as well as a higher increase in the intracellular calcium concentration ($\Delta[Ca^{2+}]_i$, 45 ± 10 nM vs. 27 ± 9 nM). Between the undigested forms, Ca–dekCPP is more effective than Ca– CPP, both as a fraction of responding cells (26% vs. 15%) and as a $[Ca^{2+}]_i$ increase (40 ± 20 nM vs. 27 ± 9 nM). Digestion of Ca–dekCPP does not significantly alter the calcium uptake ($\Delta[Ca^{2+}]_i$) increment at single cell level, despite occurring in a smaller population of cells (18% vs. 26%). Interestingly, when digested complexes are supplied, the recovery of the intracellular calcium basal level occurs on much longer time scales, roughly fourfold. This feature is common to both Ca–CPPs and Ca–dekCPPs.

The administration of the digested Ca–CPP in HT-29 cells (Fig.12 and Table 11), again, produces a cellular response significantly higher than that produced by its undigested counterpart, both as a fraction of responsive cells (89% vs. 70%) and in the intracellular calcium increase (115 ± 19 nM vs. 76 ± 28 nM). As previously reported (Cosentino et al., 2010), the administration of the undigested Ca–dekCPP, induced a calcium uptake in a higher number of cells with respect to Ca–CPP (93% vs. 70%), with an overall extent reached by Ca–CPPs only after digestion. Reversely, digestion reduces the effectiveness of Ca–dekCPPs to promote the uptake of calcium (from 113 ± 59 to 79 ± 14 nM), although acting on the same fraction of cells (96% vs. 93%). The same features observed in Caco2 cells was shown in the kinetic profiles of the intracellular calcium concentration, i.e., a slower recovery of the basal level and a higher heterogeneity in the cell behaviour in the case of digested CPPs.

As a whole, these data indicate that digestion of Ca–CPPs results in an increment both in the number of cells responding with a calcium rise and in the amount of calcium taken up by the cell, ($\Delta[Ca^{2+}]_i$). If we compare the increase of the total intracellular calcium concentration reached after the administration of digested Ca–CPPs (tot $[Ca^{2+}]_i$) respect to its undigested counterpart, we can see that the Caco2 cells are notably higher in (778%) respect to HT-29 cells (192%), beyond the absolute values of the single measures in the two cell lines. Reversely, in the case of Ca–dekCPP, the digestion procedure depletes the overall increase in calcium uptake (tot $[Ca^{2+}]_i$), through a reduction either in the number of responsive cells or in the single-cell calcium increase, depending on the cell type. Anyway, results shown a reduction to less than 80% in both case (78% in Caco2 cells and 72% in HT-29 cells) (Table 10 and 11).

Treatments	% Responsive cells	$\Delta[Ca^{2+}]_i$ (nM)	tot $[Ca^{2+}]_i$ (nM)
Ca–CPPs	15	27 ± 9	405
Digested Ca–CPPs	70°	45 ± 10*	3150
Ca–dekCPPs	26°	40 ± 20*	1040
Digested Ca–dekCPPs	18^$	45 ± 13*	810

Table 10. Statistical analysis of Ca–CPP and Ca–dekCPP effects on calcium uptake in Caco2 cells before and after the simulated digestion process. The statistical significance for cell responsiveness (% responsive cells) was assessed using the χ^2 test: significantly different from Ca– CPP (°, $p < 0.005$); from digested Ca–CPP (^, $p < 0.005$); from Ca– dekCPPs ($, $p < 0.005$). The variations in the average single-cell intracellular calcium concentration ($\Delta[Ca^{2+}]_i$) were analyzed by Student's t-test (*significantly different from Ca–CPPs, $p < 0.01$). Each value represents the mean ± SD of 10–12 analogous experiments for at least 400 analyzed cells. Details of the calculations are reported in the Materials and methods section.

Treatments	% Responsive cells	$\Delta[Ca^{2+}]_i$ (nM)	tot $[Ca^{2+}]_i$ (nM)
Ca–CPPs	70	76 ± 28	5320
Digested Ca–CPPs	89°	115 ± 19*	10 235
Ca–dekCPPs	93°	113 ± 59	10 509
Digested Ca–dekCPPs	96°^	79 ± 14#	7584

Table 11. Statistical analysis of Ca–CPP and Ca–dekCPP effects on calcium uptake in HT-29 cells before and after the simulated digestion process. The statistical significance for cell responsiveness (% responsive cells) was assessed using the χ^2 test: significantly different from Ca– CPPs (°, $p < 0.005$); from digested Ca–CPPs (^, $p < 0.005$). The variations in the average single-cell intracellular calcium concentration ($\Delta[Ca^{2+}]_i$) were analyzed by Student's t-test (*significantly different from Ca–CPPs, $p < 0.01$); from digested Ca–CPPs (#, $p < 0.01$). Each value represents the mean ± SD of 6–8 analogous experiments for at least 500 analyzed cells. Details of the calculations are reported in the Materials and methods section.

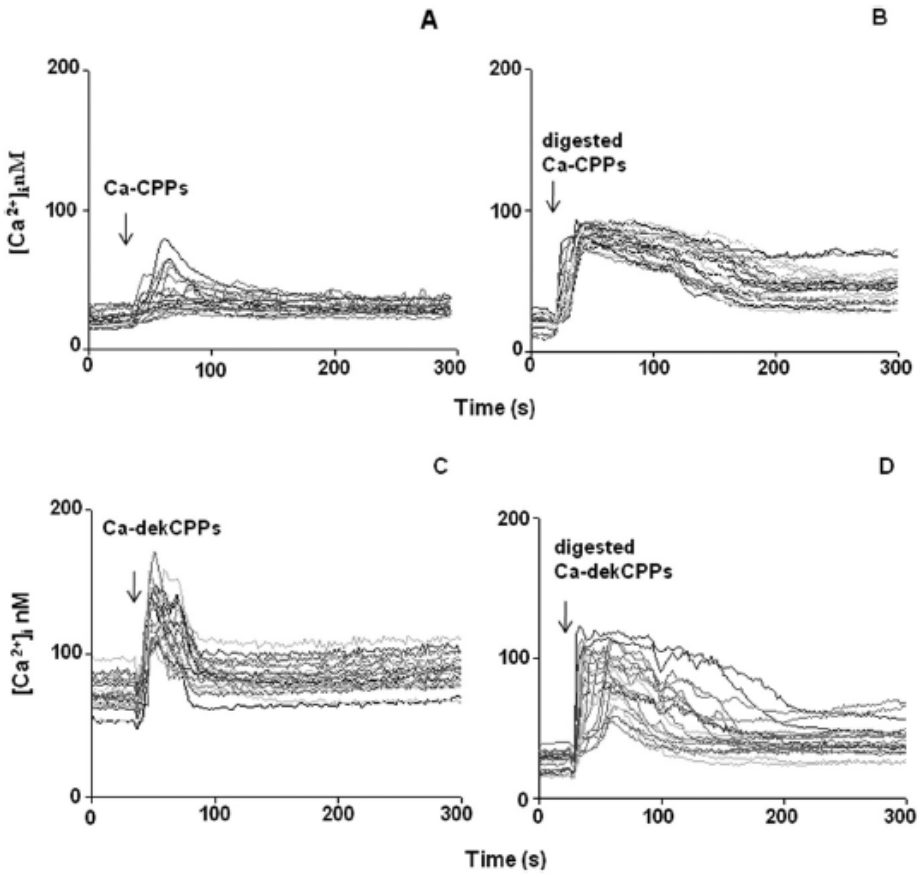

Figure 11. Effect of CPPs in Caco2 cells. The average change in cytosolic calcium, $[Ca^{2+}]_i$, after administration (1280 μM) of Ca–CPPs (A), digested Ca– CPPs (B), Ca–dekCPPs (C) and digested Ca–dekCPPs (D) is shown. Each graph represents the average behaviour of 10–12 independent experiments, each of them consisting of a minimum of 40–60 analysed cells.

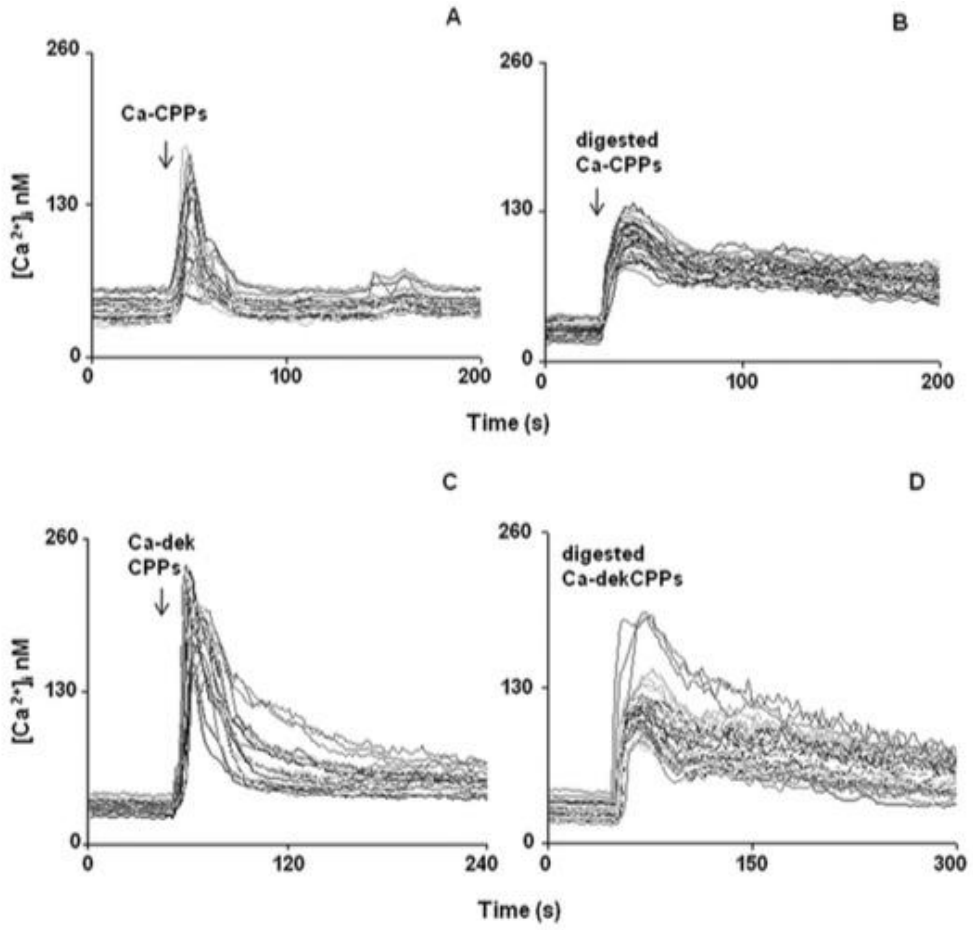

Figure 12. Effect of CPPs in HT-29 cells. The average change in cytosolic calcium, $[Ca^{2+}]_i$, after administration (1280 μM) of Ca–CPPs (A), digested Ca– CPPs (B), Ca–dekCPP CPPs (C) and digested Ca–dekCPPs (D) is shown. Each graph represents the average behaviour of 10–12 independent experiments, each of them consisting of a minimum of 70–90 analysed cells.

Data shown in figures 9-12 and in tables 9-11, are recently published (Perego et al., 2015).

GRANA PADANO AND TRENTIN GRANA CHEESES CHARACTERIZATION

After determination of proteins, lipids, calcium and humidity content in Grana Padano and Trentin Grana cheese samples, results shown a similar values to each other as represented in the table 12. In details, the average content is of 31.57% for protein, 26.75 % for lipids, 0.888 % for calcium and 34.13% for humidity.

SAMPLES	Proteins %	Lipids %	Calcium %	Humidity %
GP 13 months	31.72	27.5	0.891	34.63
GP 19 months	31.53	27	1.004	35.85
GP 26 months	32.58	28	0.844	30.21
TN 13 months	30.55	25	0.818	36.10
TN 19 months	31.62	25.5	0.863	36.06
TN 26 months	31.41	27.5	0.913	31.93

Table 12. Characterization of GP and TN cheese samples. Data are expressed as a percentage (g/100 g of grated cheese as such) and represent the assay results carried out in duplicate (proteins) or single (lipids, humidity and calcium).

Furthermore, the main differences are present only for humidity values between samples at low and high period of ripening, in both cheese typology, while they are similar between low and medium period of aging.

Caseinophosphopeptides (CPPs) released upon *in vitro* gastrointestinal digestion of Grana Padano and Trentin Grana cheeses. A qualitative point of view.

The *in vitro* gastrointestinal digestion of the GP and TN cheeses at 13, 19 and 26 months of ripening was performed according Perales et al., (Perales et al., 2005). Subsequently, the selective precipitation of CPPs from digestates was carried out at two different pH values (4.6 and 8.0) since it is known that selective precipitation can be a source of qualitative and quantitative changes (Cruz-Huerta et al., 2015). Indeed, it has been reported that at pH 4.6 di- and tri-phosphorylated peptides (including those containing the phosphorylated cluster sequence sssEE) selectively precipitated from a tryptic digest of casein. At pH 8.0, all of the cluster peptides and the diphosphorylated peptides as well as the monophosphorylated peptides containing the sequence sEE precipitated, but the other monophosphorylated peptides containing the sequence sAEE and EsTE did not (Cruz-Huerta et al., 2015; Reynolds et al., 1994).

Six different gastrointestinal digestate CPP-enriched extracts were obtained. They were further fractionated by reverse phase ultra-performance liquid chromatography (RP-UPLC), and the CPPs were identified by high resolution mass spectrometry (Michalski et al., 2011) maximizing peptide identification using data-dependent acquisition (Bateman et al., 2014). The superior sensitivity of HR-MS/MS technique guarantees the identification of the vast majority of the peptides of interest (Maarten Altelaar & Heck, 2012).
The HR-MS total ion current (TIC)-chromatographic profiles of CPP-enriched extracts (at the same pH value) of both cheese digestates were highly similar at the same ripening age (Figure 13 A and B). This "peptidic fingerprint" similarity can be justified by the quite analogous proteolytic phenomena that occur in both cheeses during ripening (Mucchetti & Neviani, 2006). During RP-UPLC separation, many CPPs co-eluted (Supplementary data Table S1), and not phosphorylated peptides co-eluted with the CPPs (data not shown). Therefore, relative semi quantitation of CPPs as described by Dupas et al. (Dupas et al., 2009) or Cruz-Huerta et al. (Cruz-Huerta et al., 2015) was not feasible.
A total of 279–346 CPPs were revealed, of which 130–170 corresponded to α_{S1}-CN, 55–79 to α_{S2}-CN, 72–95 to β-CN, and 2–6 to κ-CN depending on cheese type, ripening period and casein fraction (Table 13). The length of CPPs, released upon *in vitro* gastrointestinal digestion of both cheeses, varied from 6 to 24 amino acids. It should be noted that 10–18 of the 24–46 total identified tri-phosphorylated CPPs presented the sequence sssEE (pSer-pSer-pSer-Glu-Glu), the characteristic Ca^{2+} binding motif (Table 14; Ferraretto et al., 2001; Nongonierma & FitzGerald, 2015). The different CN fractions present this cluster at different sites of their primary sequence: α_{S1}-CN f(66–70), α_{S2}-CN f(8–12), α_{S2}-CN f(56–60) and β-CN f(17–21). The above-mentioned motif was revealed in CPPs deriving from both α-CN and β-CN. (Park et al., 1998) have reported that CPPs derived from α-CN exhibit greater calcium binding affinity (measured by a calcium selective electrode) than β-CN-derived CPPs. In our cheese digestates, 198–245 CPPs derived form α-CNs (3–8 containing sssEE motif) and 72–95 from β-CN (7–12 containing sssEE motif).

Taken together this data shown a similar peptidic profile between the different digestates. No significant biological difference appeared between the digestates derived by the two cheese types.

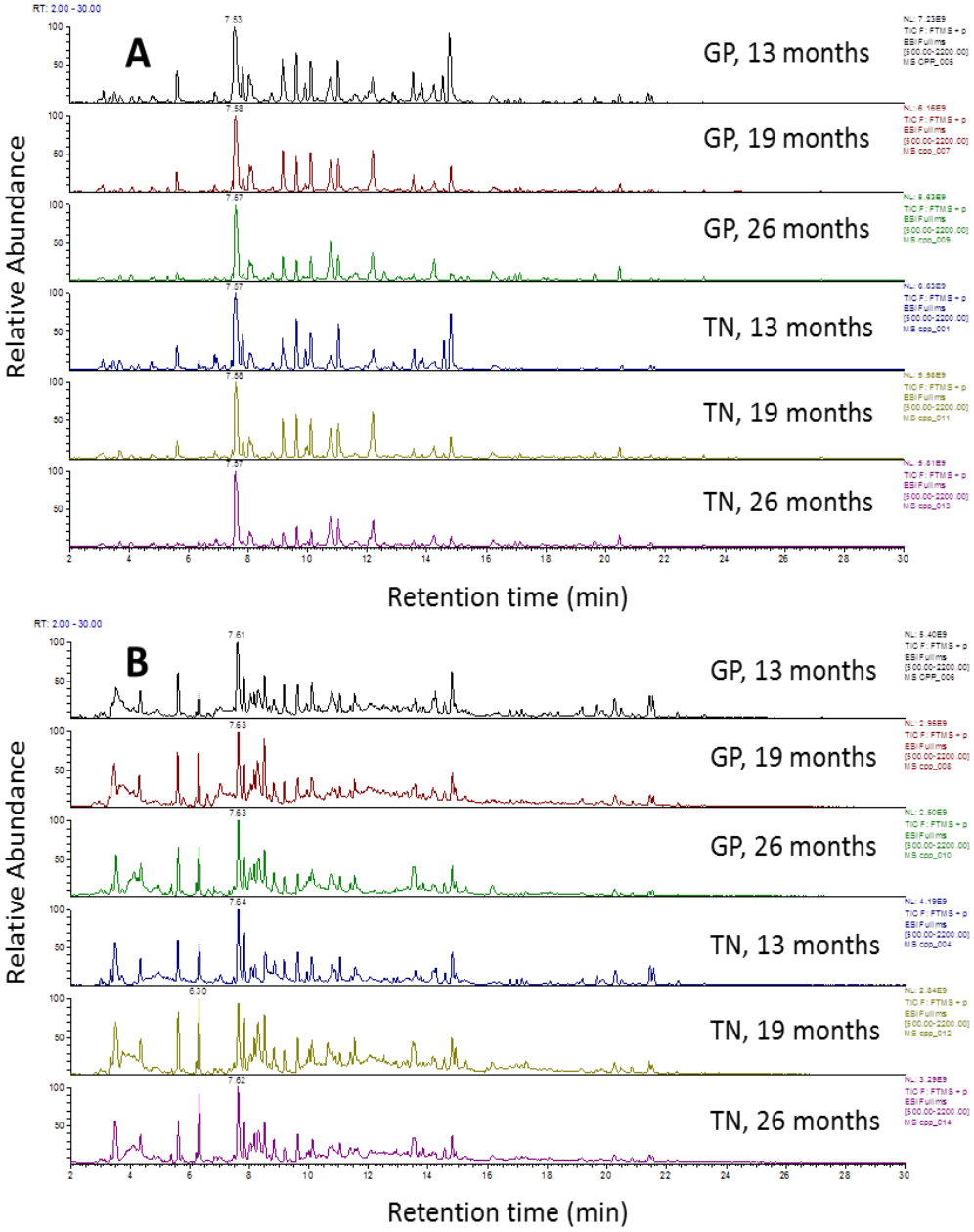

Figure 13. HR-MS total ion current (TIC) profiles of Grana Padano (GP) and Trentin Grana (TN) digestates (digestion protocol according Perales et al., 2005) after CPP enrichment by selective precipitation at pH 8.0 (**A**) or pH 4.6 (**B**). Months of ripening are indicated for each cheese sample.

Cheese	Age of ripening (months)	α_{S1}-CN	α_{S2}-CN	β-CN	κ-CN	Total
GP	13	166 (sssEE–2)	79 (sssEE–4)	95 (sssEE–9)	6 (sssEE–0)	346 (sssEE–15)
	19	170 (sssEE–2)	55 (sssEE–4)	87 (sssEE–9)	3 (sssEE–0)	315 (sssEE–15)
	26	144 (sssEE–2)	67 (sssEE–6)	72 (sssEE–10)	5 (sssEE–0)	288 (sssEE–18)
TN	13	130 (sssEE–1)	78 (sssEE–2)	87 (sssEE–7)	6 (sssEE–0)	301 (sssEE–10)
	19	134 (sssEE–1)	64 (sssEE–5)	78 (sssEE–10)	4 (sssEE–0)	280 (sssEE–16)
	26	145 (sssEE–2)	59 (sssEE–4)	73 (sssEE–12)	2 (sssEE–0)	279 (sssEE–18)

Table 13. Number of CPPs identified in enriched extracts of Grana Padano (GP) and Trentin Grana (TN) digestates at different age of ripening. sssEE, pSer-pSer-pSer-Glu-Glu amino acid motif-containing CPPs.
1P, mono-phosphorylated CPPs; 2P, bi-phosphorylated CPPs; 3P, tri-phosphorylated CPPs; sssEE, pSer-pSer-pSer-Glu-Glu amino acid motif-containing CPPs.

Cheese	Age of ripening (months)	α_{S1}-CN	α_{S2}-CN	β-CN
GP	13	f(65-74) l**sssEE**IVPN f(65-79) l**sssEE**IVPNSVEQK	f(1-12) KNTMEHV**sssEE** f(7-13) V**sssEE**S f(8-13) **sssEE**S f(56-61) **sssEE**S	f(15-24) SL**sssEE**SIT f(15-25) SL**sssEE**SITR f(16-22) L**sssEE**S f(16-24) L**sssEE**SIT f(16-25) L**sssEE**SITR f(16-26) L**sssEE**SITRI f(17-22) **sssEE**S f(17-24) **sssEE**SIT f(17-25) **sssEE**SITR
	19	f(65-74) l**sssEE**IVPN f(65-79) l**sssEE**IVPNSVEQK	f(1-12) KNTMEHV**sssEE** f(7-13) V**sssEE**S f(8-13) **sssEE**S f(56-61) **sssEE**S	f(15-24) SL**sssEE**SIT f(15-25) SL**sssEE**SITR f(16-22) L**sssEE**S f(16-24) L**sssEE**SIT f(16-25) L**sssEE**SITR f(16-26) L**sssEE**SITRI f(17-22) **sssEE**S f(17-24) **sssEE**SIT f(17-25) **sssEE**SITR
	26	f(64-74) SI**sssEE**IVPN f(65-74) l**sssEE**IVPN	f(1-12) KNTMEHV**sssEE** f(1-19) KNTMEHV**sssEE**SIISQET f(7-13) V**sssEE**S f(7-16) V**sssEE**SIIS f(8-13) **sssEE**S f(56-61) **sssEE**S	f(6-24) LNVPGEIVESL**sssEE**SIT f(15-22) SL**sssEE**S f(15-24) SL**sssEE**SIT f(15-25) SL**sssEE**SITR f(16-22) L**sssEE**S f(16-24) L**sssEE**SIT f(16-25) L**sssEE**SITR f(17-22) **sssEE**S f(17-24) **sssEE**SIT f(17-25) **sssEE**SITR
TN	13	f(65-74) l**sssEE**IVPN	f(1-12) KNTMEHV**sssEE** f(7-13) V**sssEE**S	f(15-25) SL**sssEE**SITR f(16-22) L**sssEE**S f(16-24) L**sssEE**SIT f(16-25) L**sssEE**SITR f(16-26) L**sssEE**SITRI f(17-24) **sssEE**SIT f(17-25) **sssEE**SITR
	19	f(65-74) l**sssEE**IVPN	f(1-12) KNTMEHV**sssEE** f(7-13) V**sssEE**S f(8-13) **sssEE**S f(53-70) SIG**sssEE**SAEVATEEVK f(56-61) **sssEE**S	f(15-22) SL**sssEE**S f(15-24) SL**sssEE**SIT f(15-25) SL**sssEE**SITR f(16-22) L**sssEE**S f(16-24) L**sssEE**SIT f(16-25) L**sssEE**SITR f(16-26) L**sssEE**SITRI f(17-22) **sssEE**S f(17-24) **sssEE**SIT f(17-25) **sssEE**SITR
	26	f(64-74) SI**sssEE**IVPN f(65-74) l**sssEE**IVPN	f(1-12) KNTMEHV**sssEE** f(7-13) V**sssEE**S f(8-13) **sssEE**S f(56-61) **sssEE**S	f(6-24) LNVPGEIVESL**sssEE**SIT f(12-25) IVESL**sssEE**SITR f(15-22) SL**sssEE**S f(15-24) SL**sssEE**SIT f(15-25) SL**sssEE**SITR f(16-22) L**sssEE**S f(16-24) L**sssEE**SIT f(16-25) L**sssEE**SITR f(16-26) L**sssEE**SITRI f(17-22) **sssEE**S f(17-24) **sssEE**SIT f(17-25) **sssEE**SITR

Table 14. Casein phosphopeptides containing the amino acid motif sssEE (pSer-pSer-pSer-Glu-Glu) identified in enriched extracts of Grana Padano (GP) and Trentin Grana (TN) digestates at different age of ripening.

CO-CULTURE CHARACTERIZATION

Transmission electron microscopy analysis (TEM)

Ultrastructural observations of parental Caco2 RPMI cells and co-culture are summarized in Table 15 and 16.
From the morphological point of view, the cultured cells are in continuous remodeling with the post-confluence day advancement.
In detail, upon reached confluence, the HT-29 cells are organized in a discontinuous monolayer and exhibit mucus, but are absent cell junctions and microvilli (Figure 14). On the contrary, the Caco-2 cells EMEM, organized in continuous monolayer, show many microvilli, abundant junctions, but the absence of mucous secretions (Figure 15). Similarly, in the culture of Caco-2 cells RPMI mucus is not present. These cells, also arranged in a single layer continuous, they show few junctions and sporadic microvilli (Figure 16).
On the 3rd day of post-confluence, the Caco-2 monolayer in RPMI remain organized, have no junctions, but mucus and sporadic microvilli. However, after six post-confluence days are present junctions, particularly desmosomes; microvilli increased and mucous secretions persist. Also, at this point, the cells begin to organize into multi-layer and *domes* are evident, index of polarized epithelium. This organization is also visible on the 10th day of post-confluence where the junctions decrease, but mucous secretions and the microvilli are more abundant compared to the previous stages. After 14 days of post-confluence, joints remain similar to the T10, the microvilli decrease and mucous secretions are abundant. Also, at this stage the multilayer is continuous.

CELL LINES, POST-CONFLUECE DEGREE	CELLULAR JUNCTIONS	MICROVILLI	MUCUS	CELL ARRANGEMENT
HT-29, T_0	-	-	+	Discontinuous monolayer
Caco-2 EMEM, T_0	++	++	-	Continuous monolayer
Caco-2 RPMI, T_0	±	scattered	-	Continuous monolayer
Caco-2 RPMI, T_3	-	scattered	+	Continuous monolayer
Caco-2 RPMI, T_6	+ (Desmosomes)	+	+	Continuous monolayer with multilayer
Caco-2 RPMI, T_{10}	±	++	++	Continuous monolayer with multilayer
Caco-2 RPMI, T_{14}	±	±	++	Multilayer

Table 15. Morphological and ultrastructural characteristics of the Caco-2 and HT-29 parental cell lines at different post-confluence days. The symbols + and - indicate respectively the presence or absence of a particular cellular structure.

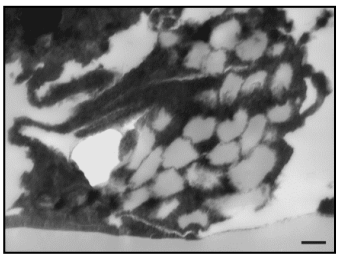

Figure 14: HT-29 T_0, (30000x).
Evident mucus granules.

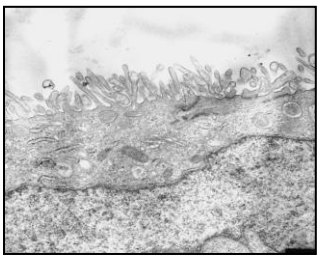

Figure 15: Caco-2 EMEM T_0, (5000x).
Evident junctions and abundant microvilli

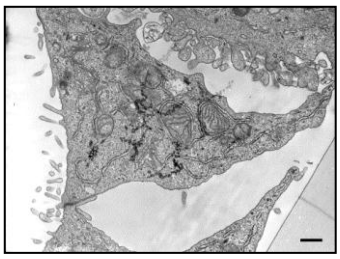

Figure 16: Caco-2 RPMI T_0, (10000x).
Discrete level of junctions and sporadic microvilli.

CELL LINES, POST-CONFLUECE DEGREE	CELLULAR JUNCTIONS	MICROVILLI	MUCUS	CELL ARRANGEMENT
T_0	±	±	±	Continuous monolayer
T_3	+	+	+	Continuous monolayer
T_6	+	+	+	Multilayer
T_{10}	+	++	-	Multilayer
T_{14}	++ (Desmosomes)	++	-	Multilayer

Table 16: Morphological and ultrastructural characteristics of co-culture at different degrees of post-confluence. The symbols + and - indicate respectively the presence or absence of a particular cellular structure.

At the confluence achievement, co-culture is organized in a cell monolayer and it presents continuous and discrete quantities of microvilli, junctions and mucous secretions (Figure 17). After 3 days of post-confluence, an increase of microvilli, mucus and junctions are visible. On the 6th day of post-confluence the morphological characteristics remain similar and in addition the cells have organized into multilayer (Figure 18). The multilayer persists even after 10 days of post-confluence, but at this stage is not longer visible mucus and an increase of microvilli is highlighted instead. After 14 days of post-confluence, cells are still organized in multilayer, with obvious junctions, including desmosomes, abundant microvilli, but are not visible mucous secretions (Figure 19). The data are summarized in table 14.

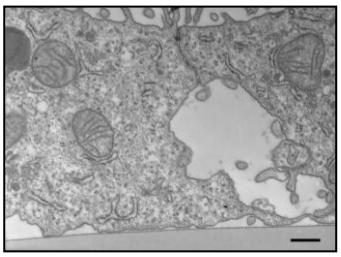

Figure 17: Co-culture T_0, (15000x). Discreet presence of junctions, microvilli and mucous secretions.

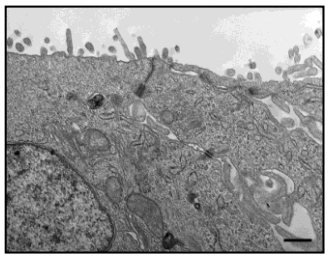

Figure 18: Co-culture T_6, (15000x). Evidence of junctions, microvilli and mucous secretions.

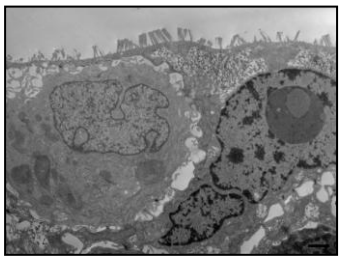

Figure 19: Co-culture T_{14}, (5000x). Aboundant junctions and microvilli.

Immunofluorescence analysis of intercellular adhesion

The tight junctions are a specific markers of the intact and functional intestinal epithelium. The tight junctions formed by co-culture, were observed by fluorescence microscopy after treatment with specific antibody for the occludin, that is a part of the junction protein structure. The same procedure was applied to the Caco-2 RPMI and EMEM cell cultures. figures 20, 22 and 23 are related to cell cultures examined at the 6th day of post-confluence. Furthermore, the presence of desmosomes in co-culture at T14 has been verified (Figure 21), to consolidate the data obtained by TEM. In this case the desmocollin-2 is the marker protein.
In all types of culture (Figures 20, 22, 23) the presence of the tight junctions between the cells is evident thanks to the contour green coloring. In co-culture at T14 protein desmocollin-2 is evident thanks to the green dyeing (figure 21). The nuclei are visible in blue thanks to DAPI. Moreover, the dyeing allows to observe the cell partial arrangement of the co-culture multilayer (figure 21 and 22) and of the Caco-2 RPMI cells (Figure 22), that are organized into *domes*.

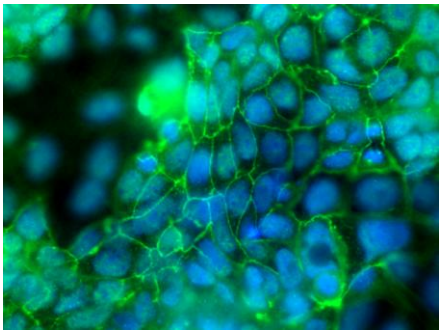

Figure 20: co-culture at 6th post-confluence day (60x). The green outline identifies the presence of occludin, proteins of the intercellular tight junctions. In blue the nucleus is evident by DAPI. The color highlights the arrangement of the multi-layer cells arranged in *domes.*

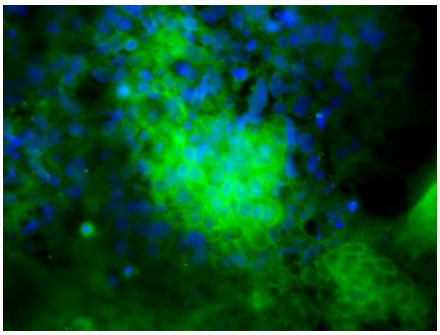

Figure 21: co-culture on 14th post-confluence day (40x). The green coloration identifies the presence of the protein of the desmosomes desmocollin-2. In blue the nucleus is evident by DAPI. The color highlights the arrangement of the multi-layer cells arranged in *domes.*

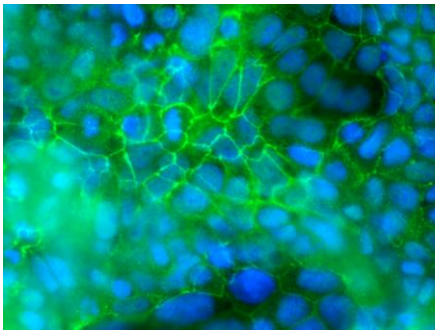

Figure 22: Caco-2 RPMI cells on 6th post-confluence day (60x). The green outline identifies the presence of occludin, proteins of the intercellular tight junctions. In blue the nucleus is evident by DAPI. The color highlights the arrangement of the multi-layer cells arranged in *domes.*

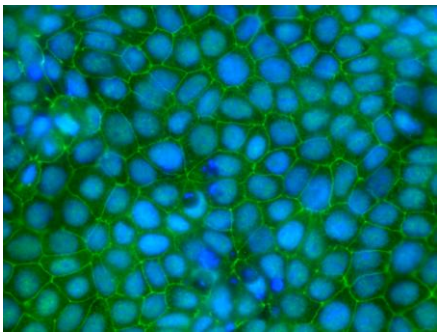

Figure 23: Caco-2 EMEM cells on 6th day of post-confluence (60x). The green contour identifies the presence of occludin, a protein of intercellular tight junctions. In blue the nucleus is evident by DAPI. The color highlights the arrangement of the multi-layer cells arranged in *domes.*

Proliferation rate (MTT)

MTT viability assay revealed that, at full confluence (T0), HT-29 cells were the most proliferative respect to both co-culture and Caco2 cells ($p<0.01$) in both growth media. In fact, from the statistical point of view, the proliferative rate of HT-29 is significantly higher than in all other cell cultures ($p <0.01$), while there are not differences in proliferative activity of Caco-2 cells with any growth medium and between Caco-2 cells compared to culture (Figure 24).

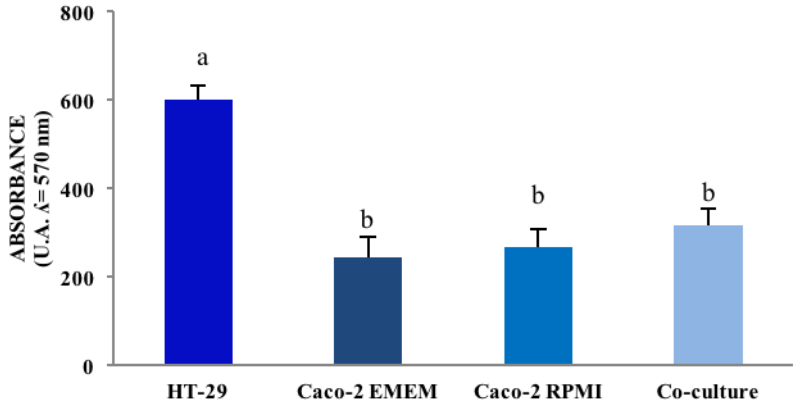

Figure 24: Viability of different cell cultures reached confluence. The values represent the averages of 3 independent experiments, each of which has provided 3 wells for each culture type. The different letters indicate statistically significant differences.

Specific activity of the Alkaline Phosphatase enzyme (ALP)

Following isolation from the original homogenate (H), the enzyme assays were performed on the cellular fraction (P2), containing the cellular brush border at different post-confluence degrees.
The specific activity of Alkaline Phosphatase showed an increase from the confluence day (T0) to the 14th day of post-confluence (T14) in both cultures. For each post-confluence days examined, the Alkaline Phosphatase specific activity of Caco-2 RPMI cells is higher than co-culture, but this difference was statistically significant only at T0, ($p < 0.05$) (Figure 25).
Analyzing in detail the progress of the Alkaline Phosphatase activity in co-cultures, it shows a statistically significant increases between the confluence day (T0) and the maximum times of post-confluence T10 and T14, ($p < 0.05$). The increase is not statistically significant in the intermediate stages of post-confluence (figure 25).
As for the alkaline phosphatase specific activity of Caco-2 RPMI, there is a first statistically significant increase ($p < 0.05$) between the 3rd (T3) and the 6th (T6) day of post-confluence. At 10th post-confluence day there is a slowdown in growth while the enzyme activity peak occurs after 14 days from the confluence (T14), reaching a statistically significant value compared to the other ($p < 0.05$) (figure 25).

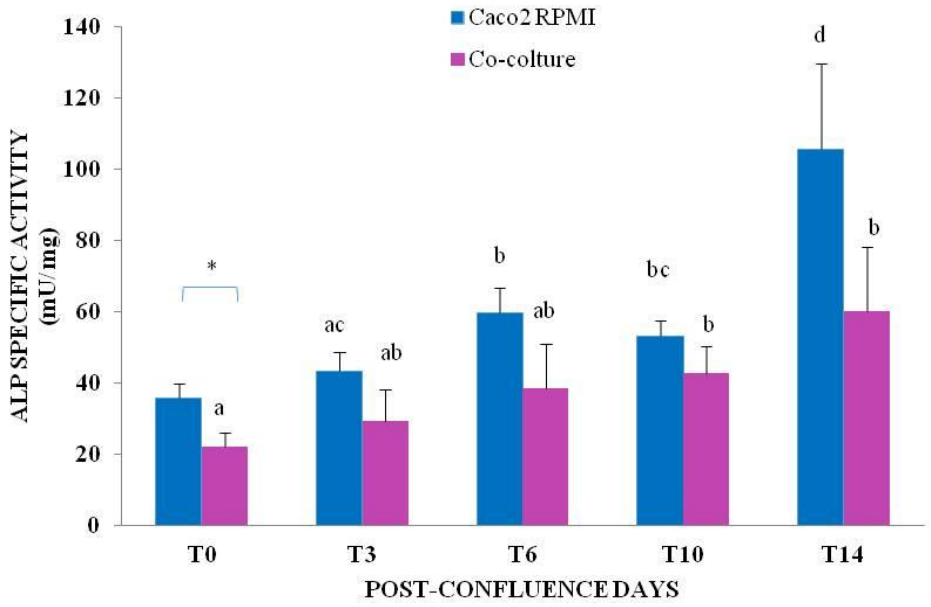

Figure 25. Alkaline phosphatase activity of parental cell line (Caco2 RPMI) and co-culture, from 0 to 14 days of post-confluence. Different letters indicate statistical significant differences within subject, while symbol * indicates statistical significant differences ($p \leq 0.05$) between subjects (two way ANOVA).

Specific activity of the Amino peptidase N enzyme (APN)

The APN enzyme values show a growing trend advancing with the post-confluence days. However, beyond the trend, there are not statistically significant differences between the values given by Caco2, while for the co-cultures statistically significant differences appear only between T0 and T14 (Figure 26).

Moreover, even if the values of the Caco2 cells appear higher than the co-cultures, in reality there are no significant statistically differences between the two culture types.

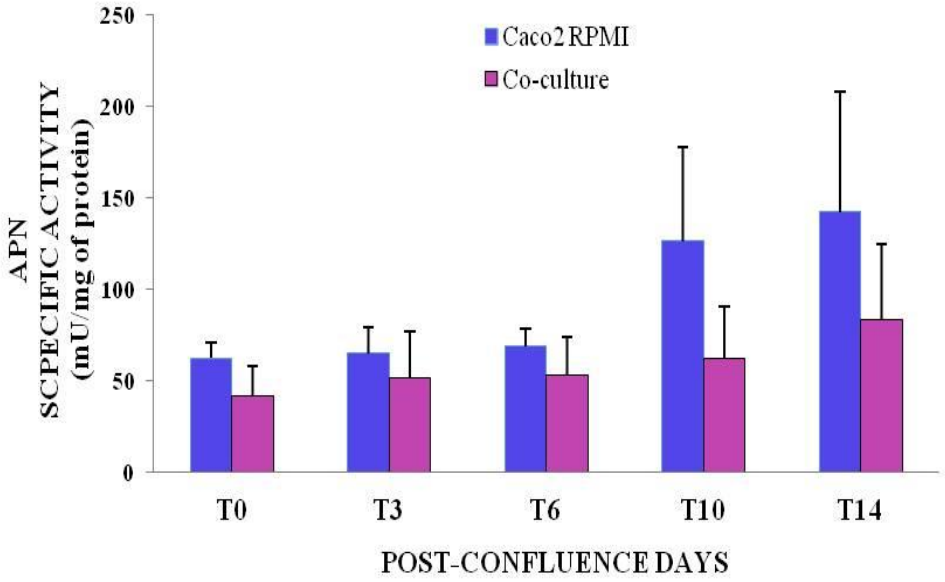

Figure 26. Amino Peptidase N activity in co-culture from 0 to 14 days of post-confluence. Different letters indicate statistical significant differences within subject (two way ANOVA).

Specific activity of the Dipeptidyl peptidase IV enzyme (DPP IV)

As for APN results, the values of DPP IV enzyme show a growing trend advancing with the post-confluence days, but there are not statistically significant differences between the values given by Caco2, while for the co-cultures statistically significant differences appear between T0 and T10 and between T0 and T14 (Figure 27).

Also for this enzyme activity, even if the values of the Caco2 cells appear higher than the co-cultures, no significant statistically differences are present between the two culture types.

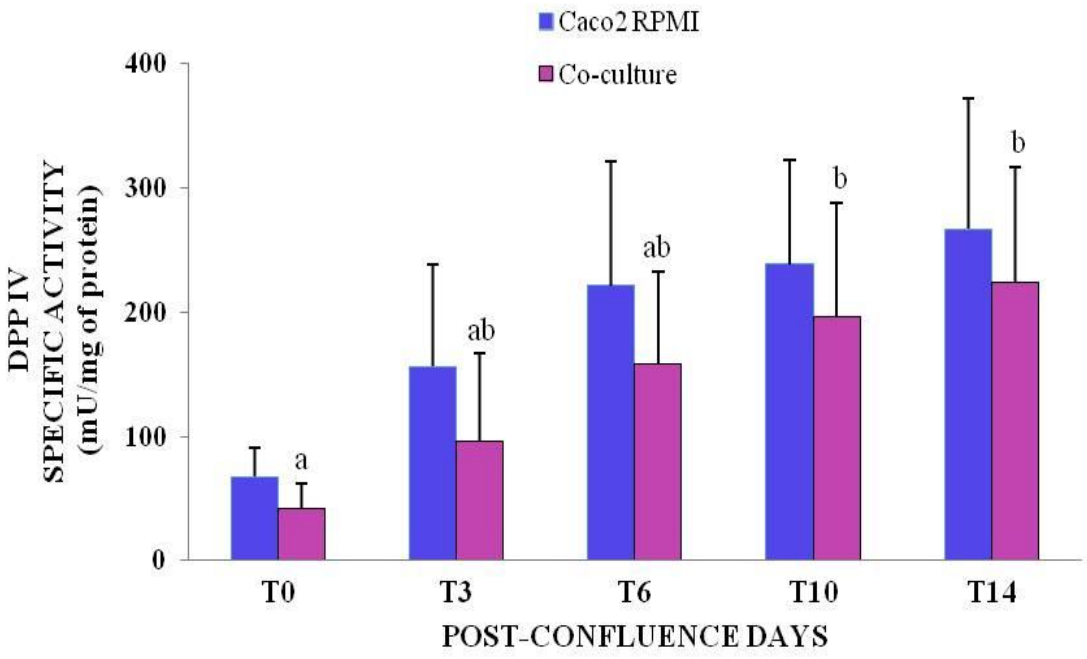

Figure 27. Dipeptidyl peptidase IV activity in co-culture from 0 to 14 days of post-confluence. Different letters indicate statistical significant differences within subject (two way ANOVA).

Transepithelial electrical resistance (TEER)

The transepithelial electrical resistance, given by the tight junctions, makes a significant contribution to the barrier function exercised by the intestinal epithelium. In fact, the tight junctions are involved in the paracellular transport regulation and their functionality may be affected by molecules present in the intestinal lumen.

For this reason, the electrical resistance monitoring over time, is fundamental for the choice of an *in vitro* model of intestinal epithelium that can simulate the interactions between itself and the food derived molecules.

TEER values of all types of culture show an increase from the confluence day (T0) until the 6th post-confluence day (T6), in which reaches the maximum values (Figure 28). Despite this similarity, the three types of culture trends show obvious differences. In fact, the co-culture presents TEER values comprised between 24 and 94 Ωcm^2, lower than those of both Caco-2 cell cultures. Caco-2 EMEM instead have the highest values, from 17-532 Ωcm^2, with a sharper peak at T6. Caco-2 RPMI TEER values have an intermediate pattern, from 26 to 182 Ωcm^2. These differences are confirmed by statistical analysis that reveals significant differences ($p < 0.01$) between the three cultures in each degree of confluence, except between Caco-2 cells and the RPMI co-culture at T0 (Figure 28) By analyzing the individual cell culture, the TEER values are always significantly higher respect to the confluence day (T0) ($p < 0.01$). The TEER increase is statistically significant also from the 3rd to 6th ($p < 0.01$) and between the 3rd and the 10th post-confluence day ($p < 0.01$ for the Caco-2 EMEM and $p<0,05$ for Caco-2 RPMI and co-culture). Subsequently to T6, the TEER trend changes within each culture and also between the three culture types. In fact, only the Caco-2 EMEM cells shows a clear and significant TEER decrease at T14, where the value shows a statistically significant difference compared to T6, ($p < 0.05$). Caco-2 RPMI and co-culture after 6th post-confluence day showed a plateau of TEER values. In fact, there is the absence of significance between T6, T10 and T14 values (Figure 28).

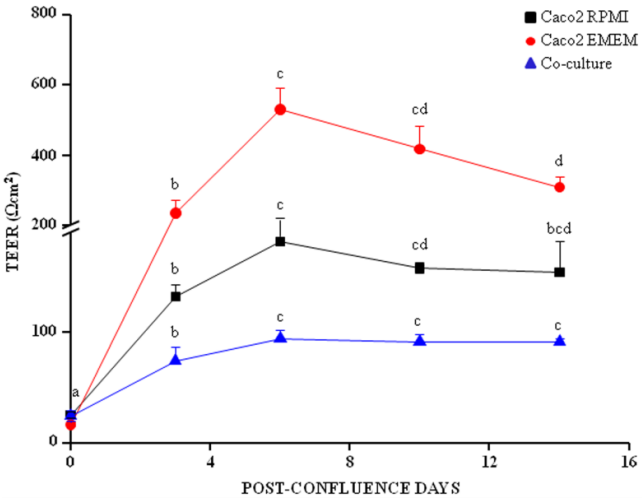

Figure 28, TEER values of parental cell lines (Caco2 RPMI and Caco2 EMEM) and of co-culture at different post-confluence stage (from T0 to T14). At different letters correspond a significant statistical differences within the same culture.

Protein assay

Protein content of the homogenate (µg/µl) of both co-culture and Caco-2 RPMI cells, expressed as the total amount of proteins in cell homogenate (H) at different post-confluence days, increases from the full confluence day (T0) to 14 days of post-confluence (T14). The progressive increase of the protein density shows a regular and similar trend for the two types of culture. In particular, a more rapid increase was detected from T0 to T6 and from T10 to T14 (Figure 29). These intervals describe a more rapid increase in protein.

Protein concentration of the cell homogenate increases from T0 to T14 progressively and similarly in co-culture and Caco2 RPMI (Figure 29).

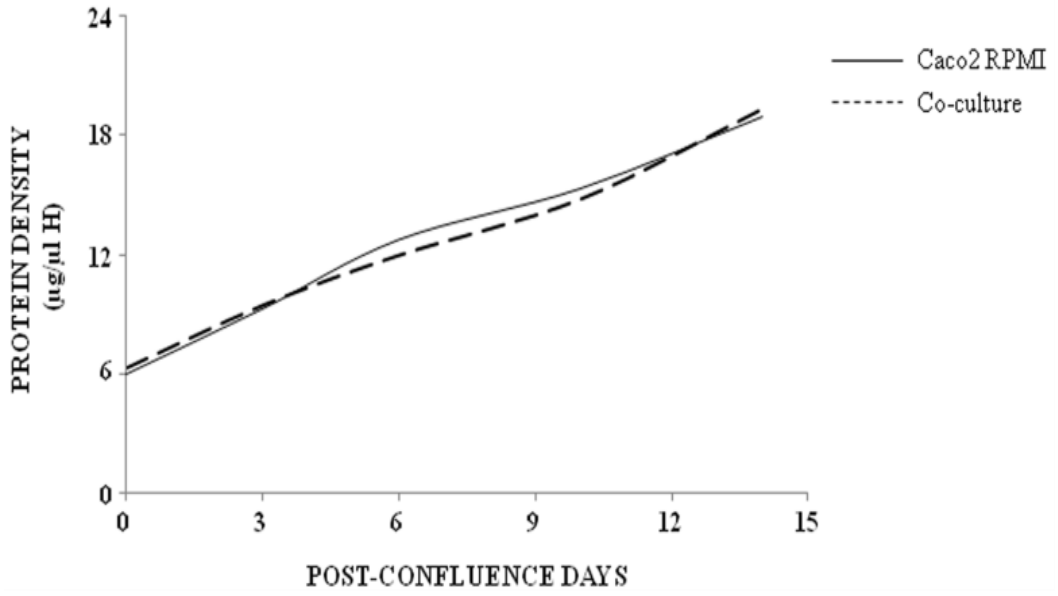

Figure 29. Protein content (µg/µl) of parental cell line (Caco2 RPMI) and Co-culture at different post-confluence stage.

EFFECTS OF GP AND TN DIGESTATES ADMINISTRATION

Effects of GP and TN digestates on cell viability

Co-culture cell viability data obtained from MTT assay after treatment for 2 and 24 h with three different doses of GP and TN digestates (50, 150 e 300 µl), shown a dose and time dependent decrease (Figure 30). In detail, the administration of 50 and 150 µl cause not always a statistically significative decline, while after administration of 300 µl of sample, cell viability was statistically lower respect to the control cells, reaching the minor value after 24 h incubation. The results after the treatment with the same dose of digestates, at different period of aging, show a significance after 24 h incubation in both digestates and only in few cases after 2 h incubation but never at the lowest dose.
After administration of the higher dose (300 µl) of GP and TN digestates at the same ripening period, almost all results are statistically different after 24 h of treatment (Figure 30).
Instead, as regards the differences between GP and TN for the same dose, ripening and treatment time, the samples show a similar trend. After two hours of treatment, the TN 13M shows higher values than the other period of aging, unlike what is shown from the GP that presents similar values between the different ripening. After 24 hours of treatment, the GP 26 M shows lower values than 19 and 26 M of ripening. TN instead, shows lower values at 19 M.

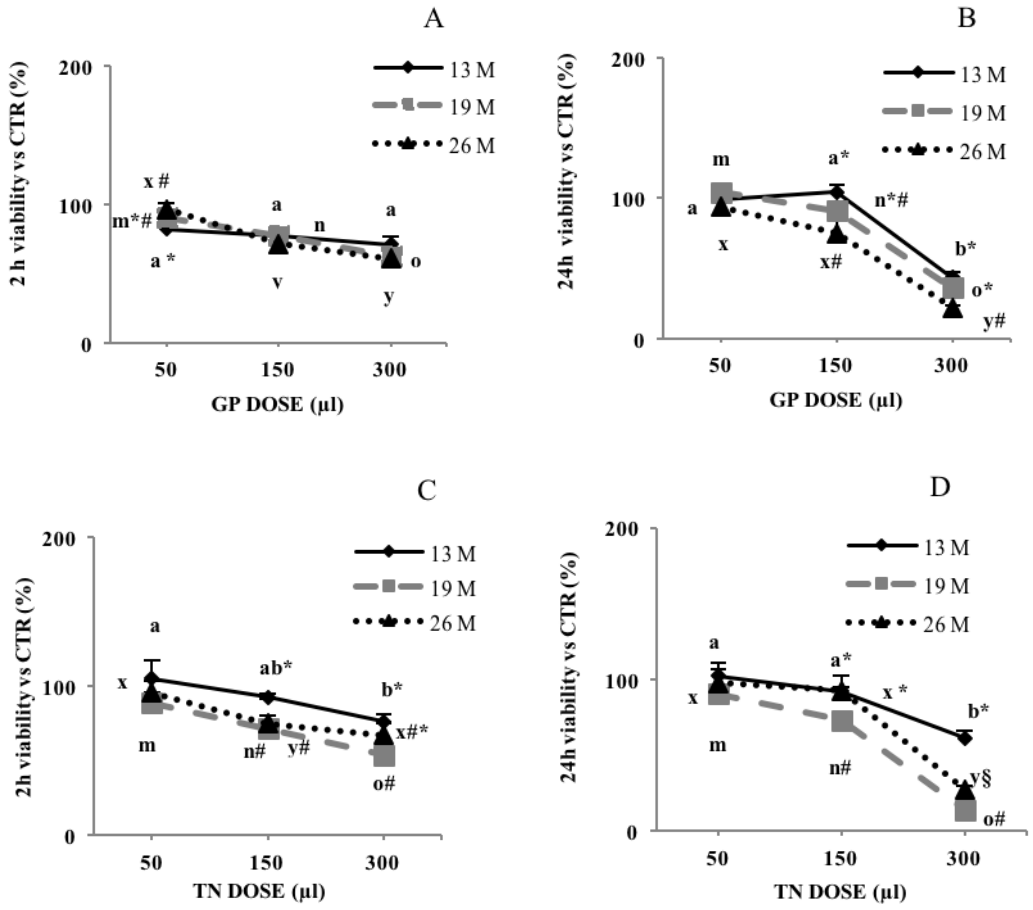

Figure 30. Cell viability after cheese digestates administration at three different doses. Within the ripening, different letters correspond to statistically significant differences.

Effects of GP and TN digestates on TEER measurements

After treatment of co-culture with digestates, TEER results do not show a decrease respect to control. Even digestate values are higher than control. This effect may be caused by the presence of electrolytes in digestates, that can alter the current passage. Moreover, TEER values are similar in all the samples. In detail, GP shows the lowest value at 19 months of aging, while at 13 and 26 M it shows similar values. The TN instead shows the highest value at 13 M and then decreased to 19 M. At 26 M the values appear similar to 19 M.

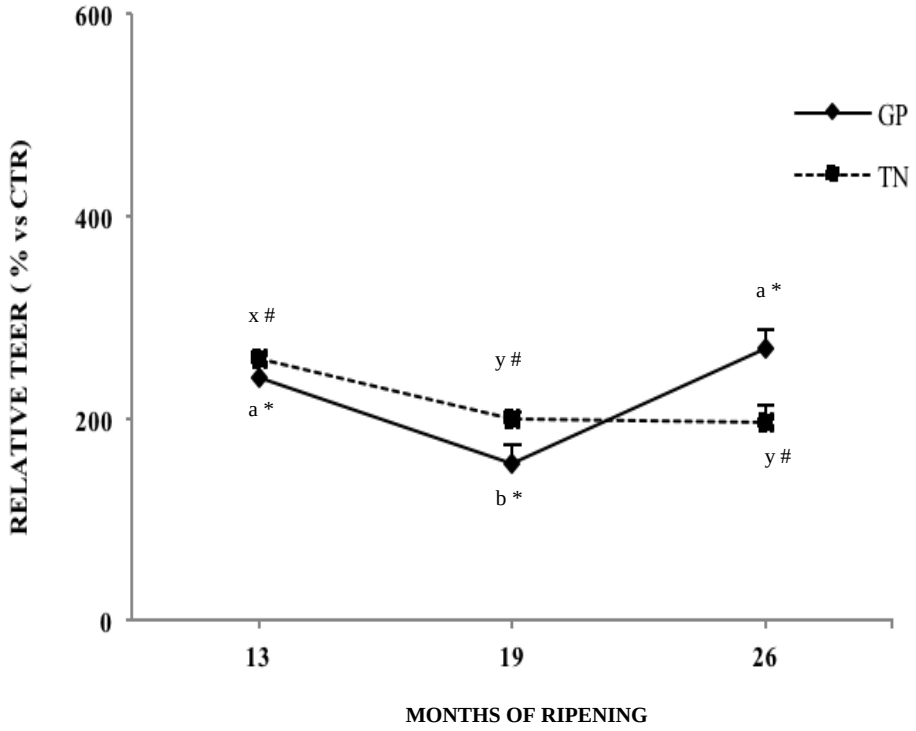

Figure 31. Paracellular permeability determination after cheese digestates administration. Within the same cheese GP or TN, different letters correspond to statistically significant differences: a, b and cfor GP and x, y for TN. In the comparison between subjects with the same ripening, the symbol * corresponds to statistically significant difference.

Effects of GP and TN digestates on intracellular calcium content

Measurement of intracellular free calcium concentration, $[Ca^{2+}]_i$, at a single-cell level after cheese digestate administration, shows an increased calcium uptake into co-culture cells. This calcium uptake is not correlated to dose and sample typology (*= $p < 0,05$).

This effect was monitored with the same feature both in nominally free calcium KRH buffer (data not shown) and in 2 mM $CaCl_2$. These results indicate that the calcium fraction internalized by cells is the one contained in the digestates. In fact, treating co-cultures with the blank of digestion in nominally free calcium KRH buffer, any increment of calcium was observed, while treating co-cultures with digestates in the same buffer, an increase of intracellular calcium was shown.
Moreover, after GP and TN digestate administration in co-cultures, the intracellular calcium increase was registered in about 20-30 percentage of cells for both samples in independent manner respect to the dose administered and the digestate ripening (Figure 32) except in the case of GP 19 M and TN 26 M (Figure 32 panels A, B). At the same way, the mean single-intracellular calcium rise, ($\Delta[Ca^{2+}]_i$) reached values in the range 28-56 nM with both samples (Figure 32). No significative differences were found between GP and TN results.

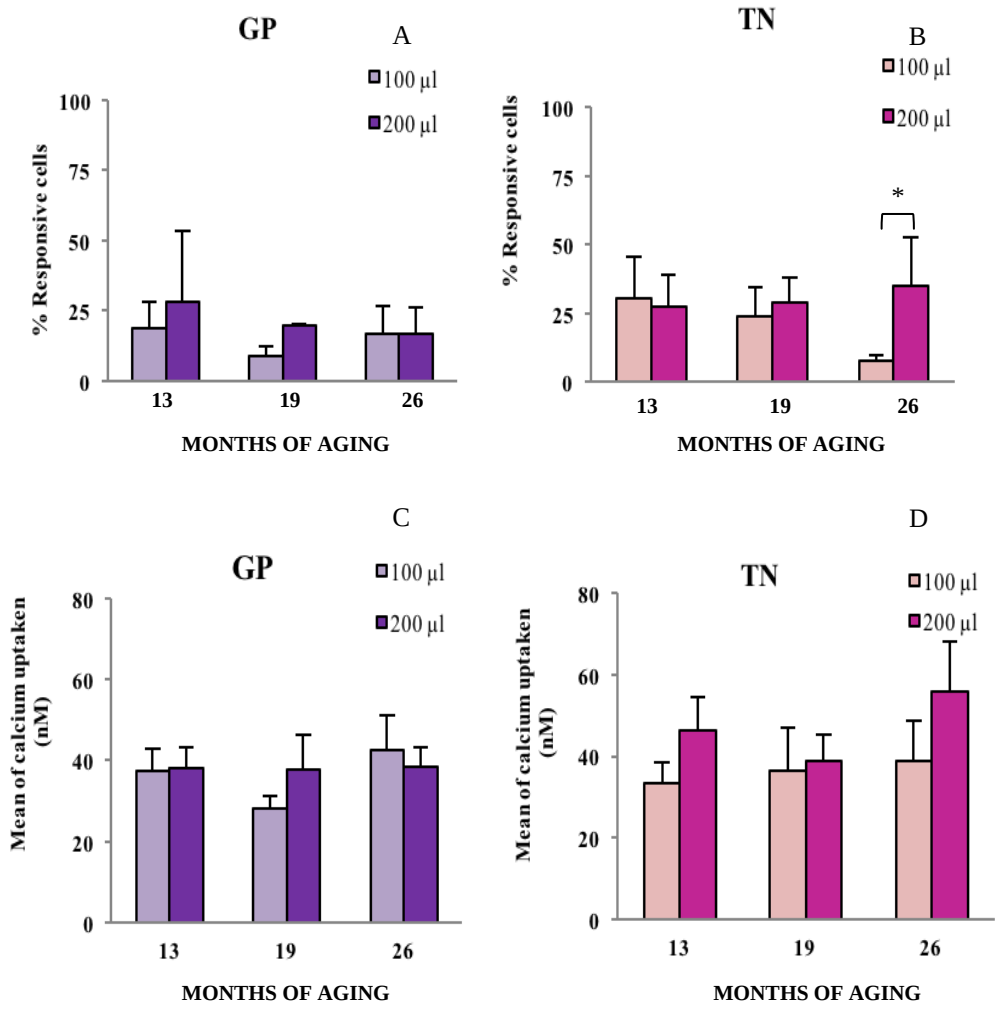

Figure 32. The graphs represent the responsive co-culture cell number after live treatment with two doses and three maturation degree of GP (panel A) and TN (panel B) digestates, at level of calcium absorption. Panels C and D represent the amount of calcium uptaken by the same cells after the same treatment. The symbol * indicates a significative statistical difference.

Evaluation of bone mineral matrix formation

After administration to Human osteoblast-like cells (Saos-2) for 28 days with the solution derived from basolateral compartment of transwell previously plated with co-culture and treated in apical compartment with digestates, Alizarin Red Staining was performed. Thanks to this staining, qualitative and quantitative bone mineral matrix apposition was evaluate. The treatment was cooperated by beta glycerophosphate and Vitamin C. For this reason, the Saos-2 cells grown with normal medium supplemeted by beta glycerophosphate and vitamin C can be considered as a real control (CTR plus). Results shown an increase of bone mineralization in all cell culture treated with the different GP and TN digestates respect to CTR plus and respect to the cell culture grown in normal medium, without any stimulus (considered as a negative control).
The bone matrix production observed was significantly higher than CTR plus and the negative control ($p<0,05$) (Figure 33), while the comparison between GP and TN samples shown never statically significant results.
Even more important, the digestates induced a bone mineral matrix formation in the same manner respect to the two typical inductors of bone mineralization represented by dexamethasone (DEX) and 1,25 dihidroxy Vitamin D (Vit D).

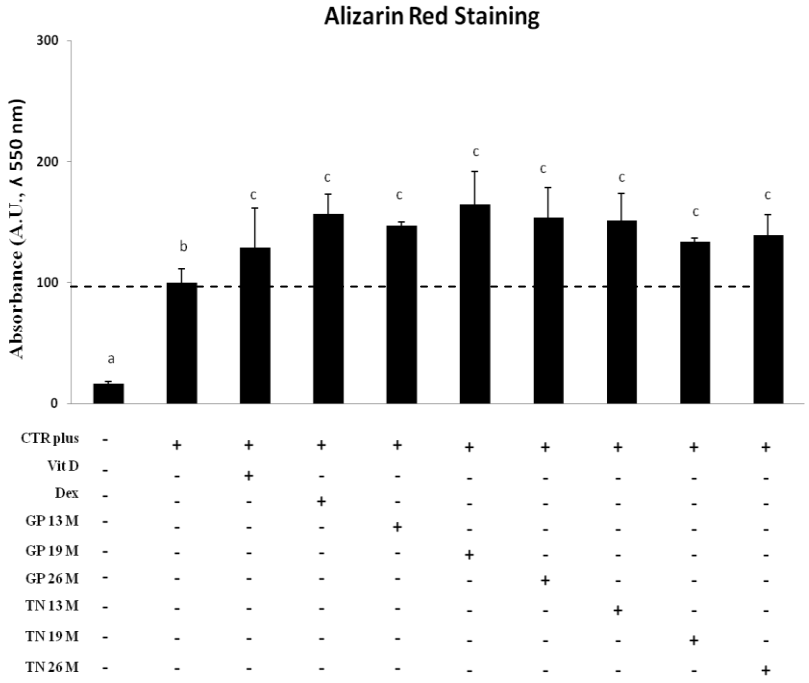

Figure 33, Alizarin Red Staining results from human osteoblast-like cells (Saos-2) after treatment with GP and TN digestates and with controls. Different letters correspond to statistically significant differences ($p < 0.05$).

Discussion

Over the last ten years, in many parts of the world, demand for beverages and foods that improve or benefit health has increased, simultaneously with the rise in healthcare costs (Diplock et al, 1999). In this context, functional foods provide a new health tool that promises specific effects related to certain food components (Doyon et al, 2008).
The term "functional foods" was first introduced in Japan in the mid-1980s and the European Commission's Concerted Action on Functional Food Science in Europe (FuFoSE), coordinated by International Life Science Institute (ILSI), and it described functional foods as: "a food can be regarded as *functional* if it is satisfactorily demonstrated to affect beneficially one or more target functions in the body, beyond adequate nutritional effects, in a way that is relevant to either an improved state of health and well-being and/or reduction of risk of disease. Functional foods must remain foods and they must demonstrate their effects in amounts that can normally be expected to be consumed in the diet: they are not pills or capsules, but part of a normal food pattern" (Diplock et al., 1999).
We can state that a functional food can be a natural food or a food that has been modified to have a functional influence on the health and human well-being through the particular component addition, removal, or modification (Diplock et al, 1999; Howlett J, 2008).
Next to the functional food term, the "nutriceutical" term has been coined for the first time by the founder and chairman of Foundation for Innovation in Medicine, Dr. Stephen De Felice, in 1989. He defined nutraceuticals as "food, or parts of food, that provide medical or health benefits including the prevention and treatment of diseases". While a functional food is essentially a food, a nutraceutic is an isolated or concentrated form.
Nowadays, thanks to separation techniques in the food industry and enzyme technology, it is possible to isolate, concentrate or modify the compounds, so that their application in functional foods, nutraceuticals, dietary supplements and medical foods became possible.
Among functional foods, particular importance is given by milk and dairy products. In fact, numerous studies have established the presence of bioactive peptides in diary products (Nakamura et al, 1995; Saito et al, 2000). The digestion of casein, the major protein component, produces high amounts of bioactive peptides (Meisel & Olieman, 1998).
Numerous claims have been made with respect to the CPP applications, in order to enhance mineral bioavailability. In fact, for bone development or ricalcification following bone fracturing, in the osteoporosis prevention and during the treatment of rickets, an adequate Ca^{2+} supply is required.
Currently, several multinational companies, especially in Europe and Japan, market CPP containing products, in order to increase the calcium or iron bioavailability.
In vivo, *in vitro* and human *in situ* experiments have demonstrated that synthetic caseinphosphopeptide-amorphous calcium phosphate (CPP-ACP) nanocomplexes are anticariogenic and they are incorporated into a wide range of products such as toothpaste, chewing gum, topical gels, toothpowder, dental filling material, mouthwashed, lozenges, tablets, yogurt, nutritional supplements for children, mineral drinks, confectionery and products for dental care (Reynolds et al., 2003; Iijima Y et al., 2004; Ferrazzano et al., 2008).
A basic prerequisite to define a food as a functional food or a molecule component as a nutraceutical, is the ability to retain or acquire a specific biological activity after the digestion process.
So far, the CPPs role has always been studied on samples such as, and never after further digestion process. Even if they represent purified peptides, already deriving from digestive process, after use as supplements in foods, they are further subjected to digestion.
These CPPs have shown a higher fraction of serine residues than casein (10.3% vs 6.1% w/w). This concept is fundamental, because the phosphorylated serine are the most responsible for the binding with calcium ions (Cosentino et al, 2010).
Since the bioactive potential of the CPP is given by their ability to bind calcium ions, making them more bioavailable to intestinal cells, the first step was to evaluate the persistance of the CPP aggregates with calcium ions even after digestion.
Moreover, in the present project, the aggregation properties of calcium-CPPs (Ca-CPPs) were studied by laser light scattering and the internal structure of CPP complexes and their evolution during the digestion process were assessed by SAXS measurements.
Results have shown the presence of a large-scale structure of some hundreds of nanometers and a small substructure characterized by many ramifications (conformation similar to the polycondensates), that is different from the parent whole-casein, in which is present a network with reticulated amorphous calcium-phosphate nanoclusters (ellipsoid conformation).
The digestion process changed the CPP aggregate features: on the large scale, they are still present but the size was reduced. In these conditions, CPP are able to preserve their ability to form aggragates respect to casein. At acid pH, that simulate the gastric phase, the charges on the peptide chains are neutralized, as in casein, and the interaction with calcium ions is lost. The aggregate size become smaller (few tens of nm) than undigested Ca-CPP. At pH 6 (intestinal phase of digestion) large aggregates quickly reform and the condensation nuclei are still present.
This suggests that, the digestion process with acidification effect and enzyme action, induced a decrease in the radius of gyration of the subchains of internal aggregate Ca-CPP substructures. In this manner, calcium ions become more finely distributed in the peptide matrix. In our biological study, we used two cell lines, namely Caco2 and HT-29 cells that represent different intestinal morphological tracts and functions. Using these cell lines, it was possible to evaluate the calcium uptake by the two main different mechanisms activated by CPPs as previously demonstrated (Perego et al., 2012; Perego et al., 2013). In fact, after *in vitro* differentiation, Caco2 cells resemble the duodenum cells with a higher

presence of digestive enzymes as it appears in the intestinal tract more involved in the food digestion. Fundamental is the presence of the TRVP6 channel (Perego et al., 2013), indicative of the transcellular calcium absorption as the main route, as it was observed in duodenum (Kellett., 2011).
Otherwise, HT-29 cells represent a more heterogeneous population, prevalently the secretory cell type, with a minor amount of digestive enzymes (Quaroni and J. Hochman, 1996). They present L-type calcium channel, characteristic of the jejenum and ileum tract in which calcium is absorbed through paracellular route.
The digestion of Ca-CPP aggregates increased the calcium uptake in both Caco2 and HT-29 cells. In particular, in Caco2 cells, the increase is eight time higher respect to the undigested Ca-CPP administration. In HT-29 cells, instead, the calcium uptake is increased by only two times.
This result is supported, *in vivo*, by the transcellular calcium absorption that takes place in duodenum, according to the saturable kinetics, when the extracellular calcium concentration is low. This transcellular route is regulated by vitamin D and it occurs in Caco2 cells through TRVP6 channels.
Reversely, paracellular calcium absorption takes place in the distal jejunum and ileum when the extracellular calcium concentration is very high, for instance after a meal (Kellett, 2011). This paracellular route is not vitamin D-dependent and it occurs in HT-29 cells through L-Type channels.
The digestion causes great modifications in the structure-function relationship of CPPs involving the interaction with the cell membranes. For the first time, this data demonstrated that the digestion process was able to influence significantly and in a positive manner, the pre-formed Ca-CPP aggregate state.
Probably, the radius shortening of the complexes calcium-CPP and the greater dispersion of calcium ions inside them, facilitates contact between calcium and membrane surface.
This is very important because Ca-CPP aggregates make calcium ions more bioavailable toward the intestinal cells.
According to these reasons and to the CPPs origin from the digestion of casein contained in milk and diary products, the next step of this project was the evaluation of the biological activity of caseinophospopetides conteined in a complete food such as cheeses.
In order to permform this experimental phase, a new model of *in vitro* human intestinal epithelium has been developed for the first time. It is represented by a co-culture of Caco2 and HT-29 cells, previously used individually.
The choice of the co-culture model is motivated by the cytological heterogeneity present *in vivo*. This characteristic is fundamental for the natural development of the main enteric functions such as the digestion, absorption and secretion, together with the maintenance of a protective barrier (Shimizu, 2010; Hingeldorf et al, 2000). The use of a single human intestinal cell line, although widely used and described in the literature (Vreeburg et al., 2012; Suzuky & Hara, 2009; Amasheh et al, 2008), does not allow to mimic in a perfect way the differentiated intestinal epithelium, composed at least by 4 different cell types, from the cell absorbent to the mucus-secreting one.
The co-culture characterization has shown a good correspondence between the ultrastructure and the functional parameters related to cell differentiation at the various post-confluence stages.
This morphological development has a physiological confirmation in transepithelial electrical resistance (TEER).
However, the co-culture demonstrated an adeguate differentiation degree in all examined post-confluence stages, in each case prevails specific morpho-functional markers.
Moreover, the co-culture can be considered a versatile model that allows to select a specific post-confluence stage, depending on the intestinal features and functions that are required in an experiment.
The co-culture, showed a good correlation between the morpho-functional charactheristics and the tight junctions development at different post-confluence stages. In fact, the results revealed the highest expression of tight junctions and desmosomes at the 6^{th} post-confluence day.
Probably, the coexistence of two different cell lines in co-culture leads to a more marked differentiation towards their cellular characteristics: absorbing function of Caco2 and secretory function of HT-29.
An important advantage offered by the co-culture is the TEER, whose values, comprised between a minimum of 24 $\Omega \cdot cm^2$ at T0 and a maximum of 94 $\Omega \cdot cm^2$ at T6, are comparable to the human small intestinal epithelium *in vivo*. In fact, the TEER values of human intestinal epithelium ranges from 50 to 100 $\Omega \cdot cm^2$ in the jejunum and ileum and from 300 to 400 $\Omega \cdot cm^2$ in the the colon.
In our opinion co-culture, at the sixth day of post-confluence, offer a suitable compromise between functional and morphological development, in order to represent as best as possible the human small intestinal epithelium, in which most of the nutrient absorption takes place.
The study of interactions between food and intestinal epithelial cells is important to understand how dietary substances and not only a single nutrient, regulate our body systems and keep us healthy.
For this reason, we decide to analyze the behaviour of whole digestates, in which various nutrients interact with each other in order to modulate the biological effect.
The HR-MS total ion current (TIC)-chromatographic profiles of CPP-enriched extracts (at the same pH value) of both cheese digestates were highly similar at the same ripening age. This "peptidic fingerprint" similarity can be justified by the quite analogous proteolytic phenomena that occur in both cheeses during ripening (Mucchetti & Neviani, 2006). During RP-UPLC separation, many CPPs co-eluted, and not phosphorylated peptides co-eluted with the CPPs (data not shown). Therefore, relative semi quantitation of CPPs as described by Dupas et al. (Dupas et al., 2009) or Cruz-Huerta et al. (Cruz-Huerta et al., 2015) was not feasible.

It should be noted that 10–18 of the 24–46 total identified tri-phosphorylated CPPs presented the sequence sssEE (pSer-pSer-pSer-Glu-Glu), the characteristic Ca^{2+} binding motif (Ferraretto et al., 2001; Nongonierma & FitzGerald, 2015). The CN fractions present this cluster at different sites of their primary sequence: αS_1-CN f(66–70), αS_2-CN f(8–12), αS_2-CN f(56–60) and β-CN f(17–21). The above-mentioned motif was revealed in CPPs deriving from both α-CN and β-CN. In contrary Miquel et al. (Miquel et al., 2005) reported the motif-containing CPPs to derive only from α_{S1}-CN and α_{S2}-CNin infant formula digesta. This observation could be interesting in terms of mineral bioavailability, because Park et al. (Park et al, 1998) reported that CPPs derived from α-CN exhibit greater calcium binding affinity (measured by a calcium selective electrode) than β-CN-derived CPPs. Nonetheless, it is important to underline that the *in vitro* digestion method applied by Miquel et al. (Miquel et al., 2005) was adapted for toddler rather than adult, which is the case of the present study. More recently, Adt et al. (Adt et al., 2011) identified 17 CPPs containing the motif sssEE in digesta of Beaufort cheese. Despite the research concerned the presence of CPPs in undigested GP and TN cheeses, there is no data regarding the release of this type of tri-phosphorylated CPPs after *in vitro* gastrointestinal digestion of GP and TN cheeses.

Analyzing the qualitatively content of caseinophosphopeptides in cheese digestates, profiles appear very similar, between the various aging period in the same type of cheese and between the two cheeses. In addition, the characteristic acid motif responsible for the binding with calcium ions is always maintained after digestion, in all types of samples, in a similar manner.

Afterwards, in order to identify the suitable dose of GP and TN digestates for the intestinal cell model, a cytotoxic test was performed with three different doses (50, 150 and 300 µl) and two times of treatment (2 and 24 h).

Two hours treatment mimics the physiological duration of digestion and absorption phases, while the 24 hours treatment is considered in order to understand whether the digestate components are able to interfere with cell viability.

According to hypotesis, the digestates induce a dose and time dependent decrease in cell viability. In fact, the lower values were obtained after 24 hours treatment using the higher digestates dose of each cheese typology. Probably, the digestion mixture contains components that can damage cells in the long period.

The measurement of the TEER has provided information about the cell monolayer integrity. Tight junctions (TJ) are the most important element responsible for the intestinal barrier functionality and they are positioned around the epithelial cell rhyme side. The TJ structure involved a wide spectrum of proteins such as occludin, claudin, the zonula occludens (ZO) and other molecules such as the family of protein kinase C (PKC) (Suzuky & Hara, 2009). It has been demonstrated (Berkes et al, 2003; Brandtzaeg et al. 2002) that an alteration in the TJ structure, caused by stress, pathogens, pro-inflammatory cytokines or food components, results in an increase of the permeability of the intestinal epithelium which allows the passage of unwanted substances.

Afterwards, the effect of the digestates on the tight junctions integrity was examined by measuring TEER. Results showed an increase in TEER values compared to its control (untreated co-cultures). This behavior was observed by Vreeburg et al. (Vreeburg et al. 2012): the exposure of Caco2 to an homogenate raw apple induced an increase of paracellular electrical resistance. (Suzuky & Hara, 2009).

Frequently, the manifested biological effect cannot be attributed to the individual components present in the food because its the result of a synergy between many food elements. Similarly, we evaluated the effect induced by GP and TN digestates *in toto* and not by the individual constituent, in order to emphasize the importance of the food matrix used and the interaction between the different nutrients.

Clearly, the results suggested that GP and TN do not determine an increase in paracellular permeability, but an opposite behavior, indicating that the cell permeability were not damaged by digestates administration (Suzuky & Hara, 2009; Amasheh et al, 2008).

Sforza et al. disagree with Mucchetti et al. (Sforza et al., 2004) because they demonstrated that the lysozyme used in the Grana Padano production, modified the cheese peptidic profile (< 5000 D fraction) during ripening process.

However, Sforza et al. (Sforza et al., 2004), have demonstrated that Grana Padano phosphopeptides level increased, reaching a maximum at 12 months of ripening and then decreased, while Parmigiano Reggiano phosphopeptides level was usually lower at the same period of aging and showed a less regular trend. In Grana Padano cheese the proteolysis is faster than in Parmigiano Reggiano and Trentin Grana because the lysozyme induces Lactic Bacteria lysis and then the releasing of citoplasmatic proteolysis enzymes. In fact, the lysozyme employment determines a different proteolitic evolution in Grada Padano respect to Parmigiano Reggiano and Trentin Grana.

Anyway, in the present project, the calcium uptake results showed a quite similar cell calcium increase after administration of the GP or TN digestates. Moreover, we do not have a dose-dependent response. In fact, although the only statistically significant value was found between the two doses of the highest period of aging TN, this result does not appear relevant from the biological point of view.

Our results do not agree with those provided by Sforza et al. and this is explained because our samples underwent to the further *in vitro* proteolytic digestion.

Research about the biomineralization mechanisms and the mineral phases chemistry was the topic of various recent reviews (Georgeet al., 2008; Wang et al., 2009; Dorozhkin et al., 2011). Hard tissues, including bone, cementum, dentine and enamel, contain a basic calcium phosphate mineral called apatite, or hydroxyapatite. (Kawasaki et al, 2004; Kawasaki et al, 2003).

Our previous study (Donida et al., 2009) showed that CPPs play a role as a modulator of bone cell activity. In particular,

the results about human osteoblast-like cells, highlight that CPP, and calcium-CPP, display the ability to enhance the calcification nodule production. These CPPs samples were administered without further modifications, because they were considered by a technological and not nutritional point of view.
According to the improvement of the calcium solubility and of the calcification of embryonic rat bones in the diaphyseal area due to CPPs (Meisel, H., & FitzGerald 2003), these peptides are used to coating orthopedic metallic implants, in order to improve the calcification process (Liguo et al, 2015).
The aim of the present project, was to verify the Grana Padano and Trentin Grana digestates ability to induce a bone mineralization. For this purpose, the digestates were firstly administered to the intestinal cells, for two hours. During this period, the intestinal cells absorbed nutrients contained in digestates, transporting them in the basal compartment, that simulates the bloodstream.
The content of the bloodstream compartment was harvested and administered to osteoblast-like cells for 4 weeks. After, the bone matrix apposition was evaluated in these cells from the qualitative and quantitative point of view.
The results clearly showed that digestates induced bone mineralization behaving like bone differentiation agents such as Vitamin D and dexamethasone.

In conclusion, present data show that after digestion the preformed aggregates of calcium and CPPs still maintain their conformation and retain their bioactivity as promoters of calcium uptake in intestinal cells, regardless of calcium mechanism transport (TRPV6 in Caco2 cells and depolarizing L-type calcium channels in HT-29 cells). Moreover, *in vitro* digestates of Grana Padano and Trentin Grana were able to induce a calcium uptake in a co-culture of Caco2 and HT-29, a complete and useful model of human intestinal epithelium. An important result is poitend out by the digestates capacity to induce the bone mineralization in human osteoblast-like cells.
For this reasons, the use of CPP as food supplement or the usual ingestion of cheeses such as GP and TN, characterized by high digestibility, becomes important in particular conditions like pregnancy, lactation, growth and in all those circumstances in which the mineral requirements is fundamental.

References

Addeo F. et al., 1992, Characterization of the 12-percent trichloroacetic acid-insoluble oligopeptides of Parmigiano-Reggiano cheese; J Dairy Res 59: 401-411.

Addeo F. et al., 1994, Characterization of the oligopeptides of Parmigiano-Reggiano cheese soluble in 120 g trichloroacetic acid/l. J Dairy Res 61: 365-374.

Addeo F. et al., 1995, Gel-electrophoresis and immunoblotting for the detection of casein proteolysis in cheese. J Diary Res 62: 297.

Adt et al., 2011, Identification of CPPs generated through in vitro gastro-intestinal digestion of Beaufort cheese. International Dairy Journal 21: 129-134.

Amasheh M. et al., 2008, Quercetin Enhances Epithelial Barrier Function and Increases Claudin-4 Expression in Caco-2 Cells. J Nutr 138: 1067.

Andrews AT. Alichanidis E., 1983, Proteolysis of caseins and the proteose-peptone fraction of bovine milk. J Dairy Res 50: 275.

Arienti G., 2010, Le basi molecolari della nutrizione. Piccin editore.

Armbrecht HJ. et al., 2003, Effect of age and dietary calcium on intestinal calbindin D-9k expression in the rat. Arch Biochem Biophys 420: 194-200.

Arsenio L., Strata A, 1996, Alimentazione ed esercizio fisico. Barilla, Parma, Italia.

Artursson P., (1990), Epithelial transport of drugs in cell culture. I: A model for studying the passive diffusion of drugs over intestinal absorbtive (Caco2) cells. J Pharm Sci 79: 476–482.

Bachmann et al., 1997, Prediction of flavour and texture development in Swiss-type cheeses. Food Sci. Technol. - Lebensm-Wiss. Technol. (1997) 32: 284.

Bärtschi F. et al., 2006, Determination of lysozyme in cheese by LC-MS. Mitt Lebensm Hyg 97: 478.

Bateman F. et al., 2014, Maximizing Peptide Identification Events in Proteomic Workflows Using Data-Dependent Acquisition (DDA). Mol Cell Proteomics 13: 329-338.

Berkes J. et al., 2003, Intestinal epithelial responses to enteric pathogens: effect on the tight junctional barrier, ion transport and infiammation. Gut 52 (3): 439.

Berman MC., 1999, Regulation of Ca2+ transport by sarcoplasmic reticulum Ca2+-ATPase at limiting [Ca2+]. Biochim Biophys Acta 1418: 48-60.

Berrocal R. et al., 1989, Tryptic phosphopeptides from whole casein. II. Physicochemical properties related to the solubilization of calcium. J Dairy Res 56: 335-341.

Bianchi A. et al., 1993, Aminoacid composition of granules and spots in Grana Padano cheeses. J Dairy Sc 57: 1504.

Bishop JM. et al., 1990, Natural history of cow milk allergy: clinical outcome. J Pediatr 116: 862.

Bottazzi V. et al., 1994, I cristalli nel formaggio Grana. Scienza e tecnica lattiero-casearia 45 (1): 7.

Bottazzi V., Battistotti B., 1999, Lisozima e formaggio grana: combinazione di complessi aspetti. Il latte 24 (3): 58-65.

Bouchoux A. et al., 2010, How to squeeze a sponge: Casein micelles under osmotic stress, a SAXS study. Biophys J 11:3754-3762.

Brandtzaeg PE., 2002, Current understanding of gastrointestinal immunoregulation and its relation to food allergy. Ann N Y Acad Sci 964: 13-45.

Bronner F., 1988, Gastrointestinal absorption of calcium. In Calcium in human biology: 93-124. Ed Springer. Berlin: B.E.C. Nordin

Bronner F., Pansu D, 1999, Nutritional aspects of calcium absorption. J Nutr 129: 9-12.

Brown JM., Attardi LD, 2005, The role of apoptosis in cancer development and treatment response. Nat Rev Cancer 5: 231-237.

Bruno J., 2013, Basics and recent advances in peptide and protein drug delivery. Ther Deliv 4 (11): 1443-1467.

Buras R. et al., 1995, The effect of extracellular calcium on colonocytes: evidence for differential responsiveness based upon degree of cell differentiation. Cell Proliferation 28: 245-262.

Castano P., Donato RF., 2008, Anatomia dell'uomo. Edi-Ermes, seconda edizione; 8: 221-226.

Celik-Bilgili S. et al., 2005, The predictive value of specific immunoglobulin E levels in serum for the outcome of oral food challenges. Clin Exp Allergy 35: 268-273.

Cereijido M. et al., 1978, Polarized monolayers formed by epithelial cells on a permeable and translucent support. J Cell Biol 77: 853-880.

Cerruti L., Residui, additivi e contaminanti degli alimenti. Tecniche Nuove, III Edizione, 2006.

Chan GM. et al., 1995, Effects of dairy products on bone and body composition in pubertal girls. J Pediatr 126: 551-556.

Cho E. et al., 2004, Dairy foods, calcium and colorectal cancer: a pooled analysis of 10 cohort studies. J Natl Cancer Inst 96: 1015-1022.

Cho MJ. et al., 1989, The Madin Darby canine kidney epithelial cell monolayer as a model cellular transport barrier. Pharm Res 6: 71–77.

Choi KC., Jeung EB., 2008, Molecular mechanism of regulation of the calcium-binding protein calbindin-D9k, and its physiological role(s) in mammals: a review of current research. J Cell Mol Med 12: 409-420.

Choisy C. et al., La biochimie de l'affinage. A. Eck, & J.-C. Gillis (Eds.), Le Fromage 1997.

Collins YF. et al., 2003, Lipolysis and free fatty acid catabolism in cheese: a review of current knowledge. Int Dairy Journal 164 (13): 841-866.

Colombo R., Olmo E. Biologia dei tessuti. Edi-Ermes, 2007.

Cosentino S. et al., 2010a, Calcium ions enclosed in casein phosphopeptide aggregates are directly involved in the mineral uptake by differentiated HT-29 cells. Int Dairy J 11:770-776.

Cosentino S. et al., 2010b, Caseinphosphopeptide-induced calcium uptake in human intestinal cell lines HT-29 and Caco2 is correlated to cellular differentiation. J Nutr Biochem 21: 247-254.

Costantini A.M., Cannella C., Tomassi G. Alimentazione e Nutrizione umana. Il Pensiero Scientifico Editore, seconda edizione; 2006.

Creff A.F., Bernard L. Dictionnaire de la nouvelle dietetique. Laffont, Parigi, 1984.

Crippa G., Bosi M., Cassi A., Fiorentini L., Rossi F. Blood pressure lowering effect of dietary integration with Grana Padano cheese in hypertensive patients. 21° European Meeting on Hypertension, 17-20 giugno, Milano, 2011.

Cruz-Huerta E. et al., 2015, Caseinophosphopeptides released after tryptic hydrolysis versus simulated gastrointestinal digestion of a casein-derived by-product. Food Chem 168: 648-655.

De Kruif CG. et al., 2012, Casein micelles and their internal structure. Adv Colloid Interface Sci 172: 36-52

Diplock AT. et al., 1999, Scientific concepts of functional foods in Europe: consensus document. Br J Nutr 81:1-27.

Donida BM. et al., 2009, Casein phosphopeptides promote calcium uptake and modulate the differentiation pathway in human primary osteoblast-like cells. Peptides 30: 2233-2240.

Dorozhkin SV., 2011, Calcium orthophosphates: occurrence, properties, biomineralization, pathological calcification and biomimetic applications. Biomatter 1(2):121-164.

Doyon M., Labrecque J., 2008, Functional foods: a conceptual definition. Br Food J 110: 1133-1149.

Dupas C. et al., 2009, A chromatographic procedure for semi-quantitative evaluation of casein phosphopeptides in cheese. Dairy Sci Technol 89: 519-529.

Edwards ST., Sandine WEN, 1981, Public health significant amines in cheese. J Dairy Sci 64: 2431-2438.

Eigel WN. et al., 1979, Plasmin-mediated proteolysis of casein in bovine milk. Proc Natl Acad Sci USA 76: 2244-2248.

Ellegard KH. et al., 1999, Process scale chromatographic isolation, characterization and identification of tryptic bioactive asein phosphopeptides - Proteins. Int Dairy J 9:639-652.

Erba D. et al., 2002, Effect of the ratio of casein phosphopeptides to calcium (w/w) on passive calcium transport in the distal small intestine of rats. Nutrition 18: 743-746.

Farrell Jr. et al., 2004, Nomenclature of the proteins of cows' milk – sixth revision. J Dairy Sci 87, 1641-1674.

Fernandez-Garcia E. et al., 2000, Formation of biogenic amines in raw milk hispanico cheese manufactured with proteases and different levels of starter colture; J Food Protec 11: 1551-1555.

Ferranti P. et al., 1997, Combined high resolution chromatographic techniques (FPLC and HPLC) and mass spectrometry-based identification of peptides and proteins in Grana Padano cheese. Lait 77: 683-697.

Ferranti P. et al., 1997, Phosphopeptides from Grana Padano cheese: nature, origin and changes during ripening. J Dairy Res 64: 601-615.

Ferraretto A. et al., 2001, Casein phosphopeptides influence calcium uptake by cultured human intestinal HT-29 tumor cells. J Nutr 131 1655-1661.

Ferraretto A. et al., 2003, Casein-derived bioactive phosphopeptides: role of phosphorylation and primary structure in promoting calcium uptake by HT-29 tumor cells. FEBS Lett 551: 92-98.

Ferraretto A. et al., 2007, New Methodological Approach to Induce a Differentiation Phenotype in Caco-2 Cells Prior to Post-confluence Stage; Anticancer Research (2007), 27: 3919-3926.

Ferraretto A., Fiorilli A, 2010, Phosphopeptides of casein and calcium uptake. In Biochemical aspects of human nutrition, pp 69-86. Eds L Avigliano & L Rossi. Kerala India: Transworld Research Network.

Ferraretto A., Modelli cellulari in vitro per lo studio dei meccanismi alla base delle funzioni cellulari; III symposium of cellular biology of epithelia-atti del convegno, Aracne editore, 2006.

Ferrazzano GF. et al., 2008, Aust Protective effect of yogurt extract on dental enamel demineralization in vitro. Dent J 53(4): 314-319.

Ferruzza S. et al., 2012, A protocol for differentiation of human intestinal Caco-2 cells in asymmetric serum-containing medium. Toxicol in Vitro 26: 1252-1255.

FitzGerald RJ., 1998, Potential Uses of Caseinophosphopeptides. Int Dairy J 8: 451-457.

Fox PF., McSweeney PLH., 1996, Proteolysis in cheese during ripening; Food Rev Int 12: 457-509.

Gaiaschi A. et al., 2001, Proteolysis of β-Casein as a Marker of Grana Padano Cheese Ripening. J Dairy Sci 84: 60-65.

Ganjam LS. et al., 1997, Antiproliferative effects of yogurt fractions obtained by membrane dialysis on cultured mammalian intestinal cells. J Dairy Sci 80: 2325-2329.

Ganong WF., Barrett KE, 2005, Gastrointestinal Function Digestion and Absorption. Review of Medical Physiology 25: 384-393.

Gatti M. et al., 1999, Presence of peptidase activities in different varieties of cheese. Lett Appl Microbiol 28: 368-372.

George A. et al., 2008, Phosphorylated proteins and control over apatite nucleation, crystal growth, and inhibition. Chem Rev 108(11): 4670-4693.

Gravaghi C. et al., 2007, Casein phosphopeptide promotion of calcium uptake in HT-29 cells - relationship between biological activity and supramolecular structure. FEBS J 274: 4999-5011.

Grufferty MB., 1988, Milk alkaline proteinase. J Dairy Res 55: 609-630.

Grynkiewicz G. et al., 1985, J Biol Chem 260: 3440-3450.

Gueguen L., Pointillart A, 2000, The bioavailability of dietary calcium. J Am Coll Nutr 19: 119S-136S.

Ha YL. et al., 1987, Anticarcinogen from ground beef: heal alterated derivatives of linoleic acid. Carcinogenesis 8: 1881-1887.

Hartmann R. et al., 2000, Cytochemical model systems for the detection and characterization of potentially bioactive milk components. Kieler Milchwirtschaftliche Forschungsberichte 52: 61-85.

Hashida S. et al., 2002, Concentration of egg white lysozyme in the serum of healthy subjects after oral administration. Clin Exp Pharmacol Physiol 29: 79-83.

Hekmati M. et al., 1990, A morphological study of a human adenocarcinoma cell line (HT29) differentiating in culture. Similarities to intestinal embryonic development. Cell Differ Dev 31: 207-218.

Hingeldorf C. et al., 2000, Caco-2 versus Caco-2/HT29-MTX Co-cultured Cell Lines: Permeabilities Via Diffusion, Inside- and Outside-Directed Carrier-Mediated Transport. Journal of Pharmaceutical Sciences; 89 (1): 63-75.

Hoenderop JG. et al., 1999, Molecular identification of the apical Ca2+ channel in 1, 25-dihydroxyvitamin D3-responsive epithelia. J Biol Chem 274: 8375-8378.

Hoenderop JG. et al., 2000, Localization of the epithelial Ca(2+) channel in rabbit kidney and intestine. J Am Soc Nephrol 11:1171-1178.

Hoenderop JG. et al., 2005, Calcium absorption across epithelia. Physiol Rev 85: 373-422.

Holmes R., Lobley RW., 1989, Intestinal brush border revisited. Gut 30: 1667-1678.

Holt C. 2013, Unfolded phosphoproteins enable soft and hard tissues to coexist in the same organism with relative ease. Curr Opin Struct Biol 23:420-425.

Howlett J. ILSI Europe Concise Monograph on Functional Foods: from Science to Health and Claims. Brussels, Belgium: The International Life Sciences Institute; 2008.

Hu FB. et al., 1999, Dietary saturated fats and their food sources in relation to the risk of coronary heart disease in women; Am J Clin Nutr 70: 1001-1008.

Iaconelli A. et al., 2008, Absence of Allergic Reactions to Egg White Lysozyme. J Am Coll of Nutr 27(2): 326-331.

Iijima Y. et al., 2004, Acid resistance of enamel subsurface lesions remineralized by a sugar-free chewing gum containing casein phosphopeptide-amorphous calcium phosphate. Caries Res 38(6): 551-556.

Ip C. et al., 1994, Conjugated linoleic acid suppresses mammary carcinogenesis and proliferative activity of the mammary gland in the rat. Cancer Res 54: 1211-1215.

Jia-Li Y. et al., 2014, Initial Characterization of Osteoblast Differentiation and Loss of RUNX2 Stability in the Newly Established SK11 Human Embryonic Stem Cell-Derived Cell Line. J Cell Physiol 230:237-241.

Johnson JA., Kumar R., 1994, Renal and intestinal calcium transport: roles of vitamin D and vitamin D-dependent calcium binding proteins. Semin Nephrol 14: 119-128.

Jovaní M. et al., 2001, Calcium, Iron, and Zinc Uptake from Digests of Infant Formulas by Caco-2 Cells. J Agric Food Chem 49: 3480-3485.

Jumarie C., Malo C., 1991, Caco-2 cells cultured in serum-free medium as a model for the study of enterocytic differentiation in vitro. J Cell Physiol 149: 24-33.

Kawasaki K. et al., 2004, Genetic basis for the evolution of vertebrate mineralized tissue. Proc Natl Acad Sci USA 101(31): 11356-11361.

Kawasaki K., Weiss KM, 2003, Mineralized tissue and vertebrate evolution: the secretory calcium-binding phosphoprotein gene cluster. Proc Natl Acad Sci USA 100(7): 4060-4065.

Kellett GL., 2011, Alternative perspective on intestinal calcium absorption: proposed complementary actions of Ca(v)1.3 and TRPV6. Nutr Rev 69(7): 347-370.

Khanal RC. & Nemere I, 2008a, Endocrine regulation of calcium transport in epithelia. Clin Exp Pharmacol Physiol 35: 1277-1287.

Khanal RC, Nemere I, 2008b, Regulation of intestinal calcium transport. Annu Rev Nutr 28: 179-196.

Kitts DD., Yuan YV., 1992, Caseinophosphopeptides and calcium biovailability. Trends Food Sci Tech 3: 31-35.

Kris-Etherton P., S. Yu. Individual fatty acids on plasma lipids and lipoproteins: human studies. Am J Clin Nutr (1997) 65 (Suppl): 1628S.

Lacroix IME., Li-Chan ECY., 2012, Dipeptidyl peptidase-IV inhibitory activity of dairy protein hydrolysates. Int Dairy J 97-102.

Lallès JP., 2014, Intestinal alkaline phosphatase: novel functions and protective effects. Nutr Rev 72(2): 82-94.

Lambeir AM. et al., 2003, Dipeptidyl-Peptidase IV from Bench to Bedside: An Update on Structural Properties, Functions, and Clinical Aspects of the Enzyme DPP IV. Crit Rev Clin Lab Sci 40(3): 209-294.

Larsson D. et al., 1998, Ca^{2+} uptake through voltage-gated L-type Ca^{2+} channels by polarized enterocytes from Atlantic cod Gadus morhua. J Membr Biol 164: 229-237.

Larsson SC. et al., 2005, High fat dairy food and conjugated linoleic acid intakes in relation to colorectal cancer incidence in the Swedish Mammografy Cohort. Am J Clin Nutr 82: 894-900.

Lentz KA et al., 2000, Development of a more rapid, reduced serum culture system for Caco-2 monolayers and application to the biopharmaceutics classification system. Int J Pharm 200: 41-51.

Liguo Q. et al., 2015, Preparation and bioactive properties of chitosan and casein phosphopeptides composite coatings for orthopedic implants. Carbohyd Polym 133: 236-244.

Lowry O. et al., 1951, Protein measurement with the Folin phenol reagent. J Biol Chem 193: 265-275.

Maarten A. et al., 2012, Trends in ultrasensitive proteomics. Curr Opin Chem Biol 16:206-213.

Mace OJ. et al., 2007, Sweet taste receptors in rat small intestine stimulate glucose absorption through apical GLUT2. J Physiol 582:379-392.

Magnano SLE. et al., 2011, In vivo and in vitro digestibility of the calcium contained in foods of animal and plant origin. Med J Nutr Metabol 4:105-110.

Malacarne M. et al. Proteolisi e lipolisi nel P.R. a differenti periodi di stagionatura: 12, 24, 55 e 96 mesi; Ann. Fac. Medic. Vet. di Parma Vol. XXVI (2006) 145.

Mariani A. et al., 2006, Alimentazione e nutrizione umana; il pensiero scientifico editore, 193.

Martinez-Palomo A. et al., 1980, Experimental modulation of occluding junctions in a cultured transporting epithelium. J Cell Biol 87: 736-745.

Masotti F. et al., 2010, Hogenboom J.A., Rosi V., De Noni I., Pellegrino L. Proteolysis indices related to cheese ripening and typicalness in PDO Grana Padano cheese. International Dairy Journal 20: 352.

Matar C., Goulet J., 1996, β-Casomorphin-4 from milk fermented by a mutant of Lactobacillus helveticus; Int Dairy J 6: 383.

Matkovic V. et al., 1990. Factors that influence peak bone mass formation: a study of calcium balance and the inheritance of bone mass in adolescent females; Am. J. Clin. Nutr. 52: 878.

Matkovic V., 1979, Bone status and fracture rate in two regions of Yogoslavia; Am.J.Clin.Nutr. 32: 340.

McDonagh D. & FitzGerald RJ., 1998, Production of Caseinophosphopeptides (CPPs) from Sodium Caseinate Using a Range of Commercial Protease Preparations. International Dairy Journal 8 39-45.

Meisel H. & Frister H., 1988, Chemical characterization of a caseinophosphopeptide isolated from in vivo digests of a casein diet. Biol Chem Hoppe Seyler 369 1275-1279.

Meisel H. & Schlimme E., 1990, Milk proteins: precursors of bioactive peptides. Trends in Food Science & Technology 1 41-43.

Meisel H., & FitzGerald R. J., 2003, Biofunctional peptides from milk proteins: mineral binding and cytomodulatory effects. Current Pharmaceutical Design, 9, 1289–1296.

Meisel H., & Olieman C., 1998, Estimation of calcium-binding constants of casein phosphopeptides by capillary zone electrophoresis. Analytica Chimica Acta, 372, 291–297.

Mellander O. & Olsson N., 1956, The influence of peptide bound calcium and phosphorus on bone calcification in rickets. Bol Med Hosp Infant Mex 13 243-246.

Michalski A. et al., 2011, Mass spectrometry-based proteomics using Q Exactive, a high-performance benchtop quadrupole Orbitrap mass spectrometer. Molecular & Cellular Proteomics, 10 (9), No. M111.011015.

Middlebrooks B. et al., 1998, Effect of storage time and temperature on the microflora ad amine development in Spanish Mackerel, J.Food Sci 4: 1024.

Millan JL., 2006, Alkaline Phosphatases : Structure, substrate specificity and functional relatedness to other members of a large superfamily of enzymes. Purinergic Signalling; 2(2): 335–334.

Miquel E. at al., 2005, Identification of Casein Phosphopeptides Released after Simulated Digestion of Milk-Based Infant Formulas. Journal of Agricultural and Food Chemistry, 53, 3426–3433.

Moorman PG., Terry P.D, 2004, Consumption of dairy products and the risk of breast cancer: a review of the literature. Am. J. Clin. Nutr. 80: 5.

Morgan EL. et al., 2003, A role for Ca(v)1.3 in rat intestinal calcium absorption. Biochem Biophys Res Commun 312 487-493.

Morgan EL. et al., 2007, Apical GLUT2 and Cav1.3: regulation of rat intestinal glucose and calcium absorption. In J Physiol, pp 593-604. England.

Morita T. et al., 1983, Hyperproduction of phosphate-binding protein, phoS, and pre-phoS proteins in Escherichia coli carrying a cloned phoS gene. Eur J Biochem 130:427-435.

Mosmann T., 1983, Rapid colorimetric assay for cellular growth and survival: application to proliferation and cytotoxicity assays. J Immunol Methods 65:55-63.

Mozes S. et al., 2004. Obesity and Changes of Alkaline Phosphatase Activity in the Small Intestine of 40- and 80-day-old Rats Subjected to Early Postnatal Overfeeding or Monosodium Glutamate. Physiological Research; 53: 177–186.

Mucchetti G., & Neviani E., 2006, Microbiologia e tecnologia lattiero-casearia. Qualità e sicurezza. Tecniche Nuove: Milano, pp. 489–496.

Mullally M.M. et al., 1996, Synthetic peptides corresponding to alpha-lactalbumin and beta-lactoglobulin sequences with angiotensin-I-converting enzyme inhibitory activity. Biol. Chem Hoppe Seyler 377: 259.

Munaron L., et al., 2004, Blocking Ca^{2+}entry: a way to control cell proliferation. Curr Med Chem 11 1533-1543

N Li, et al., 2004, Glutamine regulates Caco-2 cell tight junction proteins. Am J Physiol Gastrointest Liver Physiol 287: 726.

Naito H., Kawakami A. & Imamura T., 1972, In vivo formation of phosphopeptides with calcium-binding property in the small intestinal tract of the rat fed on casein. Agric. Biol. Chem 36 409-415.

Nakamura Y. et al., 1995. Purification and characterization of angiotensin-I-converting enzyme inhibitors from sour milk. Journal of Dairy Science, 78, 777–783.

Nakkrasae LI. et al., 2010 Transepithelial calcium transport in prolactin-exposed intestine-like Caco-2 monolayer after combinatorial knockdown of TRPV5, TRPV6 and Ca(v)1.3. J Physiol Sci 60 9-17

Nelson DL. & Cox MM., 2006, I principi di biochimica di Lehninger: Zanichelli.

Nemere I., 2005, The 1,25D3-MARRS protein: contribution to steroid stimulated calcium uptake in chicks and rats. Steroids 70 455-457.

Neviani E., Carini S., 1994, Microbiology of Parmesan cheese, M.A.N. 12: 1

Nongonierma A.B. et al., 2013, Inhibition of dipeptidyl peptidase IV and xanthine oxidase by amino acids and dipeptides. Food Chemistry; 644–653.

Nongonierma A. B., & FitzGerald, R. J., 2015, The scientific evidence for the role of milk protein-derived bioactive peptides in humans: A Review. Journal of Functional Foods, 17, 640–656.

Ophir I., et al., 1995, Apical polarity in human colon carcinoma cell lines. Tissue & Cell 27: 659.

Orrenius S. et al., 2003, Regulation of cell death: the calcium-apoptosis link. Nat Rev Mol Cell Biol 4 552-565.

Ortega N. et al., 2009, J. Agric. Food Chem., 2009, 57, 5743–5749.

Otani H. et al., 2001, Effects of bovine beta-casein (1-28) and its chemically synthesized partial fragments on proliferative responses and immunoglobulin production in mouse spleen cell cultures. Biosci Biotechnol Biochem 65 2489-2495.

Park O., Swaisgood, H. E., & Allen, J. C. ,1998, Calcium Binding of Phosphopeptides Derived from Hydrolysis of a_S-Casein or β-Casein Using Immobilized Trypsin. Journal of Dairy Science, 81, 2850–2857.

Parodi MW., 1999, Coniugated linoleic acid and other anticarcinogenic agents of bovine milk fat; J.Dairy Sci. 82: 1339.

Patrick H. & Bacon JA., 1957, The effect of vitamin D upon bone mineralization of Ca45 and Sr89 as chlorides and as phosphopeptides. J Biol Chem 228 569-57.

Pellegrino L. et al., 2003, Valutazione del Grana Padano grattugiato attraverso determinazione per elettroforesi capillare di frazioni caseiniche e di loro peptidi di degradazione; Sci. Tecn.Latt.Cas. 54: 321.

Peng JB., Brown EM. & Hediger MA., 2003, Epithelial Ca^{2+} entry channels: transcellular Ca^{2+} transport and beyond. J Physiol 551 729-740.

Peng JB. Et al., 1999, Molecular cloning and characterization of a channel-like transporter mediating intestinal calcium absorption. J Biol Chem 274 22739-22746.

Perales, S. et al., 2005, Bioavailability of Calcium from Milk-Based Formulas and Fruit Juices Containing Milk and Cereals Estimated by in Vitro Methods (Solubility, Dialyzability, and Uptake and Transport by Caco-2 Cells). Journal of Agricultural and Food Chemistry, 53, 3721–3726.

Perego S. et al., 2012, Casein phosphopeptides modulate proliferation and apoptosis in HT-29 cell line through their interaction with voltage-operated L-type calcium channels. J. Nutr. Biochem., 23, 808–816.

Perego S. et al., 2013, Evaluation of a possible direct effect by casein phosphopeptides on paracellular and vitamin D controlled transcellular calcium transport mechanisms in intestinal human HT-29 and Caco2 cell lines J. Funct. Foods, 5, 847–857.

Perego S. et al., 2015, Calcium bioaccessibility and uptake by human intestinal like cells following in vitro digestion of casein phosphopeptide–calcium aggregates Food Funct., 6, 1796.

Petersen OH. & Fedirko NV., 2001, Calcium signalling: store-operated channel found at last. Curr Biol 11 R520-523.

Pignata S. et al., 1994, The Enterocyte-like Differentiation of the Caco-2 Tumor Cell Line Strongly Correlates with Responsiveness to cAMP and Activation of Kinase A Pathway'; Cell Growth and Differentiation. 5: 967.

Pinto M. et al., 1982, Biology of the cell, 1982 44: 193.

Pointillart A. & Gueguen L., 1989, Absence of effect of the incorporation of a milk phosphopeptide on the utilization of calcium and phosphorus in the young pig. Reprod Nutr Dev 29 477-486.

Polverino et al., 2002, Partly folded states of members of the lysozyme/lactalbumin superfamily: a comparative study by circular dichroism spectroscopy and limited proteolysis. Protein Sci. 11(12): 2932.

Prignano F. et al., 2015, Tuscany consensus for the diagnosis, treatment and follow-up of moderate-to-severe psoriasis. G Ital Dermatol Venerol. Accepted.

Proctor V., Cunningham F., 1988, The chemistry of lysozyme and its use as a food preservative and a pharmaceutical; Crit. Rev. Food Sci. Nutr, 26: 359.

Putney JW., 1999, Calcium. In Basic Neurochemistry, Molecular, Cellular and Medical Aspects, pp 453-469. Ed BWA

Quaroni A. and J. Hochman., 1996, Development of intestinal cell culture models for drug transport and metabolism studies. Adv. Drug Delivery Rev 22, 3–52.

Resmini P. et al., 1993, Gli amminoacidi liberi nella caratterizzazione analitica del formaggio Grana Padano; Scienza e Tecnica Lattiero-Casearia (1993) 44: 7.

Resmini P. et al., 1996, Valutazione chimico-analitica comparativa dei processi maturativi del formaggio Grana Padano; il latte: tecniche nuove 21: 110.

Restani P, et al., 1996, B -Casein as a marker of ripening and/or quality of Grana Padano cheese. J. Agric. Food Chem. 44: 2026

Review A. et al., 2013, Role of Chemical and Analytical Reagents in Colorimetric Estimation of Pharmaceutical. International Journal of Medicine and Pharmaceutical Research; 1(5): 433–445.

Reynolds EC. et al., 2003, Retention in plaque and remineralization of enamel lesions by various forms of calcium in a mouthrinse or sugar-free chewing gum. J Dent Res. 2003, 82(3):206-11.

Reynolds EC. et al., 1994, A selective precipitation purification procedure for multiple phosphoseryl-containing peptides and methods for their identification. Analytical Biochemistry, 217, 277–284.

Riggs et al., 1987, Dietary calcium intake and rates of bone less in women; J. Clin. Invest. 80: 979.

Rinni et al., 2006, Fisiologia Umana, IX edizione, tomo II, Utet editore.

Rossetti et al., 2008, Grana Padano cheese whey starters: microbial composition and strain distribution; International Journal of Food Microbiology 127 (A) 168.

Rossi F. et al., 2011, Immonological response in Egg-sensitive Adults challenged with cheese containing or not containing Lysozyme; Jacn. 385.

Rossi F. et al., Effect of lysozyme and ripening time on in vitro Ca digestibility of Grana Padano DOP cheese. Istituto di Scienze degli Alimenti e della Nutrizione, Facoltà di Agraria, Università Cattolica del Sacro Cuore, Piacenza.

Saito et al., 2000, Isolation and structural analysis of antihypertensive peptides that exist naturally in gouda cheese. Journal of Dairy Science, 83, 1434–1440.

Salvatore, 2013, Biochimica umana. Idelson-Gnocchi; 186−200.

Sampson et al., 1997, Relationship between food specific IgE concentrations and the risk of positive food challenges in children and adolescents; J.Allergy Clin Immunol 100: 444.

Sandri et al., 1997, Osservazioni sull'andamento della lipolisi nel corso della maturazione del P.R.; Sci.Tec. Lat. Cas. 48: 243.

Santon, 1996, Biogenic amines: their importance in food; Int. J. Food Microbiol. (1996) 29: 213

Sato et al., 1986, Casein phosphopeptide (CPP) enhances calcium absorption from the ligated segment of rat small intestine. J Nutr Sci Vitaminol (Tokyo) 32 67-76.

Sato et al, 1991, Characterization of phosphopeptide derived from bovine beta-casein: an inhibitor to intra-intestinal precipitation of calcium phosphate. Biochim Biophys Acta 1077 413-415.

Schlimme & Meisel, 1995, Bioactive peptides derived from milk proteins. Structural, physiological and analytical aspects. Nahrung 39: 1-20.

Schneider N. et al., 2011, Prevalence and stability of lysozyme in cheese. Food Chem. 128: 145.

Sefcíková et al., 2008, Different Functional Responsibility of the Small Intestine to High-Fat/High-Energy Diet Determined the Expression of Obesity-Prone and Obesity-Resistant Phenotypes in Rats. Physiological Research; 57(3): 467-474.

Sforza S. et al., 2004, Study of the oligopeptide fraction in Grana Padano and Parmigiano-Reggiano cheeses by liquid chromatography-electrospray ionisation mass spectrometry. European Journal of mass spectrometry 10(3), 421-427.

Sforza S. et al., 2011, Cheese peptidomics: A detailed study on the evolution of the oligopeptide fraction in Parmigiano-Reggiano cheese from curd to 24 months of aging; J. Dairy Sci. 95:3514.

Sforza S. et al., 2003, Extraction, Semi-Quantification, and Fast On-line Identification of Oligopeptides in Grana Padano Cheese by HPLC−MS. J. Agric. Food Chem. 51, 2130−2135.

Shah NP., 2000, Effects of milk-derived bioactives: an overview. Br J Nutr 84 Suppl 1 S3-10.

Shimizu M., 2010, Interaction between Food Substance and the Intestinal Epithelium. Bioscience. Biotechnology. Biochemstry; 74 (2): 232-241.

Siliciano JD. & Goodenough DA., 1988, Localization of the tight junction protein, ZO-1, is modulated by extracellular calcium and cell cell contact in Madin-Darby canine kidney epithelial cells. J Cell Biol 107: 2389-2399.

Sjogren P., et al., 2004, Milk-derived fatty acids are associated with a more favourable LDL particle size distribution in healthy men, J. Nutr. 34: 1729.

Suzuki Y. et al., 2008, Mechanisms and regulation of epithelial Ca^{2+} absorption in health and disease. Annu Rev Physiol 70 257-271.

Suzuky T., 2009, H. Hara. Quercetin enhances intestinal barrier function through the assembly of Zonnula Occludens-2, Occludin and Claudin-1 and the expression of Claudin-4 in Caco2 cells, J. Nutr. 139: 965.

Taylor A., 1993, Aminopeptidases: structure and function. FASEB Journal; 7(2): 290–298.

Tsuchita H., et al., 1996, Dietary casein phosphopeptides prevent bone loss in aged ovariectomized rats. J Nutr 126 86-93.

Twentyman P.R. &. Luscombe M, 1987, A study of some variables in a tetrazolium dye (MTT) based assay for cell growth and chemosensitivity. Br. J. Cancer. 56: 279-285.

Vreeburg R.A.M. et al., 2012, Apple extract induces increased epithelial resistance and claudin 4 expression in Caco-2 cells; J Sci Food Agric 92: 439.

Wang L., Nancollas GH., 2009, Pathways to biomineralization and biodemineralization of calcium phosphates: the thermodynamic and kinetic controls. Dalton Trans 15:2665–2672.

Wasserman RH. & Fullmer CS., 1995, Vitamin D and intestinal calcium transport: facts, speculations and hypotheses. J Nutr 125 1971S-1979S.

Wright SC., 1994, Inhibition of apoptosis as a mechanism of tumor promotion. FASEB J 8 654-660.

Zemel M.B., 2004, Role of calcium and dairy products in energy partitioning and weight management. Am J Clin Nutr, 79 (suppl) 907S-12S.

Zheng B., Cantley LC., 2007, Regulation of epithelial tight junction assembly and disassembly by AMP-activated protein kinase. Proc Natl Acad Sci 104: 819–822.

Zhuang L. et al., 2002, Calcium-selective ion channel, CaT1, is apically localized in gastrointestinal tract epithelia and is aberrantly expressed in human malignancies. Lab Invest 82 1755-1764.

Zweinbaum A. et al., 1985, Journal of Cellular Physiology, 122: 21.

RINGRAZIAMENTI

Un immenso ringraziamento è rivolto a Giuseppe, perfetto compagno di vita che mi ha sempre sostenuto nelle scelte professionali, accettando tutto ciò che esse hanno comportato.
Ringrazio la mia famiglia, che se pur distante fisicamente è quotidianamente presente nella mia vita costituendo per me un fondamentale supporto psicologico.
Un profondo grazie lo rivolgo alla Prof. ssa Fiorilli, che con la sua esperienza mi ha sempre saggiamente consigliata sia dal punto di vista professionale, sia da quello personale, ed alla Dott.ssa Anita Ferraretto che in questi anni, con fiducia e pazienza, mi ha supportata professionalmente mantenendo sempre il rispetto nell'individualità delle scelte.
Mille grazie anche alle compagne di questa esperienza, Margherita, Michela, Manu e Valentina, senza le quali nulla sarebbe stato così stimolante, divertente e appassionante.